DV1.1b Stress Drivers and Outline of Proposed Numerical Modelling Campaign

Organisation(s)	Rockfield, NGI, BP, GEUS
Author(s)	Lars Grande, Nazmul Haque Mondol, John Hopper, Dan Roberts, Dan Phillips
Reviewer	Adam Bere, Stephen Dee
Type of deliverable	Report
Dissemination level	Public
WP	1
Issue date	October 2022
Document version	v1

Keywords: Stress, Pore Pressure, Geomechanics, Structural Geology, Constitutive Modelling, Numerical Modelling

Summary

A current synthesis of the understanding of the *in situ* stress state is presented for the Horda Platform, Endurance Structure and Greater Bunter sandstone area, Aramis, Lisa and Nini structures in the North Sea (section 2). Highlighted stress generation mechanisms include ridge push, sediment and progradational loading, continental margins, glacioeustatic adjustments, and uplift/erosion. Assessment of the relative importance of these mechanisms throughout the areas is displayed as a stress matrix (Table 2-1); which provides invaluable information for site characterisation. Following the assessment of relevant stress drivers, a proposal of relevant geomechanical models to encapsulate significant processes present at each site is presented in sections 3 and 4. Empirical laws and relevant rheological properties implemented in models are highlighted in section 3.2. Recent modifications to relevant rheologies are also considered, new for WP1. Three types of geomechanical forward models are proposed (A-C) (section 4) that explore stress in various dimensions and scales. Type A models explore the influence of mineralogy, stress translations at depth and loading/unloading processes in a uniaxial 1D model. Results can be calibrated to well data and provide estimates of minimum subsurface stress. Type B models involve regional 2D/3D modelling and provide a means for an investigation into the relative contributions of *in situ* stress along large-scale transects, as well as the analysis of spatial trends in the magnitude and orientations of stresses. Modelled stress outputs can also be compared to focal mechanism data to give insights as to the degree of coupling between thick and thin-skinned deformation. Type C (2D/3D) models explore site-specific contributions to stress variability from structures such as evaporite diapirs, stress field coupling and glacioeustatic responses of subsurface structures. Model results will provide insights into the evolution, in-situ state and potential risks linked to CO2 injection into the areas of interest. This provides invaluable information for other work packages as well as a general contribution to advancing CCS site characterisation.

Contents

1 Introduction

Accurate *in situ* stress determination is fundamental to any site characterization and risk assessment workflows associated with geological carbon storage operations. Present day stress conditions impose constraints on storage operations as they are integral to any efforts aiming to better understand injection pressure limits, caprock and seal integrity, fault reactivation, and induced seismicity. This is reflected in the emphasis accorded to understanding stress conditions local to storage sites (and regionally) in assessing rock-failure risks that have been undertaken in other SHARP work packages (SHARP Deliverable 4.1 2022).

Establishing the *in situ* stress is, however, non-trivial. Stress conditions can exhibit significant variability both temporally and spatially as determined by different driving processes that may operate locally or regionally. Stress characterization is compounded by a general paucity of calibration data and challenges associated with accurately determining specific stress components. Where there is well data available, the minimum stress at select locations can be estimated from casing shoe tests and the overburden stress may be calculated based on density integration over depth. In compressive environments where reverse faulting regimes may be encountered, the minimum stress is equal to the overburden, and therefore field measurements provide a singular measurement of the stress state. Whilst procedures exist for *estimating* the maximum horizontal stress, it is emphasized that this cannot be measured directly. It is therefore useful for characterization workflows to be supported by geomechanical modelling to reduce uncertainties associated with stress inputs for rock failure risk assessment, which will have a first-order influence on the operational limit design and potential risks.

The aim of this report is therefore to lay the foundations for improved stress characterization efforts by reviewing the potential mechanisms and processes that contributed to both paleo- and present-day stress conditions. An important aspect here is to develop an appreciation of the mechanisms that are inferred to have an influence on stress and particularly those that are active or significant across the majority of the target storage sites. The outcomes of the assessments are condensed into a *stress drivers* matrix which provides a quick overview of the important processes and helps ensure that the geomechanical modelling framework can appropriately represent them. The modelling framework is introduced and the procedures and tools for incorporating the stress drivers are described. Special attention is given to the constitutive models, as robust material laws are required to provide the link between the driving mechanisms/processes (realised as *loads* or *boundary* conditions) and the predicted stress states/paths.

Based on the key stress drivers several model designs are offered to tackle specific scientific questions and generate data and insights that can be offered to other work packages.

2 Sites Descriptions and Understanding of State of Stress

This section is concerned with a broad characterisation the stress state and describing the regional structural geology at each of the storage sites based on literature reviews. This is complemented by an assessment of key stress driver mechanisms that are thought to contribute to the present stress state. The goal of undertaking this exercise is to develop an improved understanding of the mechanisms so that they can be incorporated into subsequent geomechanical modelling tasks.

2.1 Horda Platform Area

2.1.1 Present Understanding of Insitu Stress State

Stress magnitudes and stress orientations for the Horda platform area have been documented in Thompson et al., (2022). Trends of minimum horizontal stresses (σ_h) from the Horda-Tampen area include 46 XLOTs at casing shoes, 8 XLOTs performed at intermediate depths as formation barrier tests (through perforations) and 11 minifrac results (from reservoir sandstones). All tests shallower than 3000 m with greater than 10% normal hydrostatic pore pressure are removed to reduce any overpressure effects on the dataset. There are two linear trends visible, with a shift at ~2900–3000 m TVD below the sea surface, corresponding to the depth where significant pore fluid overpressure begins. A similar shift in trend at ca 3000 m is also observed in other places based on a recent regional study, including North Sea (78 XLOTs) and Norwegian Sea (30 XLOTs) (Thompson, Andrews, Reitan, et al. 2022). XLOT from Eos 31/5-7 well, indicate that σ_h in Drake test (9 5/8 in. XLOT) is at the lower end of the Tampen-Horda trendline and the Draupne (13 5/8 in. XLOT) are more in-line with general trendlines. The Drake test was performed in a ca. 4 m long open-hole interval below the casing shoe in the transition from the Upper Drake Fm. 1 and Intra Drake intervals; it is therefore not known definitively within which formation the fracturing occurred. The XLOT data in the Drake is considered to be of high quality, however, fractures may have propagated upwards into a lower stress interval (as indicated from log data). An alternative interpretation of σ_h is therefore suggested, giving a higher K_0 of 0.5 (stress gradients of 1.55sg) compared to the main interpretation of K_0 of 0.4 (1.43sg). This corresponds to K_0 of ca 0.4-0.5, which is still in low range of observations of K_0 ca 0.4-0.8 in the Tampen-Horda area.

The general in-situ stress regime in the shallower sediments (<3000 m) can be characterized as normal-faulting/extensional. Local perturbations in close proximity to faults cannot be ruled out, however, the major principal stress is vertical. A degree of horizontal stress anisotropy exists, constrained to lie between $1.01 \leq \sigma_H/\sigma_h \leq 1.27$. It is suggested to consider even the most extreme value in the presence of a normal-faulting stress state. A value of the σ_H/σ_h ratio of 1.05 is often considered reasonable/applicable for the Northern North Sea area of the NCS (Andrews et al., 2016). In-situ stresses at Smeaheia site are reported in Statoil (2016). Nine overburden XLOT and three minifrac were available from nearby areas. Of these, two overburden XLOT tests come from the shallow (<1500 m TVDMSL) Troll area; the three reservoir minifrac tests also come from the Troll area. These five test results were chosen to define the final stress profiles, but all twelve test results fell along a consistent σ_h profile. σ_V values from the two overburden XLOT tests were used to create the σ_V profile. Values of stresses at two depth levels from these gradients are reported below. Top reservoir (1304 TVDmsl); σ_V = 23.4MPa, σ_H = 18.7 MPa, σ_h = 17.8 MPa, initial pore pressure (Pp_{ini}) = 9.17 MPa. Injection point (1488m TVD msl); σ_V = 27.2 MPa, σ_H = 21.6 MPa, σ_h = 20.6 MPa, initial pore pressure (Pp_{ini}) = 11.0 MPa. Note that the horizontal stress values presented above do not account for any reduction due to the assumed 40 bar depletion from Troll, and if depletion is to be accounted for,

1.81MPa should be subtracted from the horizontal stress values presented above. Normal faulting stress regime ($\sigma_V > \sigma_H > \sigma_h$) with equal horizontal stresses ($\sigma_H = \sigma_h$) is the basic assumption, and values above correspond to high values of σ_H =1.05x σh. Pore pressures in the Norwegian part of the North Sea are normally hydrostatic down to 2.5 km with exception of Tampen Spur Area and block 35/9 (Gjøa) and this includes the areas around Troll and Oseberg (Grollimund et al. 2001). All fields in the Tampen Spur area have hydrostatic pore pressure down to 1.0-1.5 km, where a transition zone starts and pore pressures quickly rise to 10-15MPa overpressure (Jørgensen and Bratli 1995). As a consequence of pore pressure buildup, σ_h increases in all fields and in Gullfaks and Snorre the σ_h is close to σ_v.

2.1.2 Regional Structural Geology

The structural geology of the Horda platform has been summarized recently (Wu et al. 2021). The Horda Platform is a N–S-trending structural high along the eastern margin of the northern North Sea, with the North Viking Graben to its west. The regional setting and tectonic evolution of the Horda Platform and the northern North Sea have been well documented and widely discussed in the published literature and references (see Wu et al. (2022) for the complete references). There are two major extensional events observed on the Horda Platform: The Permo–Triassic rifting (Syn-rift 1) and the Late Jurassic–Early Cretaceous rifting (Syn-rift 2). The Permo–Triassic rifting, as a result of the break up of Pangea, affected the entire northern North Sea Basin with the rift axis beneath the Horda Platform. This rifting event resulted in the formation of a series of easterly tilted, pre-Jurassic half-grabens, bound by several N–S-trending, large displacement normal fault systems. The N–S-trending strikes of the Permo–Triassic faults offshore and the Permian dykes observed onshore western Norway suggest an E–W extension orientation during this rifting event.

The Jurassic rifting event in the northern North Sea area was diachronous. To the west of the Horda Platform, the evidence of extensional episodes during the mid-Jurassic has been observed near the central segment of the northern North Sea, especially around the Viking Graben and Sogn Graben areas. On the Horda Platform's northern margin, several faults were active in the Uer Terrace area in the mid-Jurassic (since Bajocian). On the western margin of the Horda Platform, the Brent Group sequences on the hanging wall side of the Troll Fault System also shows minor fault-controlled thickness changes, suggesting Late Bajocian-to-Middle Callovian aged faulting. However, observations of active faults in the mid-Jurassic has not been reported within the Horda Platform. In this region, from Late Triassic to Late Jurassic times, the Horda Platform was stable and experienced a phase of tectonic quiescence (marked as Post-rift 1). Several fluvio-deltaic to shallow marine systems were deposited during this phase, including the Statfjord Group, the Dunlin Group, the Brent Group, and the Viking Group. In seismic sections, these sedimentary packages are nearly tabular across the Horda Platform). During the Late Jurassic–Early Cretaceous rifting (Syn-rift 2, pre-existing N–S-trending major faults were reactivated and formed several half-graben depocenters on the Horda Platform. The Draupne Formation, which is composed of deep-marine mudstones, deposited during the early phase of this rifting event and has shown minor rotated onlaps and thickness changes toward the Tusse fault. The Cromer Knoll Group shows clear wedge-shapes and rotated onlaps in the half-grabens, which marks the main phase of the faulting on the Horda Platform. Figure 1 shows main structural elements and geological cross-section of the Horda Platform area, showing rotated fault blocks and potential storage locations in Smeaheia and Aurora (Wu et al. 2021).

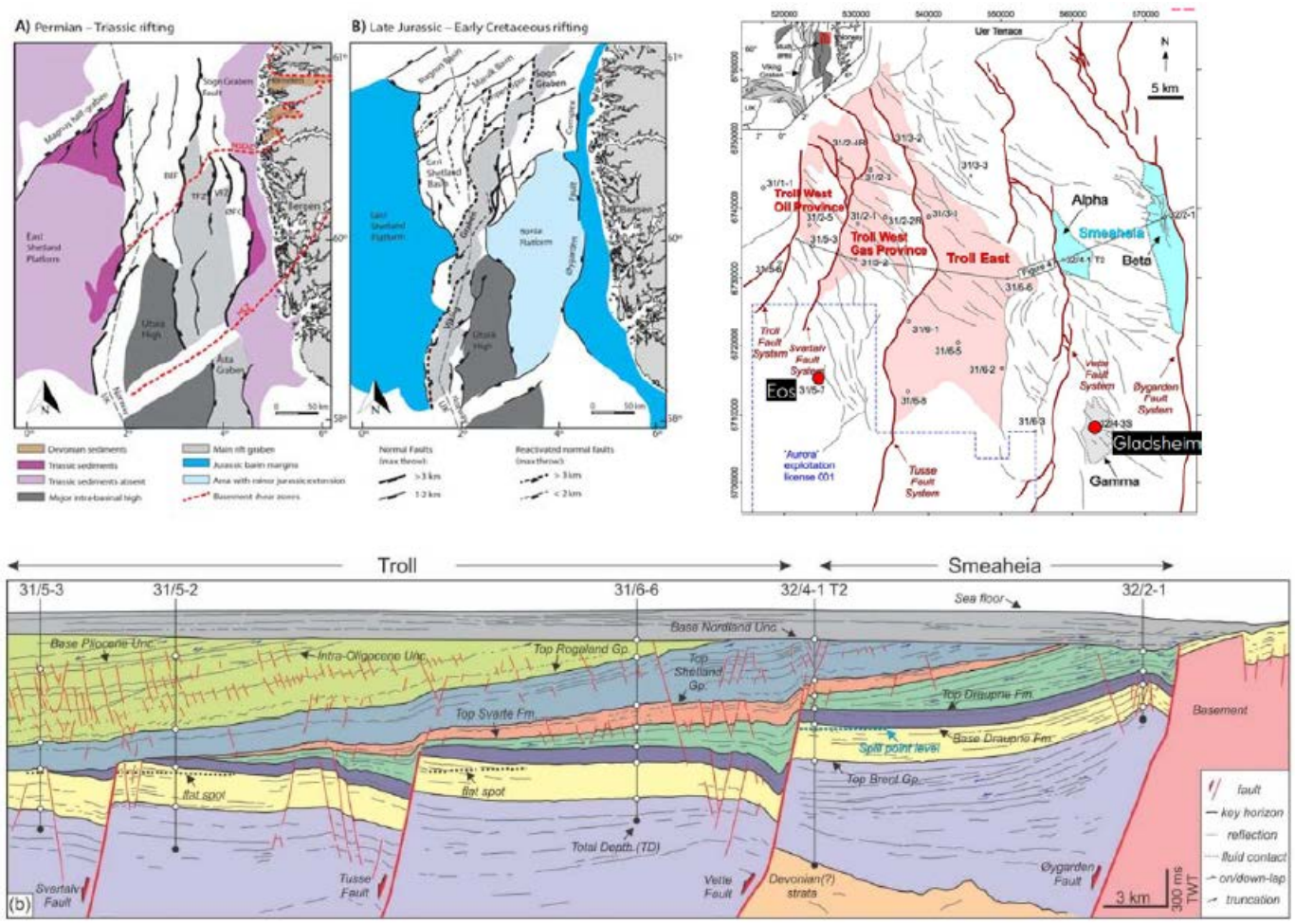

Figure 2-1 *Upper left, Structural map of area with two main rifting episodes. Main Structural elements of the northern North Sea resulting from (A) Permian-Triassic rifting (Rift Phase 1) and, (B) Late Jurassic-Early Cretaceous rifting (Rift Phase 2). (Holden, 2021, Modified from Færseth, 1996). Abbreviations: NSDZ = Nordfjord-Sogn Detachment Zone, HSZ = Hardanger Shear Zone, ØFC = Øygarden Fault Complex, VFZ = Vette Fault Zone, TFZ = Tusse Fault Zone, BEF= Brage East Fault. Upper right, map of the CCS sites (Smeaheia, Alpha, Beta, Gamma) and Aurora (Wu et al., 2021). Lower, Geological cross-section of the Horda Platform area showing rotated fault blocks and potential storage locations in Smeaheia (Wu et al. 2021).*

2.1.3 Stress Generating Mechanisms

An evaluation of stress-generating mechanisms in the Norwegian provinces has been discussed in Fejerskov (1996). The relevant information for the Northern North Sea and Horda platform area are summarized below. The suggested main mechanisms are Ridge push, Continental margin, sediment loading, deglaciation, and topographic.

2.1.3.1 Ridge Push/Compression

Since the late Paleocene (60Myr), spreading has occurred from both the mid-Atlantic ridge and its northward continuation, the Arctic mid-oceanic ridge (Fejerskov 1996). The mid-Atlantic spreading ridge induces a NW-SE deviatoric stress field in the order of 20-30MPa in the oldest oceanic crust, and its maximum values are in the thinner part of the crust, as is the case under offshore rifted basin (Mid-Norwegian Margin, Viking and Central Graben). In some places in the northern North Sea and western Norway, the NW-SE directions of Ridge push fit well with observations from logs and Focal mechanisms.

The deviatoric stress associated with ridge push increases with age and reduces with depth, and values from literature indicate tectonic stress in order of 20-40 MPa for upper crust based on modelling (M. H. P. Bott 1991; M. H. Bott and Kusznir 1984; Stein et al. 1989; Dahlen 1981; Fleitout and Froidevaux 1983).

The local thinning of crust under the Viking Graben may amplify the stresses in this area; however, this is also where the thickness of the sedimentary package is deepest. The Crystalline basement may be in order of 16, 12, and 26 km thick in the Horda platform, Viking graben, and East Shetland platform, respectively (rough numbers from figures in Maystrenko, Ottesen, and Olesen (2021) across E-W cross section). The depth to the crustal basement varies in range ca 4-12 km in the East-West cross section, and in the Horda platform, depth to the basement is ca 6-9 km. Devonian sandstone is present at depth of ca 3 km at Smeaheia and 4 km at Troll East. Large scale numerical models from the Vøring plateau in the Norwegian Sea give horizontal stress of 45 MPa in the thinner (ca 10km) crustal basement, of 45 MPa below Rås basin and 15 MPa in the thicker (ca 25km) crust under Halten Terrace when applying a later tectonic stress of 30 MPa (Kjeldstad et al. 2003). From this example, the crustal stress in the thicker basement below the East Shetland Platform should be smaller than in the thinner Viking Graben, and Horda Platform which may experience something in between.

2.1.3.2 Continental Margins

Continental margins are suggested to have an impact in the Norwegian Sea and the Barents Sea, where continental crust is characterized by tensional stresses and deviatoric compression in the oceanic crust normal to the continental margin (Fejerskov 1996). However, in the North Sea, the continental margin bends around the western side of the United Kingdom and is relatively distant from Viking Graben and Horda Platform area, and therefore the effect of the continental margin is assumed to be insignificant.

2.1.3.3 Sediment Loading Rate

High sedimentation loading rate and pore pressure buildup i.e during Pliocene is another stress driving mechanism; however, the importance is more significant on the Mid-Norwegian shelf and the Barents Sea, where the sedimentation rate was high (0.8 mm/yr and 1.6 mm/yr, respectively) (Fejerskov 1996). Viking Graben and Central Graben subsided with a relatively low sedimentation rate (ca 0.1 mm/yr), and the effect of sediment loading might be negligible.

2.1.3.4 Deglaciation

More detailed assessment of deglaciation in the North Sea has been captured in an accompanying SHARP report (SHARP Deliverable 1.1a 2022). The direction of principal stress is normal to isostatic rebound, which follows the coastline of Norway. In the Horda Platform area, the direction of principal stress should then be E-W. This is also in agreement with the majority of the stress azimuth observation reported for this area (Thompson, Andrews, Wu, et al. 2022).

2.1.3.5 Prograding Sedimentary Wedge – Differential Loading

Differential loading from a prograding sedimentary wedge may set up significant excess pore pressures in the sedimentary layers below and ahead of the load, which may again give increased lateral stresses from pore pressure. This has been demonstrated from numerical loading for the Vøring platform (Kjeldstad et al. 2003).

2.1.3.6 Uplift

The early Quaternary sedimentation in the central and northern North Sea was dominated by the progradation of hundreds of meters of thick clastic wedges in response to uplift and glacial erosion of

eastern source areas (Sejrup et al. 1996; Eidvin and Rundberg 2001; Faleide et al. 2002; Eidvin, Riis, and Rasmussen 2014; Baig 2018). A significant period of uplift and erosion along the northern North Sea basin margin is also indicated by the strong tilting of the entire Cenozoic succession below the mid-late Quaternary glacial unconformity (Riis 1996; Faleide et al. 2002). Neogene uplift in order of 1200m close to the coast has been suggested from exhumation studies from sonic logs and vitrinite reflectance (Baig et al. 2019). In general, the uplift is highest at the cost and reduces westwards. A recent uplift estimate generated under the SHARP project is presented in Figure 2-2.

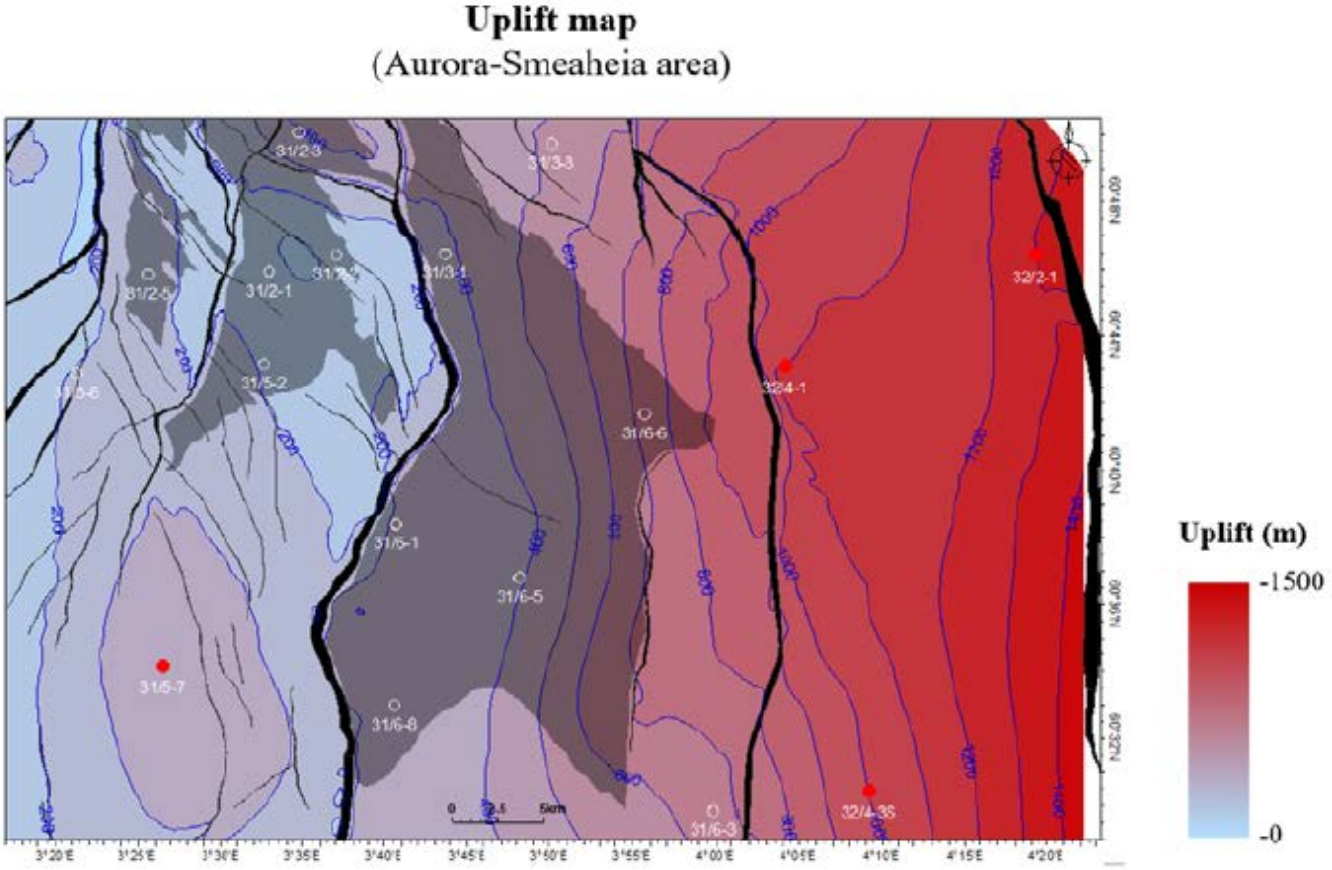

Figure 2-2 *Uplift map of the selected area in the Horda Platform, offshore Norway (Mondol, 2022 in progress, for SHARP). The potential CO2 injection locations of Alpha (32/4-1), Beta (32/2-1), Gamma (32/4-3 S) and Eos (31/5-7) are shown on the map (red dots).*

2.1.3.7 Diagenesis and Sediment Composition

Chemical compaction remineral transformations and cementation (Bjorlykke and Hoeg 1997) are the most important diagenetic processes that the Drake Formation has experienced both at their present depth (~2.6-2.7 km) and maximum burial (~2.8-2.9 km) before uplift. The present- and paleo-temperatures experienced by the caprock shales (Drake Formation) is higher than 100oC, especially in the Aurora area (Eos well location) (Figure 2-3). It is noteworthy to mention that temperature has significant effect on rock properties (e.g., Young's modulus, Poisson's ratio, etc.) where rocks experiencing higher temperatures will have high cementation compared to the same rocks exposed at low temperatures. This may involve dissolution of smectite and precipitation of microquartz and illite which occurs at temperatures of 70-100oC (2.0-3.0 km) and dissolution of kaolinite and precipitation of micro-quartz and illite at higher temperatures (>120-103oC) (Peltonen et al. 2009). The high illite content in Drake may partly be a result of transformation from a sediment richer in smectite with higher plasticity. An open question is how K0 will develop during mineral transformations (e.g., smectite to illite and kaolinite to illite), uplift of quartz-cemented rocks under stress changes and when diagenetic processes are still ongoing during the uplift phase. Therefore, the diagenetic

effects and rock property evolutions are the most relevant questions to evaluate for seal integrity of both Drake and Draupne Formation shales. The variation of mineralogical compositions of Drake and Draupne Formation shales will also influence their rock properties and likely also the stresses, where Draupne Formation shale is organic-rich compared to no organics in the Drake Formation shales (J. Rahman, Fawad, and Mondol 2020; M. J. Rahman et al. 2022).

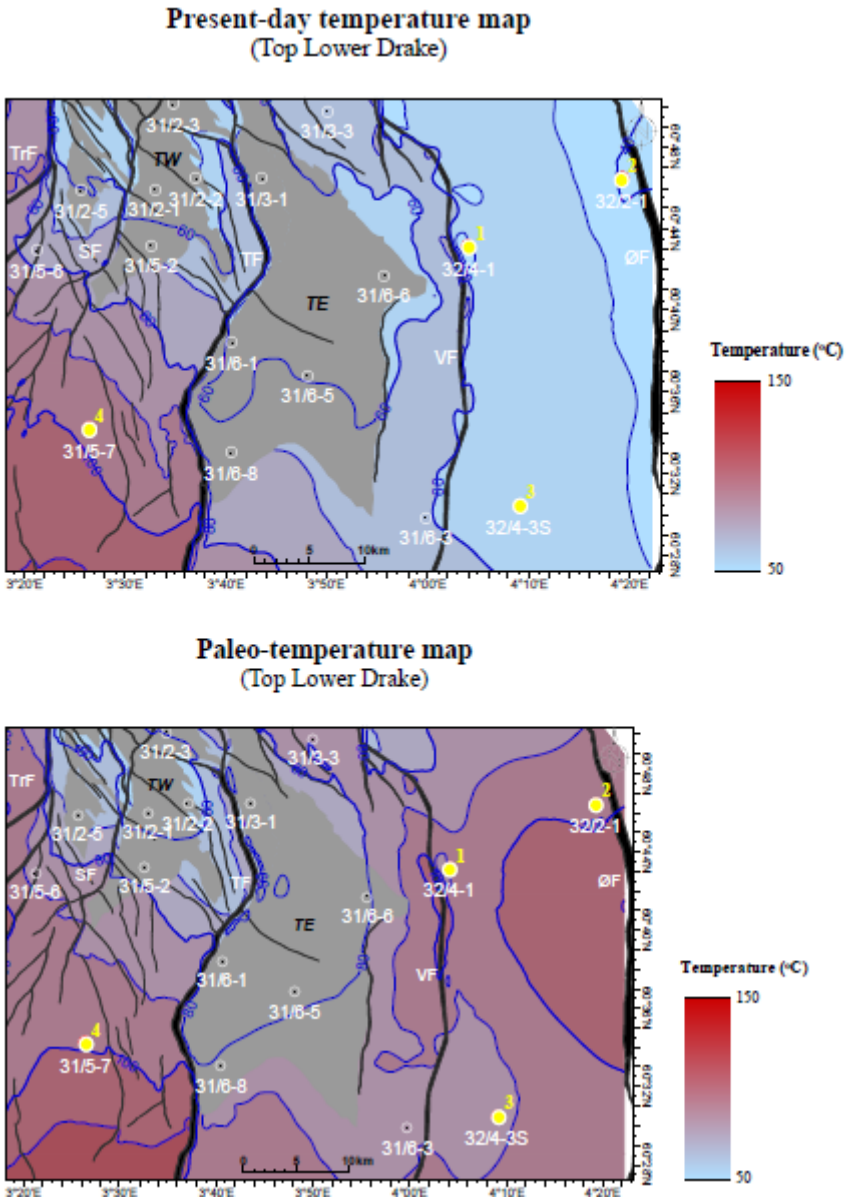

Figure 2-3 *The present (left) and paleo (right) temperature distribution maps of the caprock shale (lower Drake unit) calculated using exhumation and temperature gradient analysis display the variation and the maximum temperature experienced by the caprocks in the study area. The paleo-temperature map on top of the caprock surface represents both the mechanical and chemical compaction zones.*

2.1.3.8 Thermal Anomalies

Thermal anomalies are present in the North Sea due to the variable thickness of the basement and flexural effects from erosion and deposition i.e Fjeldskaar and Amantov (2018); Maystrenko, Ottesen, and Olesen (2021). Transient analysis of repeated thermal cycling from cooling during glaciations indicates a temperature decrease of about 5o C below areas covered with ice, and the temperature will gradually reduce

for each cycle until stabilizing and reaching equilibrium after several cycles (i.e. 20 cycles during 2 Myr (Fjeldskaar and Amantov 2018). Permafrost beneath the ice could potentially increase the thermal conductivity and increase cooling, and a steady state analysis indicates a cooling of 27◦C at 1 km from this effect (Fjeldskaar and Amantov 2018). However, steady state analysis will significantly overestimate the cooling, as there is not sufficient time for each glacial cycle to reach equilibrium. When including the effect of erosion and deposition of sediment according to isostatic corrections, the thermal pattern changes both laterally and with depth due to variations in conductivities and nature thermal equalization. In E-W profile across Viking Graben, there seems to be a thermal anomaly from this effect varying between -5◦C in the west to +5◦C in the east at 2 km depth (from figures in Maystrenko, Ottesen, and Olesen (2021). So there is an indication that erosion and sedimentation effects, overrules the effect of glacial cooling.

Such thermal anomalies could potentially generate lateral stress variations. The impact of isostasy from deglaciations and resulting temperature variations on the mantle viscosity and stress has been evaluated for a large depth >50 km (Barnhoorn et al. 2011). A maximum change in mean stresses (von mises) in order of 10-15 Mpa has been modelled offshore Norway at 100 km depth, with less change in stress at shallower and deeper depths. Glacial isostatic adjustment model (GIA) with composite 3-D Earth rheology for Fennoscandia has been used to evaluate sea levels and uplift rates throughout parts of glaciation history (Van Der Wal et al. 2013).

2.2 The Endurance Structure & Greater Bunter Sandstone Area

2.2.1 Present Understanding of *In situ* Stress State

Recently produced reports focused on geomechanical modelling at Endurance provide a useful summary of the understanding of the general state of stress (BEIS 2021). Analysis of casing shoe tests such as FIT, LOT and minifrac data suggest a normal fault regime where the largest (most compressive) principal stress is (near) vertical and the intermediate and smallest principal stresses lie in the horizontal plane. Furthermore, Sonic Scanner analysis from well 42/25d-3 indicates moderate horizontal stress anisotropy, with ratios of 1.05 and 1.10 in the Bunter Sandstones and Rot Clay layers respectively. Testing within the evaporites suggests that minimum stresses within the salt are close to overburden values; this is expected as deviatoric stresses are likely to be limited in the salt through viscous creep.

The statements above concerning stress regime and the degree of stress anisotropy are only valid for the post-Zechstein units. There is evidence of decoupling due to the presence of the Zechstein salt, establishing the possibility for distinct stress environments in pre- and post-Zechstein strata. This is discussed in subsequent sections.

2.2.2 Regional Structural Geology

2.2.2.1 UK Southern North Sea

Several key events have contributed to the structural evolution of the Southern North Sea basin which are described within this section. The crystalline basement in the area contains dominant NW-SE trending faults that established through Devonian age rifting and compression, and these have been reactivated by subsequent tectonic events (Stewart and Coward 1995). Other orientations, such as observed NE-SW and E-W trending faults were established during later orogenesis. Prominent faults that bound sub-basins in the area, such as the Dowsing Fault Zone (DFZ), are genetically linked to some of these deeper basement fault trends. During the Permian, a thick sequence of evaporites was deposited. Much of the regional structure in the overlying sediments is attributed to salt tecotnics (halokinesis) during the Triassic and Jurassic. These

halokinetic processes have resulted in the formation of salt structures within the Southern North Sea basin that are broadly classified as either (Stewart and Coward 1995):

(a) Elongate salt pillows that produce predominantly NW-SE trending folds in the overlying sediments; Figure 2-4.
(b) Smaller, reactive salt diapirs that may be linked to the adjacent salt pillows.

Basin tilting in the mid-Jurassic produced significant uplift and erosion, resulting in the extensive removal of material west of the DFZ. Towards the East, beyond the Cleaver Bank High (CBH) and into the Central Graben, there is greater preservation. It is important to note that locally in the Sole Pit Trough and Silverpit Basin, which sit between the DFZ and CBH, more significant erosion is observed that is attributed to uplift during the Sole Pit Inversion. In this area, it is common to find a complete absence of post Mid-Jurassic sediments, with the extent of erosion being closely related to the local expression of underlying salt.

2.2.2.2 The Endurance Structure

The formation of the structure is shown in Figure 2-4, reported to be well understood (White Rose 2016) and dominated by movement of the Zechstein salt. Most significant mobilization of salt is suggested to have occurred from Late Jurassic to Early Cretaceous. Deeper extensional faulting within the basement was accommodated by the salt, resulting in a progressive weakening of overburden sediments and subsequent halokinesis.

The structure at Endurance is representative of the typical salt structures observed within the Southern North Sea (Section 2.2.2.1). The main structure that will be targeted for storage is a large four-way closure formed above a salt pillow; Figure 2-5. The storage targets are the Triassic age Bunter Sandstones. The Bunter shale formation provides an underlying basal seal, whilst overlying evaporites and shales from the Haisborough group provide good quality top seals. Adjacent to the structure is a large salt diapir. Here the Bunter sandstones are inferred to outcrop at, or close to, the seabed.

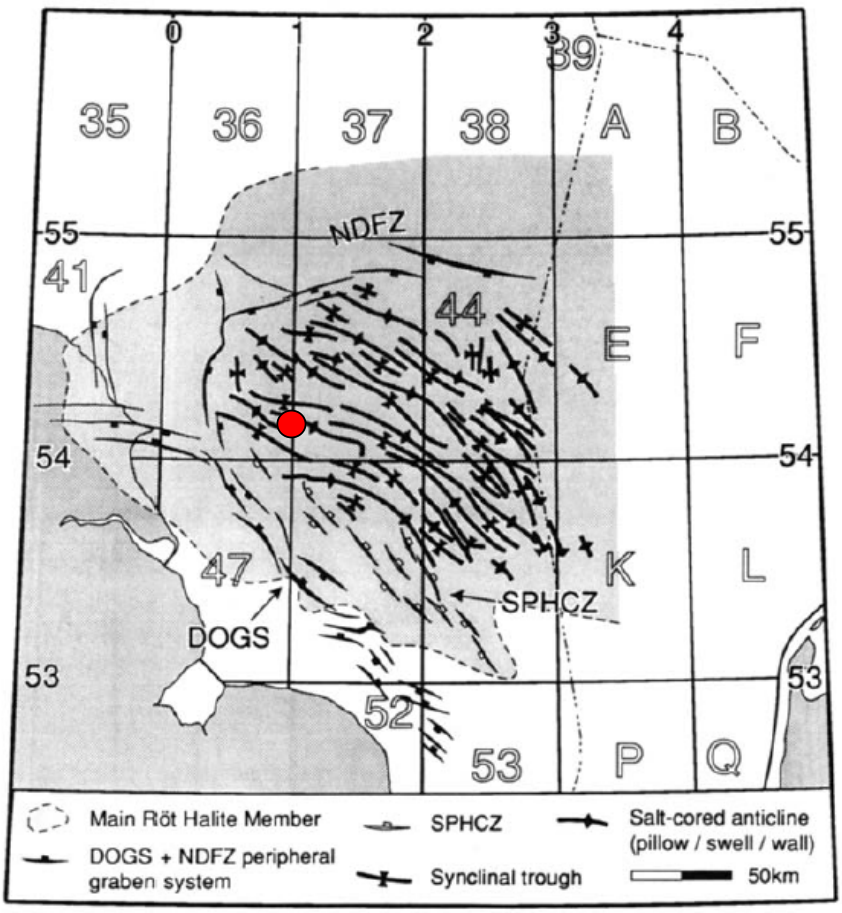

Figure 2-4 *Arrangement of salt-cored anticlines in the Southern North Sea after Steward & Coward, 1995. The approximate location of the Endurance Structure is marked with a red circle.*

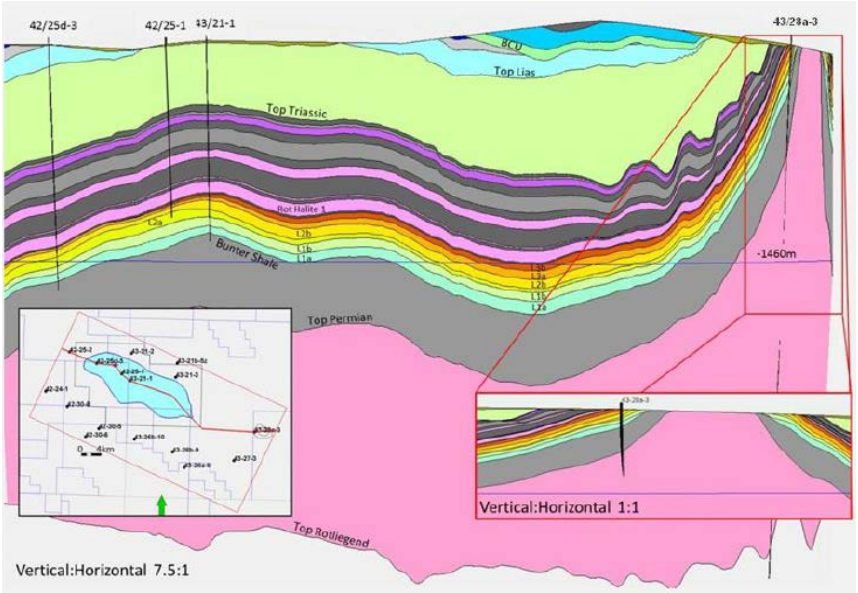

Figure 2-5 *Approximate NW-SE section through the Endurance structure. Note the almost complete absence of post mid-Jurassic sediments, and that sediments outcrop near to or at the seabed near the salt diapir to the East, (White Rose 2016).*

A number of faults are present in the overburden in the area around the proposed storage site; Figure 2-6. Above the Endurance structure itself, faults have a mainly NE-SW orientation and these likely formed due to outer-arc extension during inflation/swelling of the underlying salt (White Rose 2016). Faults typically have modest throw (10-40m) and appear to “root” at the top of Rot halite suggesting some additional decoupling at this level. In the saddle area, fault orientations appear to be increasingly East-West and have more variable orientations around the adjacent salt diapir. In these regions, there is evidence that the faults can locally cut down into the Bunter Sandstone (BEIS 2021).

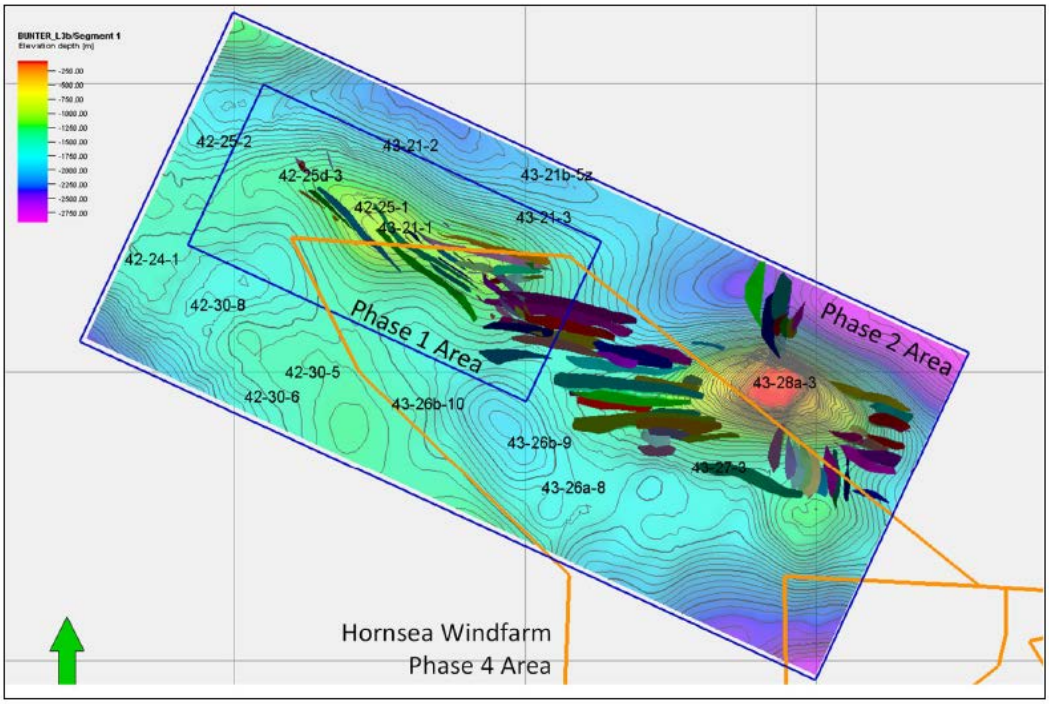

Figure 2-6 *Faulting within Endurance overburden shown relative to Top Bunter Sandstone (BEIS 2021).*

2.2.3 Stress Generating Mechanisms

2.2.3.1 Ridge Push/Compression

The contribution of ridge push from Mid-Atlantic spreading has been introduced in Section 2.1.3.1. Maximum horizontal stress orientations in the Southern North Sea are predominantly NE-SW for pre-salt strata (Williams et al. 2015). This direction is inferred to correlate with the axis of predominant ridge push direction. Similar conclusions have been drawn by Yale (2003) and Edwards (1997) in the Southern North Sea. Ridge push is therefore suggested to be a mechanism that has contributed to both the paleo (Late Mesozoic & Cenozoic) and present stress condition.

2.2.3.2 Halokinesis

The presence of the thick Zechstein evaporites has had a pronounced influence on petroleum systems within the North Sea. It is suggested that the presence of the salt has fundamentally altered the response to basin inversion in the pre- and post-salt intervals (Steward & Coward, 1995 and references therein). In the pre-salt interval, deformation is accommodated by reverse faulting, but the decoupling by weak salt permitted the post-salt to deform by buckle folding.

The influence of salt on local stress distributions is well documented in other areas of the North Sea (Carruthers et al, 2013), and discussions of the causes of such stress perturbance can be found in many publications (Luo et al. 2012; Nikolinakou et al. 2012). Within the Southern North Sea, it is suggested the

salt may have a profound influence on salt stress state by facilitating decoupling of pre- and post- Zechstein strata (Williams et al. 2015). It is possible that the pre-Zechstein stress regime might be more similar to onshore i.e. strike-slip, as opposed to a more normal stress condition in the post-Zechstein sequence.

2.2.3.3 Continental Margins

As with the Norwegian case, the continental margin is still some distance from the Endurance site, so the effect on stress might not be pronounced in contrast with the effect of ridge push.

2.2.3.4 Sediment Loading Rate

Sourcing specific sedimentation rates has proved challenging within the GBSS area. Across the Southern North Sea, Permo-Triassic successions have a maximum thickness of around 2700m accumulated over approximately 80Ma (Cameron et al. 1992). During the Jurassic, uplift resulted in the removal of material rather than emplacement (see Section 2.2.3.7). Regionally, sediment accumulations within the early Cretaceous have maximum thicknesses of 1000m near growing faults (Cameron et al. 1992), though the thickness of the Cretaceous interval at Endurance is much more modest (Figure 2-5) due to erosion.

It is not anticipated that the sediment loading rate will have resulted in significant overpressuring. Generally, there is little evidence of significant overpressures at Endurance and more regionally (SHARP Deliverable 4.1 2022), suggesting that modification of stress ratios due to excess pore pressure generation as observed elsewhere in the North Sea is perhaps unlikely.

2.2.3.5 Deglaciation

A comprehensive discussion of the influence of glacial processes at the Endurance structure can be found in the SHARP DV1.1a report. In summary, cyclical glacial loading likely occurred throughout the Pleistocene and Pliocene, possibly of smaller magnitude than areas such as the Horda Platform. This is inferred from the lack of thick seismically imaged fold and thrust complexes and far-field modelling. Estimates for the magnitude of stress caused by ice loading and ice thicknesses arise from OCR (Over-Consolidation Ratio) measurements and cap thickness models, however, these often yield ambiguous results (Cuffey and Paterson, 2010).

2.2.3.6 Prograding Sedimentary Wedge – Differential Loading

The GBSS region is more affected by unloading mechanisms and there is limited evidence of the significant overpressure variations discussed in section 2.1.3.5.

2.2.3.7 Uplift

As noted in Section 2.2.2.1 the area around the Endurance structure has been subject to various uplift events and glacial erosion. The precise amount of material removed from Mid Jurassic times is uncertain.

2.2.3.8 Diagenesis and Sediment Composition

The Bunter Sandstone is known to contain variable amounts of halite cement which likely provided early support to the rock matrix (Brook et al. 2003), and zones with little cement have very low porosities as little resistance to compaction was offered. Direct evidence of the influence of the cementation processes on *in situ* stress could not be found. However, it could be suggested that early cementation processes have influenced material state (porosity) evolution during burial and may have altered the response of this specific sequence to uplift and erosional events.

2.3 Aramis Structure

2.3.1 Present Understanding of Insitu Stress State

Generally, a normal stress regime is assumed for much of the offshore Netherlands area (SHARP Deliverable 4.1 2022). There does however appear that there is some apparent variability in the magnitude of the horizontal stress relative to the vertical stress. For example, it is noted that in several areas of the Dutch offshore area, such as the Dutch Central Graben and Terschelling Basin leak-off pressures are observed to converge on the lithostatic stress at depth (Verweij et al. 2012), and this behaviour is observed in other areas of the North Sea. Conversely, areas close to Aramis such as the Broad Fourteens Basin and Cleaverbank platform do not show this behaviour. Data in this region is noted to be scattered however which is attributed to facies/lithology dependence.

2.3.2 Regional Structural Geology

2.3.2.1 Dutch Sector, Southern North Sea

The Dutch sector of the North Sea has experienced a particularly complex geological evolution, including multiple phases of rifting, halokinesis and inversion (Maunde and Alves 2022). Folding established during the Varsican orogeny was subsequently deformed by NW-SE trending basement normal faults. Intermittent sedimentation during the Permian included deposition of the target storage sandstones of the Rotliegend formation, which were then overlain by the sealing Zechstein evaporites. Rifting became more significant during the Mesozoic, and during the late Triassic, salt tectonics and diapirism exerted a strong control on structural style (Stewart and Coward 1995; Maunde and Alves 2022).

As with other areas of the North Sea such as the Greater Bunter Sandstone area, significant erosion took place during the Mid Jurassic. The amount of material removed was influenced by tectonic events during the Kimmerian, with additional contributions from halokinesis and thermal upwelling. Further rifting and basin subsidence occurred during the Mid Cretaceous which was followed by inversion and erosion during the Late Cretaceous; dictated by the regional Alpine compression. Further periods of inversion followed during the Cenozoic; the Laramide episode (early Paleocene), the Pyrenean episode (Oligocene) and the Savian episode.

These events are well summarized in Figure 2-7 (Maunde and Alves 2022) which highlights the structural evolution of a region in the Broad Fourteens basin that is in close proximity to the Aramis AOI.

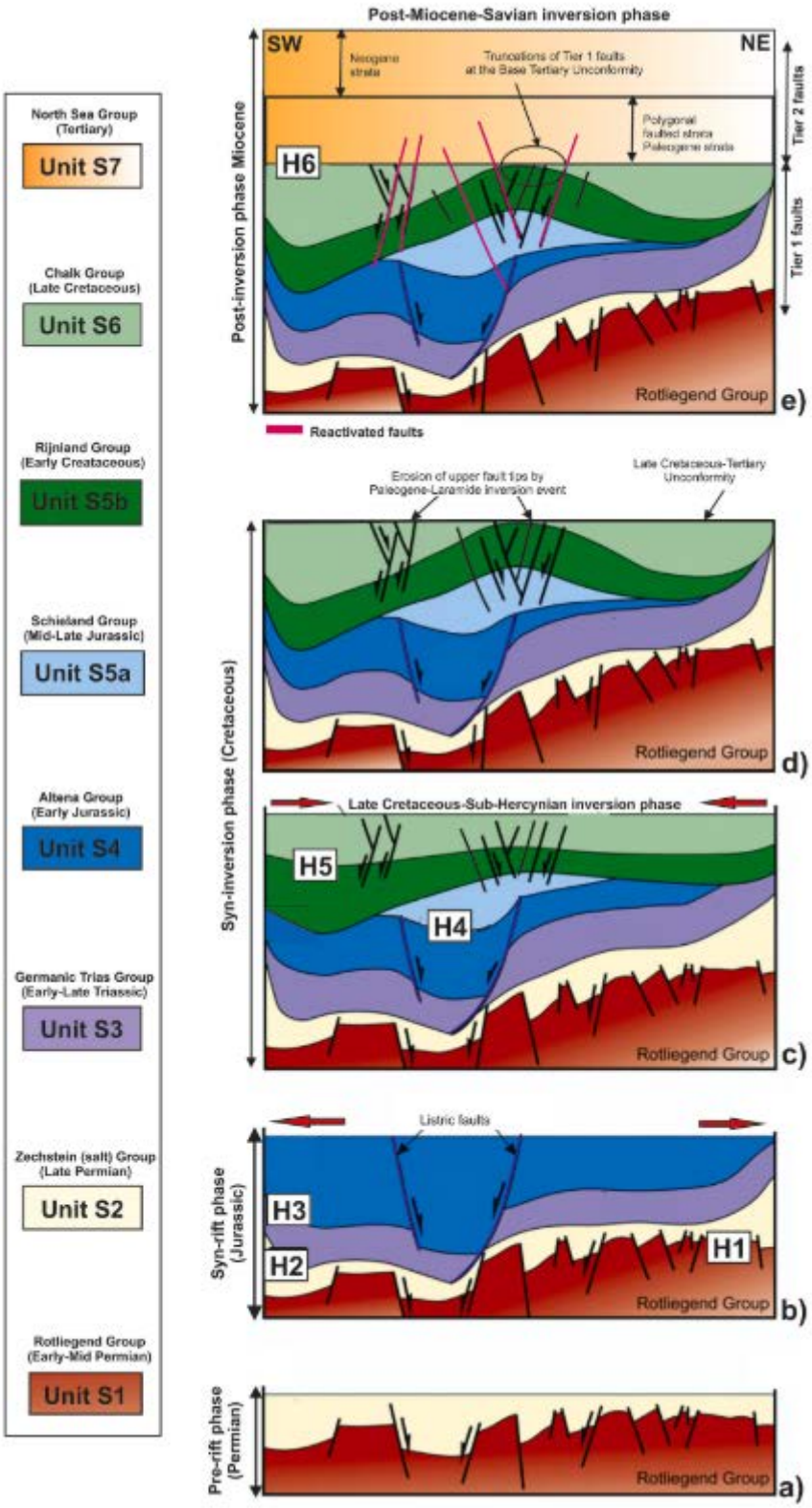

Figure 2-7 *Summary of tectonic history for a region within the Broad Fourteens Basin and close to the Aramis AOI, taken from Maunde and Alves (2022).*

2.3.2.2 Aramis Structure

Much of the previous discussion of regional structural geology relates to the Broad Fourteens basin, as much of the Aramis AOI falls within the northern tip of this basin. However, there is some complexity as the Aramis AOI actually encapsulates elements of not only the Broad Fourteens basin in the south but also the

Texel-Ijsselmeer High to the east, the Dutch Central Graben to the north, and the Cleaverbank platform to the west (Kilic et al. 2022). The AOI is therefore at the intersection of four tectonic areas with distinct structural characteristics and even potential for locally different stress regimes across the AOI. The complicated tectonic history in the AOI in particular has resulted in various trap configurations provided by faulting in the pre-Zechstein units that host the Rotliegend reservoirs. This includes horst blocks, grabens, pop-up structures and fault-dip closures. The faults in the AOI have a variety of orientations owing to the complex history and location. A large population of faults is aligned NW-SE; consistent with the grain established in the basement and the orientation of Cretaceous extensional events. Slightly smaller populations are oriented NE-SW and N-S, plus an additional population towards the Cleaverbank platform that is aligned WNW-ESE.

2.3.3 Stress Generating Mechanisms

2.3.3.1 Ridge Push/Compression

As for other areas of the North Sea, compressive events such as the ridge push effect at the Mid-Atlantic Ridge and the collision between Eurasian and African plates are suggested to be influential in terms of stress conditions in the Dutch sector. Assessment of stress orientation data within the Dutch sector would seem to suggest that this is indeed the case, with the predominant S_{Hmax} direction of NW-SE (~315°) consistent with the orientation of these plate scale processes (Figure 2-8). Based on assessment at the Gronigen field (onshore) the degree of stress anisotropy is inferred to be relatively modest, with SH:Sh ratios of 1.02 to 1.09 reported (Van Eijs 2015); the level of anisotropy offshore, and particularly in complex structural environments like Aramis, is uncertain.

2.3.3.2 Halokinesis

Thick evaporite sequences of the Zechstein group (>1km) were emplaced during the Permian. The Zechstein salt provides the regional seals for many of the Rotliegend reservoirs in the Dutch sector of the North Sea. The presence of salt strongly controls the structure in the post-Zechstein units with a direct influence on the intensity and characteristics of faulting and the amount of material removed via uplift and erosion.

Assessment of stress orientation data indicates over the Dutch sector of the North Sea (Dutch Stress Map) shows a slightly greater degree of variability in the post-salt section relative to the pre-salt section; Figure 2-9. This potentially provides evidence of some local stress reorientations in the shallow section facilitated by the salt, suggesting a degree of decoupling (Mechelse 2017). Analysis of leak-off pressures for the Dutch sector show significantly less variability in both magnitude and scatter in areas where there is no occurrence of Triassic or Zechstein salts e.g. West Netherlands Basin (Verweij et al. 2012).

It is also noteworthy that the presence of salt in the Northern area of the Dutch sector in particular influences fluid migration pathways, and therefore can locally influence overpressuring.

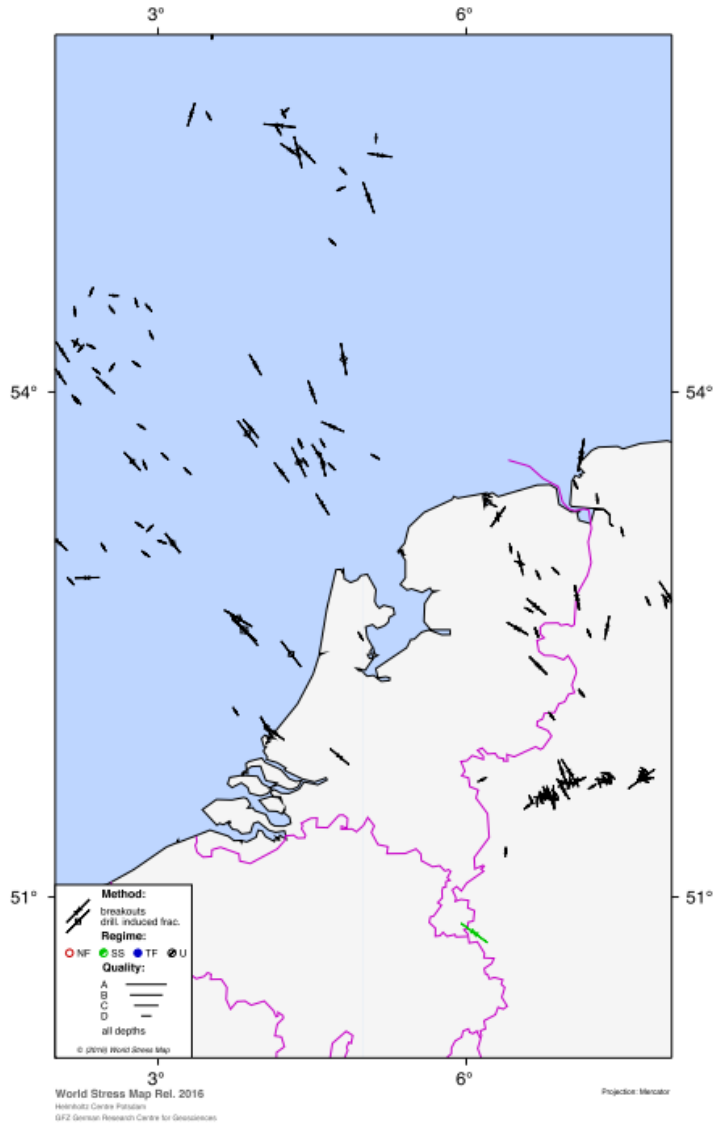

Figure 2-8 *Orientation of maximum horizontal directions for Dutch onshore and offshore areas from the World Stress Map. Note a predominant approximate NW-SE orientation in the offshore area.*

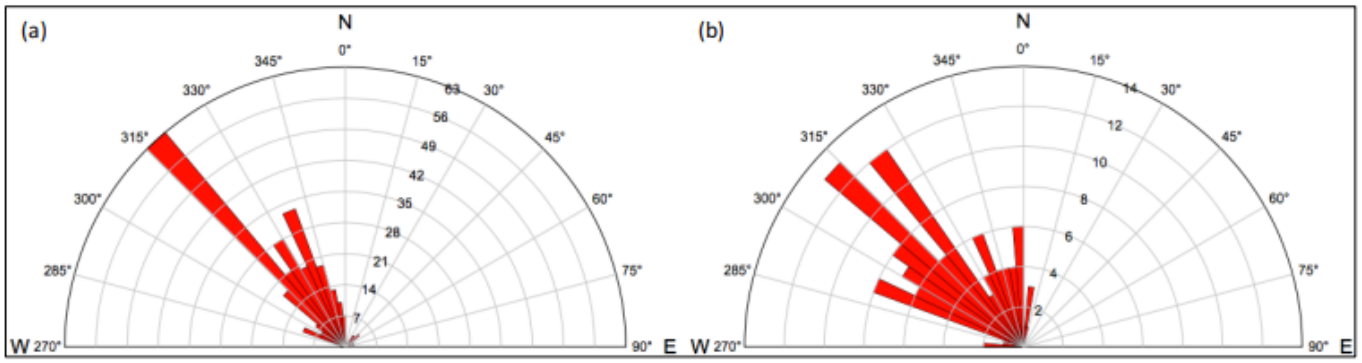

Figure 2-9 *Orientation of maximum horizontal stress in (a) pre-salt and (b) post-salt strata* (Mechelse 2017).

2.3.3.3 Continental Margins

The distance from the Dutch area to the transition between oceanic and continental crust is significant and so as for the other areas previously described the influence on stress is assumed to be minimal.

2.3.3.4 Sediment Loading Rate

Sediment loading rate varies across the Dutch sector and this is suggested to have had a direct influence on overpressure (Verweij et al. 2012), where the higher sedimentation rates (amongst other factors) have led to generally increased overpressures in the Northern area relative to the Southern areas. Here it is suggested that pore pressure converges on the minimum stress, but evidence to suggest that overpressuring drives minimum stress close to the overburden value is weak. It should be noted that the pressure conditions at Aramis are suggested to be normal (SHARP Deliverable 4.1 2022).

2.3.3.5 Deglaciation

A discussion of the influence of glacial processes in the Dutch sector can be found in the SHARP DV1.1a report. To summarise, well documented tunnel valleys incised by Quaternary glacial cycles are ubiquitous to the Danish area, from predominantly three major ice advances (Ehlers, 1990). The depth of the incisional valleys is proportional to bedrock hardness, and induced loading is thought to have facilitated the formation of crestal faults above salt structures (Wenau & Alves 2020). Cyclicity of loading is well constrained, however, ice sheet loading magnitudes and thicknesses remain poorly estimated.

2.3.3.6 Prograding Sedimentary Wedge – Differential Loading

No specific discussion of the influence of prograding sediment wedges in the Dutch sector could be located.

2.3.3.7 Uplift

The discussion of the regional structural history indicated several inversion and uplift events in the Broad Fourteens basin. Uplift during the Mid Jurassic is suggested to have removed up to 1500m of shallow strata. Erosion associated with the Alpine compression in the Late Cretaceous is thought to have removed up to 700m of shallow strata in the centre of the basin (Maunde and Alves 2022).

2.3.3.8 Diagenesis and Sediment Composition

Diagenetic processes relevant to the Aramis reservoir quality include illitization and quartz cementation (Kilic et al. 2022). The degree of diagenetic alteration is dependent on several variables and the extent of alteration changes across the storage area. No specific details regarding the influence of the diagenetic processes on local stress distributions are available. There is evidence of mineralogical/facies controls on the minimum stress in the Dutch sector in general (Verweij et al. 2012).

2.4 Lisa and Nini Structures

2.4.1 Present Understanding of *In Situ* Stress State

The present-day state of stress is known primarily from borehole breakout analyses and earthquake focal mechanisms. A limited amount of leak-off test information has also been recently compiled by GEUS. This data is available to the project but is unpublished.

Break-out data from onshore Danish wells are most relevant for the Lisa and Hantsholm structures and indicate three primary stress domains (Ask et al. 1996). The analyses focused on the Chalk and older succession, so no results from the younger Cenozoic successions are available. The areas south of the Rømø fracture zone, near the Danish-German border, have a dominant NNW-SSE maximum horizontal stress orientation, parallel to the Western European stress province (WESP) defined by Müller et al. (1992). This is a regional stress that originates from the Alpine Orogeny. In the Norwegian-Danish Basin, an ENE-WSW dominant orientation is observed, which is distinctly different from any possible regional plate forces, and is also inconsistent with the orientation expected from glacial rebound in the area. Earthquake focal mechanisms in Skagarrak indicate a dominant NW-SE maximum stress (Sørensen et al. 2011; Heidbach et al. 2018), consistent with model predictions for mid-Atlantic ridge push in this region (Pascal and Gabrielsen 2001). Ask et al., (1996) suggest that the stress is responding to local stress drivers. The wells analysed are clustered near two large salt pillows that could well be influencing the stress field in these wells. Both the Hantsholm and Lisa structures are also located over salt pillows, so likely have a stress state decoupled from the regional stress field as well. The third stress domain is the Sorgernfri-Tornquist zone (STZ), where maximum stresses are oriented sub-parallel to the lineaments and faults within the zone itself, which is suggested to indicate that the fault zone consists of non-sealing faults and open fractures that locally reorient the regional stress (Ask, Müller, and Stephansson 1996). The Lisa structure is within the STZ, so this may be important here as well, though the wells analysed are farther east in the STZ where salt is very thin to absent. Thus, salt may be the most important stress driver at reservoir levels, whereas the presence of the STZ may be important at deeper basement levels.

Breakout data from offshore wells are most relevant for the Nina field. Ask (1997) analysed 26 offshore wells, primarily in the Danish Central Graben, but included one located on the Ringkøbing-Fyn high. These wells show considerable scatter, with standard deviations of ±77°, thus no regional stress trends can be defined within the Central Graben. A majority of breakouts are found in the younger post-Chalk successions and show the largest variation, interpreted to reflect that the shallow stress is decoupled from the deeper regional stress and is responding to local drivers such as differential compaction or fluid expulsion (e.g. Clausen and Korstgård, 1993). Few breakouts are noted in the Chalk Group, but breakouts again appear in the pre-Chalk succession. Of the latter of these, three wells provided a consistent WNW-ESE maximum stress trend, which is interpreted to be from mid-Atlantic Ridge push forces (Ask 1997). There are no published earthquake focal mechanisms in the Danish North Sea.

2.4.2 Regional Structural Geology

The two main areas of interest for the SHARP project include the Lisa and Hanstholm structures just to the north the Danish Jutlandic coast, and the Nini Field in the northwestern part of the Danish North Sea. Although the Lisa structure is the main focus for the SHARP geomechanical modeling, a basic overview of all the Danish areas of interest is included here. The Lisa and Hantsholm structures are located offshore where Skagerrak meets the North Sea (Figure 2-10). Both structures are located near the Fjerritslev Fault

(FF), an east-dipping basement involved structure that forms the southwestern edge of the Sorgenfri-Tornquist zone (STZ). Hantsholm is located west of the FF over the upthrown block, which forms a basement high/horst structure bounded to the west by an unnamed fault. The Lisa structure is located within the Fjerritslev Trough, a depression that resulted from half graben formation along the fault. Because the area is of low interest for hydrocarbon exploration, the area is data poor relative to the SHARP study sites in Norway, the UK, and the Netherlands. Vintage 2D seismic data include a reasonably dense grid in the west but a more open grid to the east. In 1970 the J-1 well was drilled to a depth of 1952 m directly on top of the Lisa Structure, and in 1987 the Felicia-1 well was drilled to a depth of 5281 m in the northeastern corner of the Hantsholm structure. All data along with interpretation of the main horizons are available to the SHARP consortium and have been incorporated into a Petrel project.

The Nini field is located on a salt dome structure approximately 30 km northeast of the Siri Field. The Siri Fairway is a 15–20 km wide erosional depression in the Top Chalk surface stretching for about 150 km from the Stavanger Platform to the Central Graben along the Norwegian and Danish North Sea sector boundary. Initial formation of the Siri Canyon took place in the Early Paleocene and was related to major retrogradational sliding/slumping of the uppermost Chalk due to the uplift of the Scandinavian hinterlands, possibly in response to plate tectonic re-organisation during the opening of the North Atlantic. The depression was subsequently filled up by deep-marine sediments of Paleocene-Eocene age. The sediment fill includes a series of sandstone units deposited from gravity-flows sourced from the Stavanger Platform, which constitute the reservoir rock of the Siri Fairway hydrocarbon fields. The sandstones are interbedded by the pelagic to hemipelagic marlstones, mudstones and diluted turbidites. The shale units and associated sand members belong to the Rogaland, Stronsay and lower part of Westray Group of Late Paleocene to Late Oligocene age (Youngest to oldest: Freja, Dufa, Hefring, Frigg, Kolga, Rind, Idun, Tyr, Bor) (Schiøler et al. 2007). The deposition of the sands may have been guided not only by the geometry of the canyon, but also by the coeval salt tectonic activity in the area. Compositionally, the quarzitic sands are very fine- to fine-grained, well sorted and with a high content of detrital glauconite (15–35 %), giving the sand its characteristic green colour. The sands are massive in appearance with rare primary depositional features. Closer analysis reveals the presence of post-depositional fluidization structures.

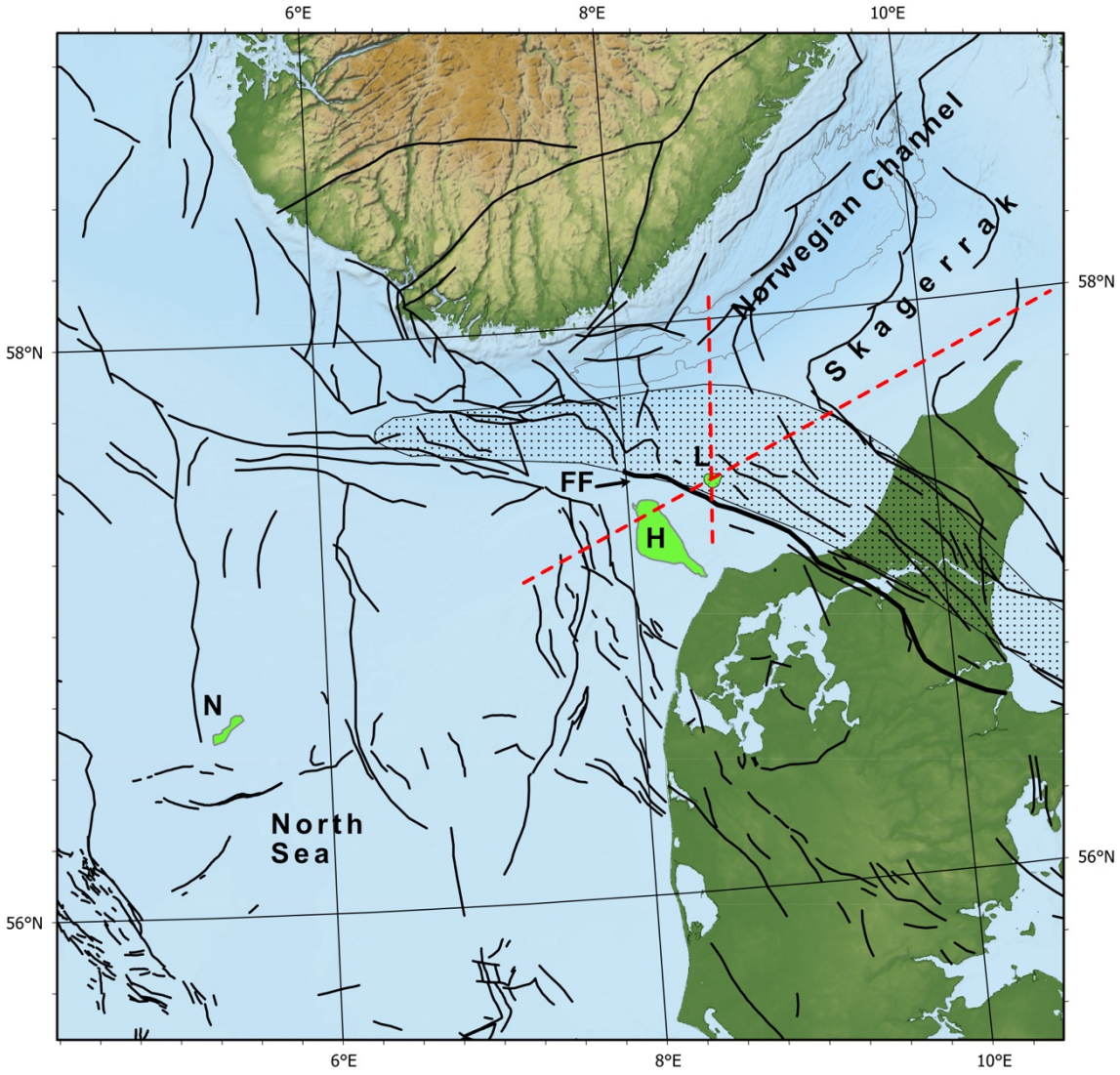

Figure 2-10 *Structural setting of the Danish North Sea and Skagerrak. Faults based on the Southern Permian Basin Atlas (Doornenbal and Stevenson 2010) combined with maps available from the Norwegian Petroleum Directorate and the NAG-TEC Atlas* (Hopper et al. 2014)*. Green polygons: L - Lisa structure; H - Hantsholm structure; N - the Nini field. Shaded region: Sorgenfri-Tornquist Zone. Red dashed lines are locations of geoseimic sections shown in Figure 2-12.*

Basin formation occurred in several phases throughout the Late Paleozoic and into the Cenozoic, including deposition of the Zechstein salt in the Permian and Upper Triassic evaporites within the Oddesund Formation. Zechstein salt thickness in the area is shown in Figure 2-11. The Nini field is located near two salt diapirs (how shallow do they reach?). Thus, the interaction of glacial loading and unloading with salt structures may be quite important to the stress history of this area. In Skagerrak, east of the FF, salt deposits are generally thin, 200 m or less, though locally up to 800 m, and have not mobilized into large diapirs. To the west, salt is very thick and numerous diapirs and large salt pillows have been mapped. Hantsholm is a large anticline over a laterally extensive pillow of Zechstein salt. Salt diapirs are mapped primarily to the west and southwest in the deeper parts of the Danish-Norwegian Basin, with the nearest located about 20 km from the Hantsholm structure. The salt beneath Hantsholm is thick, ranging from 1400-1800 m. The Lisa structure is a small anticline that is likely related to a smaller salt pillow within the Triassic section. The salt is probably a few hundred m thick beneath the structure, but this is difficult to constrain with the existing data. Geoseismic sections of the structures are provided in Figure 2-12.

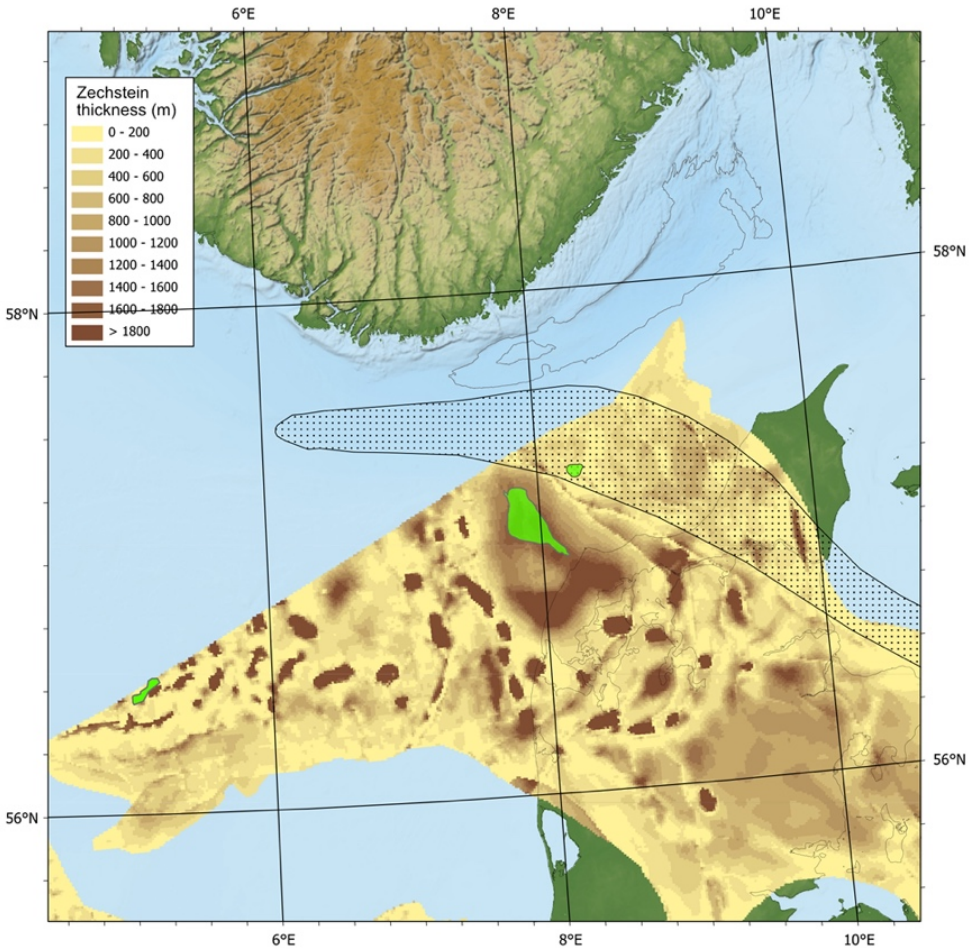

Figure 2-11 *Thickness of the Zechstein salt (from Peryt et al. 2010). Green polygons and shaded area are as in Figure 2-10.*

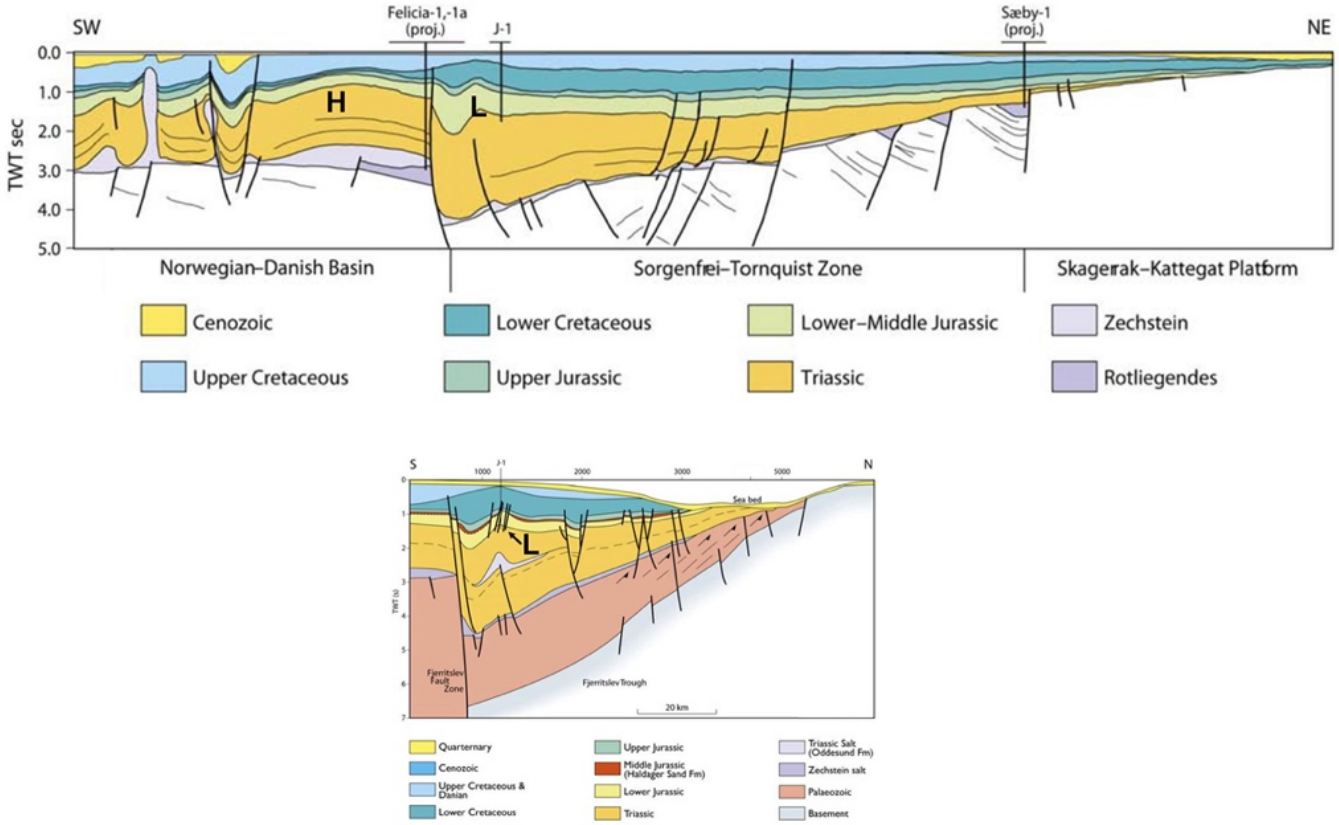

Figure 2-12 *Geoseismic sections through the Hantsholm (H) and Lisa (L) structures (based on Nielsen et al. (2011)). Location of profiles in Figure 2-10.*

2.4.3 Stress Generating Mechanisms

2.4.3.1 Ridge Push

Models predict that the maximum horizontal stress from ridge push in the Danish study areas should be oriented NW-SE (Pascal and Gabrielsen 2001). Earthquake focal mechanisms in Skagerrak near the Lisa and Hantsholm structures have this orientation as do breakouts in several pre-Chalk successions in the Danish Central Graben. Thus, the regional tectonic stress for both study areas is most likely from ridge push. South of the Rømø fracture zone near the Danish-German border, a NNW-SSE maximum horizontal stress is interpreted to be from the Alpine Orogeny. Where the transition from a regional stress in response to ridge push to Alpine compression occurs is uncertain.

2.4.3.2 Halokinesis

As noted above, Zechstein evaporites are found throughout the Danish sector. The Nini Field is located near several salt diapirs, and the Hantsholm structure is located over a large salt pillow. In addition to Zechstein, Triassic salt deposits are found in the Oddesund Formation in the region. The Lisa structure is located over a Triassic salt pillow.

2.4.3.3 Continental Margins

As described earlier for the Norwegian case in the North Sea and Viking Graben, the continental margins are quite distant from the main study area in the Danish sector and are assumed to be insignificant.

2.4.3.4 Sediment Loading Rate

In the Skagerrak near the Hantsholm and Lisa structures, the Cenozoic sediment loading rate is unknown and all post-Chalk sediments were removed by the last glaciation. Only a thin layer of recent sediments exists.

2.4.3.5 Deglaciation

Repeated glacial loading and unloading is likely to be significant throughout the Pleistocene. A more complete discussion of the glacial history relevant to the Danish sector is provided in the accompanying report (SHARP Deliverable 1.1a 2022). Concisely, the Quaternary sedimentary cover in the Danish area is generally very thin (Nielsen et al., 2008), meaning a detailed glacial history over the Lisa and Hantsholm structures is largely based primarily on the regional understanding of Pleistocene glaciations. Glacial deposits are somewhat thicker (<100m) over the Lisa structure, and a network of tunnel valley systems exists around 25km southeast of Hantsholm ((Huuse & Lykke-Andersen, 2000). Thus, it can be inferred that the evolution of such systems must have played an important role in the stress evolution of the area (Sejrup et al., 2003).

2.4.3.6 Prograding Sedimentary Wedge – Differential Loading

The Danish study areas are far from the margins where differential loading from sedimentary wedges that affect the Horda platform are located.

2.4.3.7 Uplift

The Cenozoic development is complicated by Neogene uplift and erosion that removed significant amounts of younger section. Japsen (2002) estimate that up to 1000m of pre-Pliocene sediment was removed prior to major glacial erosion in the Pleistocene and suggest that some form of tectonic uplift must have occurred in the Late Miocene. Present day uplift in northern Denmark due to glacial rebound is still occuring and is on the order of 2–2.5 mm/yr from onshore geodetic stations.

2.4.3.8 Diagenesis and Sediment Composition

In the Lisa and Hantsholm structures, the Upper Triassic to Lower Jurassic Gassum Formation is the primary reservoir for carbon storage and is capped by the Lower Jurassic Fjerritslev Formation, which provides the seal. The Gassum Formation was deposited in a shallow marine to paralic environment and consists of shore-facies sandstones interbedded with fluvial–estuarine sandstones encased in marine, lagoonal, and lacustrine mudstones (Nielsen 2003; Weibel et al., 2020). The maximum burial depths prior to Neogene exhumation are estimated at 1.4–3.8 km (Japsen et al. 2007). A detailed description of the diagenesis of the Gassum Formation is published in Weibel et al. (2017) and Weibel et al. (2020) and is briefly summarized here. The sandstones are fine- to medium-grained and dominated by quartz grains, with varying amounts of K-feldspar and albite. The matrix grains also include minor amounts of mica, clays, and rock fragments from plutonic, metamorphic, and sedimentary rocks. The authigenic phases include calcite and siderite in the shallowly buried rocks, but other carbonates, esp. anerkite, dominate in the deeply buried parts of the Gassum Formation. Additional authigenic phases comprise clay minerals (e.g. kaolinite, illite), besides albite and quartz cement in the deepest buried parts of the Gassum Formation. The cements make up an average of 2-22% of the rock volume in the wells studied. A summary diagram is shown in Figure 2-13.

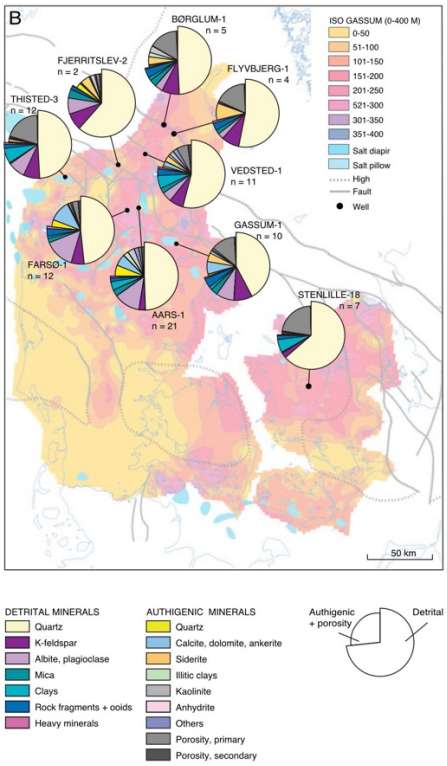

Figure 2-13 *Pie diagram showing the abundances of detrital and cement components of the Gassum Formation for a number of wells in Denmark (from Weibel et al. (2020))*

The Fjerritslev Formation is an Early Jurassic succession of marine claystones wtih laminae of silt and sandstone (Weibel et al., 2014, Nielsen, 2003). The onshore Stenlille-1 well, is dominated by quartz (30%), with less abundant amounts of illite/muscovite (25%), kaolinite (18%), and siderite (12%). Only minor amounts (< 3%) of calcite, chlorite, dolomite, and K-feldspar are found. While no diagenetic specific studies have been carried out, some information is available in a recent GEUS report by Springer et al. (2020). The formation is dominated by kaolinite, and in some intervals illite and smectite, while the non-clay part is quartz dominated. The diagenetic minerals include pyrite, calcite, and siderite. Few good quality samples and cores exist, but available analyses yield 11% average porosity, 160 µD air permeability, and mercury injection entry pressures from 60–110 bar (Springer et al. 2020). However, these may be unreliable due to the dry conditions. *In situ* analyses near Stenlille in Denmark had liquid brine permiabilities of 3nD, and other overburden measurements gave 200 nD.

2.5 Summary of Stress Drivers

Considering the assessment of stress drivers described in the preceding sections and the interpretation offered in DV1.1a (SHARP Deliverable 1.1a 2022) a “Stress Drivers Matrix” has been constructed and is shown in Table 2-1. The purpose of this matrix is to provide a summary of the mechanisms that may contribute to the present state of stress across the storage sites, and leverage this to better define the scope of the geomechanical models. Some key observations can be made:

- Faults have not been included in the preceding sections as they are considered to be an *expression of imposed deformation arising from given stress driver(s)* e.g. rifting, compression, salt tectonics. However, there is evidence that they locally modify stress magnitudes and orientations in the North Sea e.g. Yale (2003) and so have been included in the matrix simply for completeness. A high degree of structural complexity has been noted at Aramis and the Horda Platform case exploits fault-related traps. Salt related crestal and/or radial faults are noted at Endurance and Nini.
- All sites have experienced phases of unloading via uplift and exhumation and/or deglaciation and this may have a strong influence on the present stress condition. Similarly, all sites have undergone regional compression due to ridge push or orogenic events. These are therefore mechanisms that should be accorded specific consideration during planning and execution of geomechanical modelling tasks.
- Besides the Horda Platform area all sites have been strongly influenced by salt, and many of the storage sites take advantage of structural traps formed during halokinesis. As noted in the text, stress reorientation in sediments adjacent to salt is well documented and there is evidence to suggest it can facilitate decoupling of stress regimes in pre- and post-salt strata. Modelling to better understand the significance of salt on stress conditions around storage sites should be considered.
- Observations at the Horda Platform and surrounding area suggest mineralogical and diagenetic influence on stress which is supported by experimentation in the mechanical compaction regime; see section 4.1.2.3. There is some evidence of mineralogy influence from stress measurements at other sites such as Endurance (refer to Williams et al. (2022)). Whilst the evidence is not as strong this aspect is inherently incorporated into the modelling through future material characterization tasks.
- Across the sites weaker evidence was found for stress changes via overpressure and progradational loading.

Overall, the matrix provides a useful tool for understanding some of the mechanisms that need to be included in the geomechanical models and an additional column provides an assessment of whether the mechanisms can be assessed in 1D, 2D or fully 3D geomechanical models. More importantly, the matrix offers some insight into which mechanisms are regionally most significant and need to be considered during site characterisation.

The matrix could also be applied in other basins, where it is quite likely that the more significant mechanisms will be different. For example, whilst limited evidence for the influence of progradational loading was found in the North Sea, it is suggested that the geometry of prograding clastic sedimentary wedges is very significant in controlling maximum horizontal stress orientations in the Gulf of Mexico (Yassir and Zerwer 1997). The matrix can therefore be expanded and adapted for application in other basins targeted for carbon storage.

Stress Driver/Mechanism	North Sea CCUS Stores (Country)					Suggested required model type	Comments
	Endurance/GBS (UK)	Horda Platform (NO)	Aramis Structure (NL)	Lisa (DK)	Nini (DK)		
Halokinesis (salt tectonics)						2D/3D	With the exception of the Horda area, all stores are influenced by the presence of salt structures e.g. pillows, diapirs. Salt can provide regional seals and heavily influence structural configuration/trapping at the stores. It is highly probable that stresses will be locally influenced by the viscoplastic nature of salt over extended timeframes. How salt has reacted to (relatively) instantaneous loading such as glactiotectonics, and moreover how this has adjusted local stress distributions is important.
Overpressure/sedimentation rate						1D	Within the Norwegian sector there is evidence of progressively increasing horizontal stress that is likely linked to deep overpressuring that is likely related to burial diagenesis.
Diagenesis & sediment composition						1D	There are inferred direct links between diagenesis and stress at the Horda Platform and surrounding areas within the Norwegian sector. These links can be via diagenetically-sourced overpressuring in deep sediments, or due to the influence of diagenesis on fundamental rock properties which modify the response during erosion/deglaciation (this is supported via experimental evidence, see commentary in Sections 3 and 4). Whilst direct links between diagenesis and stress were not observed at other sites, evidence of diagenesis in some of the key sequences was noted. It seems likely that these processes will have had some influence on mechanical properties and by extension stress state.
Progradational loading						2D	Overall this mechanism does not seem to be especially significant for the studied sites in the North Sea basins.
Regional compression/ridge push						2D/3D	There is strong evidence to suggest that regional compression from either Mid-Atlantic ridge push or Alpine orogeny are significant contributors to in situ stress within the North Sea. The degree of horizontal stress anisotropy and orientation of the stresses may be strongly influenced by proximity to these events.
Glaciotectonics & flexural isotasy						2D	As discussed in DV1.1a all sites will have been influenced by recent glaciation and this will have had an influence on stress distributions, particularly in the shallow section.
Influence of faults and stress rotations						3D	High degree of complexity noted for the Aramis site, with intensity and direction of faults differing across the area. Presence of salt-related faults at Endurance.
Uplift & erosion						1D	All sites have experienced erosional/uplift events either associated with tilting or glacial processes.

KEY

- Direct, strong evidence for contribution to in situ stress
- Inferred or weaker evidence of contribution to in situ stress
- No evidence for contribution to in situ stress

Table 2-1 *Stress drivers matrix. Matrix is coloured according to relative significance of the process at each site.*

3 Modelling Framework

This section provides a brief overview of the main components of the numerical modelling tools that will be used for developing the geomechanical forward models described in Section 4. The modelling framework is very briefly introduced before a more comprehensive discussion on the available constitutive laws.

3.1 Computational Framework

The modelling tool that will be used to conduct forward geomechanical models is Elfen. A complete description of the modelling framework is beyond the scope of this document but can be found elsewhere (Peric and Crook 2004; Rance et al. 2013; Thornton and Crook 2013). The key elements of the modelling framework are as follows:

- Hybrid finite/discrete element formulation with a Lagrangian description of kinematics.
- Treatment of large strains typically encountered during formation of geological structures by using robust and automated adaptive remeshing techniques.
- Coupled Thermal-Hydro-Mechanical-Chemical (THMC) modelling capability.
- Explicit and implicit solvers.

Collectively, these elements are useful for geomechanical forward modelling as large strains and topology changes can be accommodated and the evolving material state is captured directly. Furthermore, an explicit solver is helpful for problems involving large plastic deformations as it avoids some numerical issues associated with implicit solution strategies e.g. consistent linearization and convergence; this is particularly important for problems with contacting interfaces. Some drawbacks associated with this methodology can involve the requirement for very small timesteps to comply with stability criteria, though mass scaling approaches can alleviate this to an extent.

With respect to simulation over geological timeframes specific tools are in place to treat some of the key stress driver mechanisms discussed in section 2:

- Sedimentation algorithms to specify the rate and type (aggradational, morphed, draped) of deposited sedimentary layers.
- Removal of material to explore stress relaxation due to uplift and erosion.
- Lateral compressive/extensional boundary loading (displacement, face loading) to replicate ridge push.
- Basement/basal loading, which may include specific mapping from an initial to a final profile (to explicitly represent uplift) or represent flexural isostasy.

3.2 Constitutive Laws

Some of the listed stress drivers arise because of the nature of the material and particularly the mechanical response. Assessing the significance of these processes via modelling will require suitable constitutive laws that describe how deformation (strains) is expressed in response to loading (stress). The requirements for constitutive modelling vary depending on the application and modelling objectives. Simpler models may assume a simple, linear elastic representation which requires only a small number of parameters. These models have the limitation that they do not incorporate any concept of a failure surface, and as such may inaccurately predict subsurface stress distributions. Furthermore, they will recover their initial state on unloading which is not typical of rocks. Plasticity models can be incorporated which represent rock failure,

but these typically have the drawbacks of more constitutive parameters and additional computational resource requirements. Fundamentally, forward geomechanical modelling aims to capture the onset and evolution of rock failure and its influence on stress, pore pressure, porosity/permeability due to various geological processes. *As such elasto-plastic models are typically required and the ability to capture responses along multiple, arbitrary stress paths is highly advantageous*. The following sections outline recommended constitutive modelling options for forward geomechanical modelling of various lithologies and outline potential data sources to aid the characterization process.

3.2.1 Clastics and Carbonates

3.2.1.1 Mechanical Deformation

At temperatures below approximately 70°C rock deformation is largely in response to increasing burial stresses (compaction) but there may exist additional contributions from local dilation due to shearing, faulting, fracturing etc. A critical-state-based failure model would be an obvious selection as this provides a unified framework for considering volumetric changes (compaction, dilation) and strength (Muir-Wood 1990). This offers greater flexibility relative to conventional models like Mohr-Coulomb or Drucker-Prager that typically can only treat shear failure. Two models based on the critical-state framework that would be suitable for application in the geomechanical modelling tasks are described in the following sections. The failure surface for these models, which represents the transition between elastic (recoverable) and plastic (irrecoverable) deformations, is presented using two stress invariants; the von Mises stress, q, and the effective mean stress, p'. These may be written as functions of principal stresses as shown below.

$$q = \sqrt{\frac{1}{2}((\sigma_1' - \sigma_3')^2 + (\sigma_2' - \sigma_3')^2 + (\sigma_1' - \sigma_2')^2)} \quad \textbf{(1)}$$

$$p' = \frac{(\sigma_1' + \sigma_2' + \sigma_3')}{3} \quad \textbf{(2)}$$

3.2.1.1.1 Elastic Deformations – Nonlinear Laws

Several elasticity laws can be applied with different levels of sophistication. Incorporating a suitable description of the elastic response is important generally, but particularly so when exploring how stresses evolve during unloading.

The simplest models assume linear elasticity and only require specification of Young's Modulus, E, and Poisson's ratio, ν. For many soft rocks it is typical to observe a dependence of the elastic moduli on porosity (ϕ) and confining stress (p'). Capturing such influence is particularly important for modelling over geological time where significant changes in material state and stress magnitude are anticipated. Several nonlinear elasticity models incorporating such features are available and are presented in Table 3-1. A constant Poisson's ratio is assumed for the Cam Clay models. The empirical model additionally offers the possibility to incorporate a stress-dependent Poisson's ratio which will influence the distribution of stress in the unloaded directions.

Model	Expression	Material Parameters	
(a) Cam Clay	$E = 3K(1-2\nu)$ with $K = K_o + \frac{1}{\kappa}\left(\frac{1}{1-\phi}\right)p'$	E – Young's modulus ν – Poisson's ratio K – Bulk modulus K_o – Bulk modulus at 0 confinement κ – slope of URL (see Figure 3-2)	***(3)***
(b) Cam Clay Variation*	$E = 3K(1-2\nu)$ with $K = K_o + \frac{1}{\kappa}\left(\frac{1}{1-\phi}\right)[(1-A_{un})p_c' + A_{un}p']$	E – Young's modulus ν – Poisson's ratio K – Bulk modulus K_o – Bulk modulus at 0 confinement κ – slope of URL (see Figure 3-2) A_{un} – lithification weighting factor p_c' - preconsolidation pressure	***(4)***
(c) Empirical Law	$E = E_{ref}\left(\frac{p'+A}{B}\right)^n \phi^c$	E – Young's modulus ϕ – Porosity E_{ref} – Reference Young's modulus (at low stress) A, B, n, c – Material constants	***(5)***

Table 3-1 *Nonlinear elasticity models *This variation is used for models incorporating chemical compaction processes by additionally weighting stiffness by the current preconsolidation pressure. With* $\boldsymbol{A_{un}}$*=1 the model recovers the conventional Cam Clay law.*

3.2.1.1.2 Plastic Deformations – Modified Cam Clay (MCC)

Modified Cam Clay (MCC) forms part of a class of constitutive models based on critical-state soil mechanics (Schofield and Wroth 1968). Whilst originally developed for soils these models can be applied to more consolidated, stronger rocks but sometimes suffer from several drawbacks such as a restrictive definition of the failure surface (Figure 3-1(a)) and the assumption of associated plastic flow (Muir-Wood 1990). A result of such constraints is a tendency to incorrectly predict the onset of yield/failure and produce an inaccurate prediction of the ratio of effective horizontal to effective vertical stresses during burial under zero-lateral strain boundary conditions. As this condition is thought to generally be representative of many passively subsiding sedimentary basins it seems prudent to apply a more robust model.

3.2.1.1.3 Plastic Deformations – Soft Rock 3 (SR3)

A proprietary soft rock model is recommended that has been extensively used for geomechanical modelling (Crook et al. 2006). This model, denoted Soft Rock 3 (SR3), is an MCC variant that overcomes the limitations associated with the original model by:

- Permitting inclusion of alternative non-linear elasticity laws.
- Replacing the failure surface in MCC with a smooth and continuous three-invariant failure surface that can be fitted more easily to experimental data. The surface includes a correction function in the deviatoric plane that adjusts strength along specific load paths. This can capture lower peak strengths in triaxial extension (RTE) relative to compression (CTC) for instance. See (Crook et al. 2006) for more detail.
- Correcting the failure surface profile to account for variable strength along different load paths.
- Assuming that plastic flow is non-associated.

The functions of the failure surface for both models are given in Table 3-2 and are visualized in q – p' space in Figure 3-1.

Model	Failure Function	Material Parameters	
(a) MCC	$F = q - M^2[p'(p'_c - p')]$	M – Gradient of critical state line p'_c – Preconsolidation pressure	***(6)***
(b) SR3	$\Psi = g(\theta, p')q + (p' - p'_t)tan\beta \left(\frac{p' - p'_c}{p'_t - p'_c}\right)^{1/n}$	p'_c – Preconsolidation pressure p'_t – Tensile intercept β – Friction parameter n – Material exponent $g(\theta, p')$ – Correction term in deviatoric plane	***(7)***

Table 3-2 *Functions of failure surfaces for MCC and SR3 constitutive laws.*

(a) Modified Cam Clay (MCC)	*(b) Soft Rock 3 (SR3)*
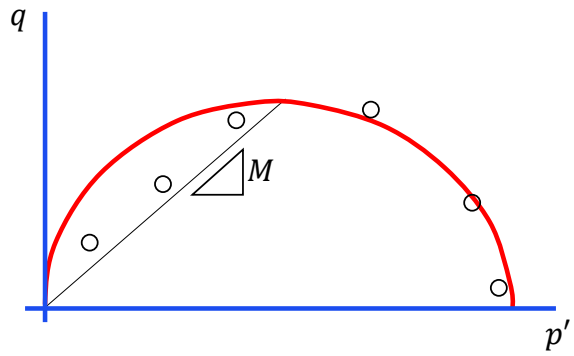	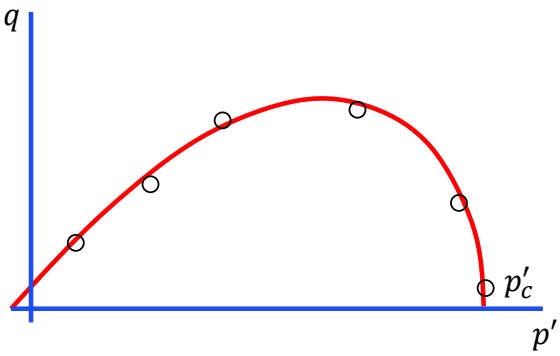

Figure 3-1 *Visualization of failure surfaces in deviatoric (q) versus effective mean stress (p') space for critical state material models. Demonstrative peak strengths from triaxial tests are shown to illustrate difficulties in fitting the MCC failure surface.*

Whilst the SR3 model has been developed specifically for poorly-consolidated and/or weakly cemented sandstones it has been generalized for applications to shales (Crook, Yu, and Willson 2002) and chalks (Crook et al. 2008). It is possible to achieve similar results with both MCC and SR3 models (Fokker 2012) however, it is emphasized that the SR3 model generally offers greater flexibility and accuracy.

A further requirement for elasto-plastic models is a means of describing how the strength of the material changes during plastic deformation, commonly referred to as a *hardening law*. Both MCC and SR3 material models incorporate hardening (compaction) and softening (dilation) by relating a measure of volume change (specific volume, v) to the effective mean stress, p'; Figure 3-2. The figure shows the initial stiffer response during elastic deformation prior to reaching the failure surface marked by the preconsolidation pressure, $p'_{c,0}$. Following this, the material yields/fails and accelerated porosity reduction is observed.

This data can be constrained by experimental testing (hydrostatic compression tests, uniaxial strain/oedometer test) or calibrated to porosity-depth data sets. The input format may be piecewise-linear or with direct input of constants defining the slope of the unloading-reloading line (url), κ, and the slope of the isotropic normal compression line (ncl), λ (see Figure 3-2).

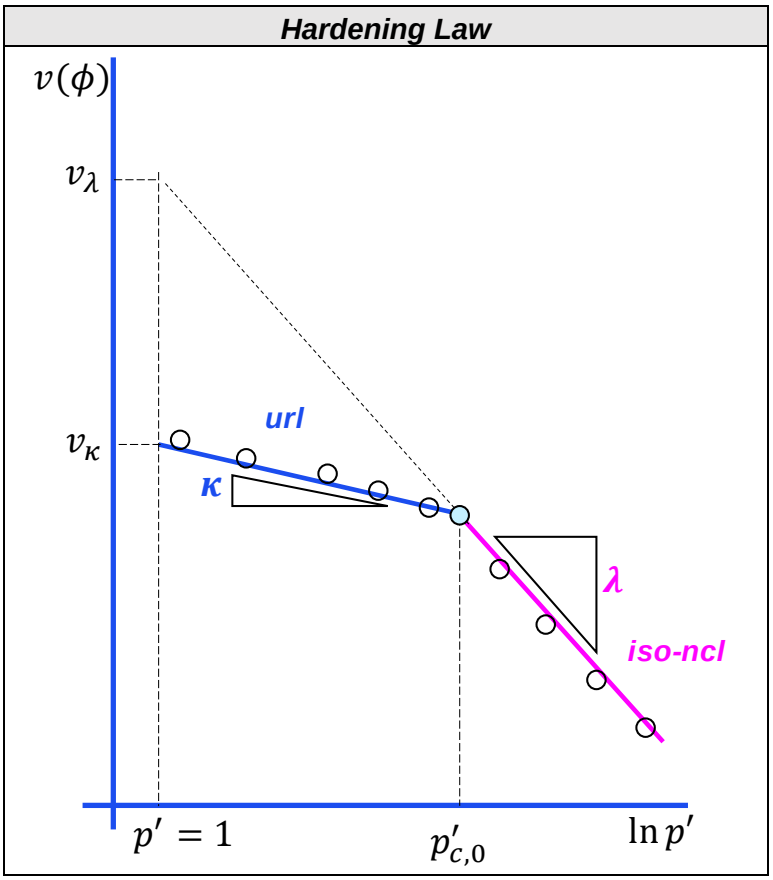

Figure 3-2 *Treatment of hardening for MCC and SR3 material models.*

3.2.1.2 Incorporating Chemical Compaction (Diagenesis)

Beyond ~2-3km depth or where temperatures exceed around 70°C chemical processes start to become more significant, and consideration of mechanical processes only is insufficient to describe porosity changes (Day-Stirrat, McDonnell, and Wood 2010). The nature of the diagenetic process depends on various factors (mineralogy, pore fluid chemistry, temperature) and several reactions may take place during burial. Whilst it is acknowledged that diagenesis becomes important at greater depths it should be noted that shallow processes such as carbonate cementation in mudstones or dolomitization in carbonates fundamentally modify how these sediments respond to further burial or tectonic loading; a stiffer and more brittle response is typical. Significant deeper reactions include the smectite-illite transformation and quartz cementation, both of which are significant generally for temperatures above 70°C.

The influence of diagenetic processes on sediment fabric is complex and detailed studies are not common; see Bjorlykke and Hoeg (1997); Croizé et al., (2010) for examples. An important study on the influence of diagenesis on the hydro-mechanical properties of argillaceous sediments was undertaken by Nygård et al., (2004). In this study the mechanical behaviour of the Kimmeridge Bay Clay (KBC) and Kimmeridge Westbury Clays (KWC) is investigated. Whilst the two clays are thought to have essentially the same origin, they have experienced very different burial histories; KWC has had a maximum burial depth of around 500m with present porosity around 50%, and KBC has been buried to over 1.7km with porosity of 22% and notable cementation. The consolidation characteristics are shown in Figure 3-3(a) and highlight a much stiffer response for the altered KBC relative to KWC that is attributed to cementation. Note that for KWC to attain the same initial porosity as KBC it would need to be compacted to approximately 200MPa effective vertical stress. Additionally, the implied consolidation coefficient is quite different, with a significantly stiffer response observed for the altered KBC sample. The samples are tested in a modified triaxial setup with confining

pressures monitored to enforce zero lateral strain conditions, and as such the ratio of horizontal to vertical effective stresses (K_0) during burial can be understood. Note that the effect of diagenetically induced pseudo-overconsolidation results in a reduced K_0 at low stress levels.

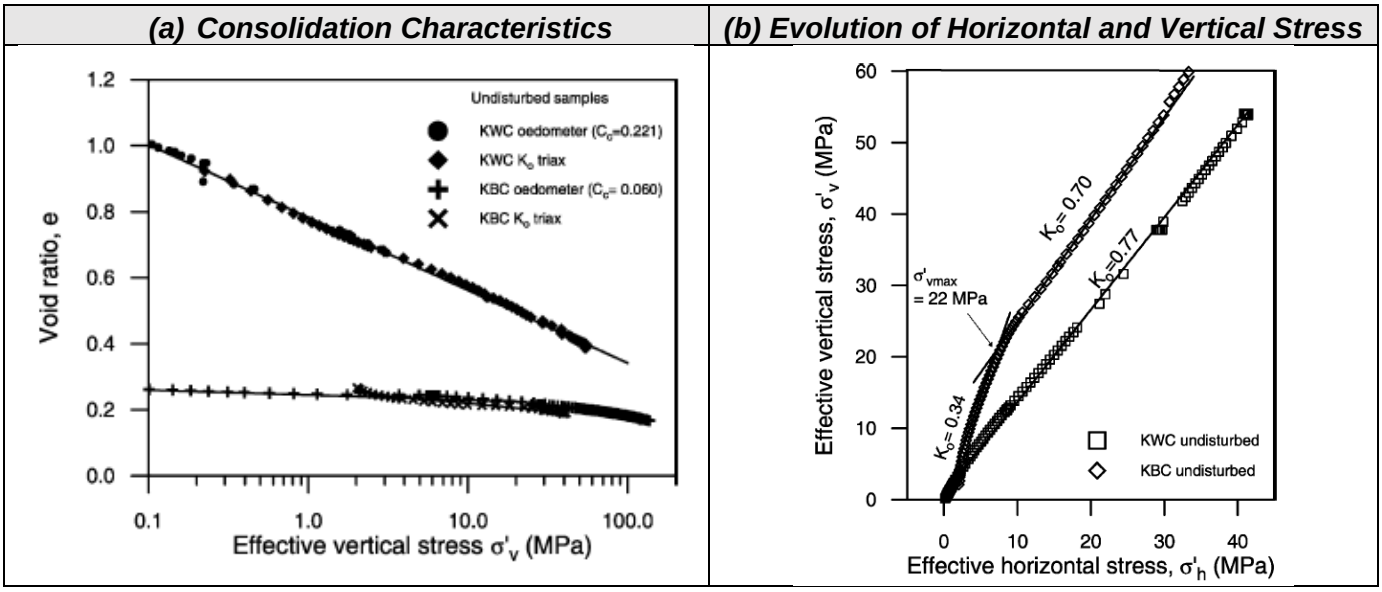

Figure 3-3 *Consolidation characteristics and stress ratios for Kimmeridge Westbury Clay (KWC) and Kimmeridge Bay Clay (KBC).*

From a modelling perspective, representing dissolution/precipitation mechanisms directly is not possible, as these processes operate at a scale much smaller than the resolution of typical field/regional scale geomechanical models. Instead, the macro-scale influence of these processes can be incorporated via their direct effect on porosity. Diagenetic processes may be coupled to the critical state framework by assuming that the current material state (porosity) is a function of both mechanical and chemical changes to porosity. Similar approaches have been applied by others (Obradors-Prats et al. 2019). It is assumed that the current porosity (ϕ) reflects a combination of the depositional porosity (ϕ_0), mechanically sourced porosity changes ($d\phi_m$), and chemically sourced porosity changes $d\phi_c$ as follows;

$$\phi = \phi_0 - d\phi_m - d\phi_c. \qquad \textbf{(8)}$$

The mechanical porosity change will reflect volumetric straining, both elastic and plastic, which is treated via the previously described SR3 constitutive model. The chemical porosity change may be determined using various laws which are described below and shown in Table 3-3.

- ***Wangen Model***: This model was developed for Quartz cementation in sandstones (Wangen 2000) and assumes that cementation is locally sourced (no transport required). The model assumes a simple Arrhenius law to represent the change of porosity due to chemical processes and an equivalent chemical viscoplastic strain rate may be derived from this (Table 3-3a).
- ***Empirical Law***: This is a simplified model that aims to incorporate the key impacts of chemical compaction with minimal required data (Roberts et al. 2014). To determine the chemical porosity change and associated strain rate, the law simply requires an initiation temperature, an upper bound temperature and reference duration that collectively control the reaction rate, together with a maximum allowable porosity change.

A comparison of the two models is also presented in Figure 3-4 where it is shown that it is possible to achieve similar trends of porosity reduction with depth for both models.

Model	Chemical Porosity Change and Strain Rate	Material Parameters	
(a) Wangen Model	$\frac{d\phi_c}{dt} = -k_f(T)S(\phi)v_q c$ $\dot{\varepsilon}_v^c = \frac{1}{(1-\phi)}\frac{d\phi_c}{dt}$	ϕ_c – Chemical porosity change $k_f(T)$ – Arrhenius function controlling rate of reaction $S(\phi)$ – function for defining evolving specific surface coating of gains with porosity v_q – the molar volume of cement c – the degree of supersaturation for cement species.	***(9)***
(b) Empirical Model	$\phi_c^{t+\Delta t} = \phi_c^{max}\left(\frac{T-T_{low}}{T_{upp}-T_{low}}\right)\left(\frac{t_c^{dur}}{t_c^{ref}}\right)$ $\dot{\varepsilon}_v^c = -\ln\left[\frac{1-\phi^{t+\Delta t}}{1-\phi^{t+\Delta t}+(\phi_c^{t+\Delta t}-\phi_c^t)}\right]$	$\phi_c^{t+\Delta t}, \phi_c^t$ – chemical porosity change evaluated at current and previous timesteps respectively T – current temperature T_{upp}, T_{low} – upper and lower (activation) temperatures for reaction t_c^{dur}, t_c^{ref} – current (since activation) and reference durations for the reaction ϕ_c^{max} – max allowable porosity change due to chemical compaction	***(10)***

Table 3-3 *Available chemical compaction models.*

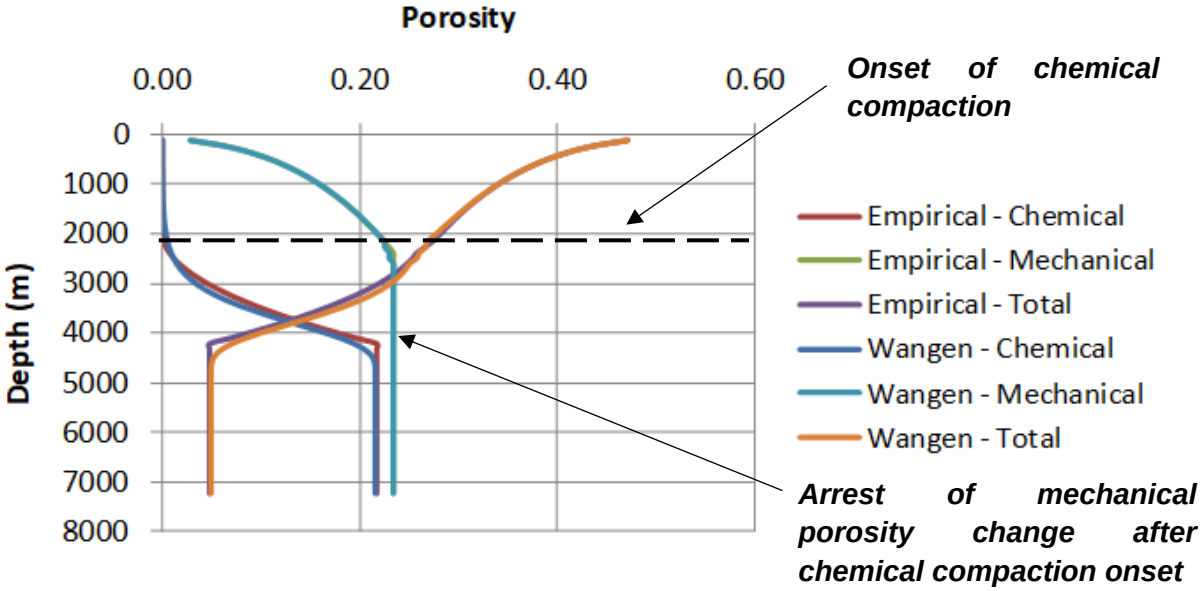

Figure 3-4 *Demonstration of chemical compaction models in a simple deposition scenario. Comparison of the Wangen and empirical models is shown.* `

For each timestep a sequential process is followed whereby the mechanical deformation and associated elastoplastic stress update is considered first. This is illustrated in Figure 3-5(a) where the size of the failure surface becomes progressively larger in response to increasing burial stress. Chemical compaction is then

considered in a subsequent stress update, Figure 3-5(b). As chemical compaction is modifying porosity the following effects arise naturally that are consistent with observations made earlier in this section:

1. Increase in stiffness associated with cementation is captured via the nonlinear elasticity laws described in section 3.2.1.1.1.
2. The chemically-sourced porosity change means that the size of the failure surface, and hence strength, is increased; Figure 3-5(b). The implication here is that as chemical compaction becomes more significant the size of the failure surface grows (pseudo-overconsolidation) and the mechanical porosity reduction will gradually become less significant (mechanical stress changes remain elastic). The piecewise-linear input of hardening also allows for differing consolidation characteristics before and after diagenesis. The implications of this are shown in Figure 3-4 where it is seen that mechanical porosity change is arrested after the onset of chemical compaction.
3. Reduction in permeability via application of appropriate porosity-permeability relationships e.g. Kozeny-Carman, Yang & Aplin. This will contribute to reduced permeability and allow for diagenetically sourced pore pressure increase (Nordgård Bolås et al. 2008). Note that the rate of pore space reduction implied by the chemical volume strain also is significant in terms of excess pore pressure generation.

It is noteworthy that experimental testing by Nygård et al., (2004) indicates that a single porosity-permeability relationship is not appropriate for representing both altered and unaltered specimens, principally due to smaller pore throats in the altered samples. As such some additional functionality could be incorporated to represent an evolving relationship between porosity and permeability as the reaction progresses. Further extensions to the material model could be incorporated to allow for the development of anisotropy due to fabric changes, which may be important in replicating the response of altered mudstones during unloading.

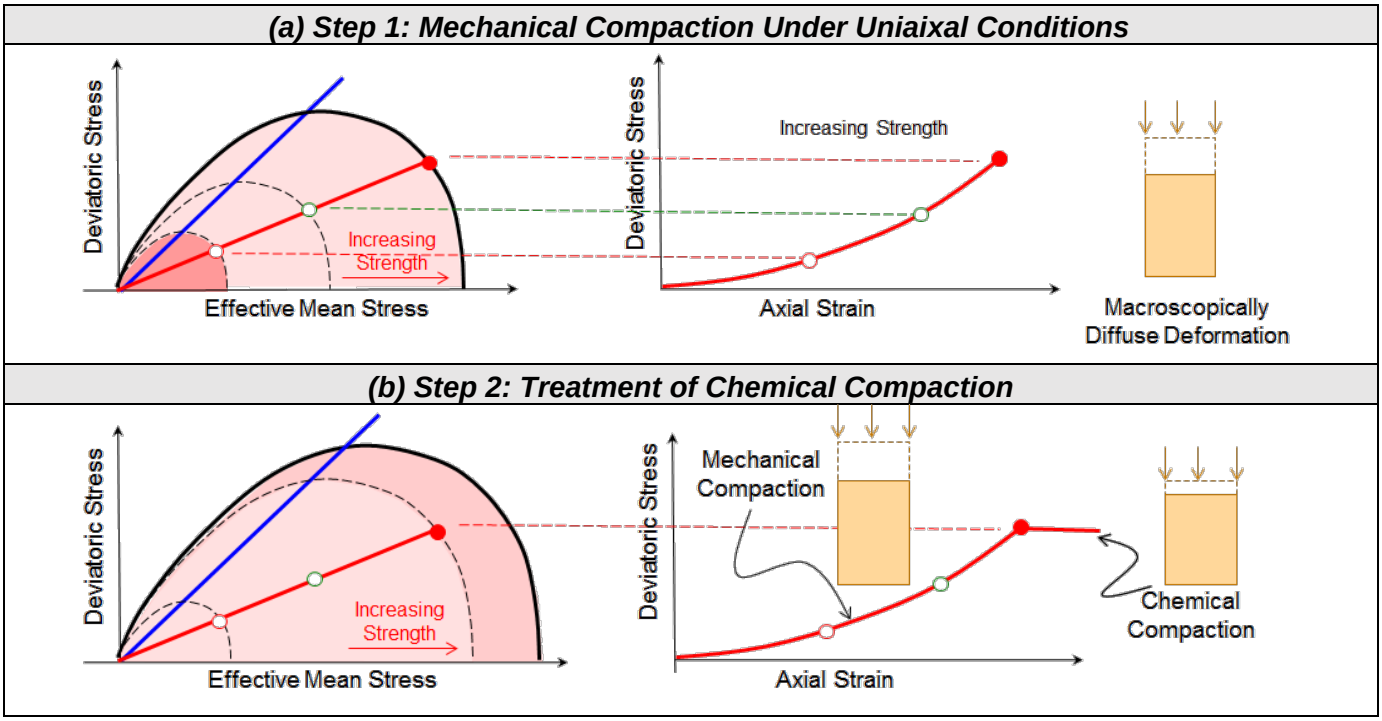

Figure 3-5 *Incorporating the influence of chemical compaction processes and influence on strain and material state.*

3.2.1.3 Data Availability

Libraries of sandstone, shale and carbonate characterisations based on open-source data sets are available to use in the absence of other data. A useful data set for consolidation characteristics and evolving lateral stress ratio has been identified in publications by NGI which are described in Section 4.1.2. It is not anticipated that any specific data will be offered with which to constrain chemical compaction properties and the influence of these processes on stress and pore pressure will likely be explored more conceptually, complimented by constraint from literature where available and field observations. This is discussed further in section 4.1.2.

3.2.2 Evaporites (Salt)

As discussed in section 2, evaporite sequences exert a strong influence on local stress states and structure across most of the storage sites. Salt modifies stresses in adjacent sedimentary sequences through its inability sustain to deviatoric stresses; non-hydrostatic stresses are resolved through various creep processes which are sensitive to temperature (Willson, Fossum, and Fredrich 2002; Fredrich, Fossum, and Hickman 2007). From a constitutive modelling perspective several laws are available which are described in the following sections.

3.2.2.1 Newtonian/Non-Newtonian Rheology

The simplest representation of salt would be to assume a Newtonian rheology for the salt. This approach is validated by acknowledging that over geological time salt behaves in a manner akin to a viscous fluid. A Newtonian flow law is characterized by a single constitutive parameter, the viscosity, which represents the proportionality between applied shear stress and shear strain rate. Whilst the assumption of a Newtonian rheology is fairly common in salt tectonics modelling over geological timeframes (Gradmann, Beaumont, and Albertz 2009; Chemia, Koyi, and Schmeling 2008; Fuchs, Schmeling, and Koyi 2011), it is widely acknowledged that this oversimplifies salt behaviour which is known to be highly nonlinear and temperature sensitive. A large range of suggested salt viscosities are reported in literature; see Mukherjee, Talbot and Koyi (2010) for a review. Salt viscosities of around 10^{18}Pa.s are normally considered representative. Values of this magnitude are supported by assessment of kinematic indicators over geological time, for example pipe trails deformed by Messinian age salt in the Levant Basin (Cartwright et al. 2018). Additional support is provided through studies of salt diapirs, extrusions and laboratory-derived flow laws for common evaporite minerals (Urai and Spiers 2007; Urai et al. 2008). Non-Newtonian constitutive models such as Herschell-Bulkley, Bingham Plastic, or Power Law fluids are also available.

3.2.2.2 Multi Deformation Mechanism Model

The Multi Deformation mechanism model (Munson 1997; Dawson and Munson 1983) has been designed to specifically model salt creep and is commonly used in geomechanical forward modelling studies (Nikolinakou et al. 2017; Nikolinakou, Flemings, and Hudec 2014; Prasse et al. 2020; Thigpen et al. 2019). Application of a reduced form of this model is proposed for geomechanical forward models in which only steady state creep is considered. This form disregards both transient (primary) creep and the contribution of the dislocation glide mechanism which is activate only at high differential stresses. The justification for these omissions is that over geological timescales it is unlikely that the salt will be subjected to very high differential stresses such as those that would be encountered during excavations, drilling operations etc.

The steady-state viscoplastic creep rate for the reduced model is written as follows:

$$\dot{\varepsilon}_c = \sum_{i=0}^{2} \dot{\varepsilon}_i^{ss} \qquad \textbf{(11)}$$

$$\dot{\varepsilon}_i^{ss} = A_i \exp\left(-\frac{Q_i}{RT}\right)\left(\frac{\bar{\sigma}}{G}\right)^{n_i} \quad \textbf{(12)}$$

Where;

$\bar{\sigma}$ is an equivalent stress measure e.g. Von Mises, Tresca, Hosford.
G is the shear modulus
R is the Boltzman constant
T is the absolute temperature
Q_i is the activation energy for the *ith* mechanism
A_i is a material pre-exponential factor for the *ith* mechanism
n_i is an exponent for the *ith* mechanism

In equations (11) and (12) subscript 1 refers to the dislocation climb mechanism and subscript 2 refers to an undefined but experimentally well characterized mechanism. More recent formulations of the model have incorporated a pressure-solution mechanism (subscript 0) which has an identical form to the other mechanisms and is known to be significant at low stress levels (Reedlunn, Argüello, and Hansen 2022). *Whilst this variant is not currently implemented it will be added as part of the SHARP project*.

Experimental data for halite samples from the various storage sites suggest it is unlikely there are a large number of halite constitutive descriptions from Gulf of Mexico/onshore US (Fredrich, Fossum, and Hickman 2007) and South Atlantic margins (Firme, Roehl, and Romanel 2016). It is noted by Firme and co-workers that the response of halite from offshore Brazil is bracketed by specimens from onshore Gulf of Mexico, and this observation provides some basis for application of the available models to other basins e.g. North Sea. A comparison of the creeping behaviour of Zechstein salt from the Asse Mine (Germany) and WIPP salt from the US; the latter generally creeps an order of magnitude faster (Dusterloh et al. 2015). Some of these publications also contain descriptions for more mobile salts like Carnallite that can be applied if necessary.

3.2.3 Deep Layers: Crystalline Basement, Upper/Lower Crust

The character of the deep basin sediments and upper portions of the basement are poorly constrained within the North Sea basins owing to very limited well penetration. What is known is that the crust is likely to be highly heterogenous with considerable lateral and vertical variations in rock fabric, in addition to the presence of fractures and ductile shear zones. Within the Northern North Sea some wells penetrate upper sections of the basement, albeit over limited depth ranges, revealing a mixed composition that can include granite (and related rocks), schist, mica, and quartzite (Fazlikhani et al. 2017). It is unlikely that specific material data will be offered for characterizing the deep crystalline basement/crustal layers. Pragmatically, the layers may be treated as linear elastic on the premise that deep, crystalline layers will likely be strong, low porosity units. Some typical elastic property values used from literature are shown in Table 3-4.

Lithology	***Material Properties***			***Ref***	***Notes***
	E (GPa)	***v***	***ρ_b (kg/m^3)***		
Continental Crust	45	0.35	2600	(Kjeldstad et al. 2003)	Continental crust
Aplite	60	0.2	2600	(J. Nevitt, Pollard, and Warren 2012)	Similar to granite
Granodiorite	74.8	0.27	2700	(J. M. Nevitt, Warren, and Pollard 2017)	Similar to granite

Table 3-4 *Examples of elastic properties for basement materials derived from literature. E – Young's modulus, v – Poisson's ratio, ρ_b – Bulk density.*

More sophisticated constitutive models may be used to represent deep basement/crust if necessary. Strength profiles within the upper crust are sensitive to composition, temperature and strain rate (Naliboff and Buiter 2018). Where strain rates are high, and the crust is cool, large differential stresses may be accommodated and deformation is typically brittle and localised (shear zones, faults). Conversely, where strain rates are low, and the crust is hot, deformation is typically more ductile via viscous creeping processes and consequently large differential stresses do not manifest. These aspects can be treated using a so-called B*rittle-Ductile Transition* model where a conventional Mohr-Coulomb (brittle) model is coupled to a viscoplastic power-law creep (ductile) model. The power law creep is defined as follows:

$$\dot{\varepsilon}_c = A \exp\left(-\frac{Q}{RT}\right) q^n \qquad \textbf{(13)}$$

Where;

A is a pre-exponential factor
q is the Von Mises stress
Q is the activation energy
n is an exponent
R is the Boltzmann constant
T is the temperature

The properties for this more complex model for the relevant rock type(s) can likely be sourced from literature. For example, properties for granodiorite compatible with Eq. (13) may be sourced from literature (Hansen and Carter 1983).

3.3 Summary and Recommendations

This section has documented some important aspects of the numerical modelling tool that will be used for modelling studies and constitutive models that may be applied to represent the various layers. In summary;

- The modelling framework is quite versatile and fundamentally has enough functionality to address the stress drivers that have been described for each of the storage sites. This includes treatment of deposition, erosion, large strain deformation and coupled processes.
- There are constitutive modelling options available for different lithologies with varying degrees of sophistication:
    - Critical state-based constitutive models such as the SR3 model are recommended for treating clastic and carbonate sediments. These are sophisticated enough to capture trends and observations made in experimental data; this is elaborated on in section 4.1.3.
    - A framework for incorporating diagenesis has already been implemented. This is important as it provides a means for exploring the influence of diagenetically-sourced changes in the character of the sediments which are not possible in the laboratory. The response of deeply buried sediments to unloading processes can then be studied. There is flexibility to either simplify the representation of these processes or conversely add additional functionality to better represent changing fabric/anisotropy.
    - Salt creep can be simulated and the influence on surrounding sediments that are targets for storage can be analysed. A minor extension to a currently implemented salt creep model has been proposed and will be undertaken as part of the project.

- Should modelling very deep layers at ‘lithospheric scale’ be required, there are appropriate constitutive models available. Pragmatically, the deeper units may be simulated as stiff and elastic.

Data for constitutive models can be sourced from existing databases and papers which have been referenced. There is therefore no perceived risk from a lack of data.

4 Proposed Designs for Forward Geomechanical Modelling

This section is concerned with providing provisional designs for geomechanical forward models that are to be developed over the course of the project. The eventual models created may exhibit deviations from the inputs and methods described here, based fundamentally on the data that is available for their construction and validation. But the overall objectives will likely remain the same. By design, the models gradually increase the level of sophistication. Areas of anticipated overlap and integration with other work packages are highlighted.

It should be noted that although the various loading scenarios can be explicitly modelled through various boundary/loading conditions it is also possible to incorporate them in alternative and potentially more straightforward ways. This could for example involve modifying the stress initialisation procedure in large 3D models to account for processes like erosion or regional compression. This understanding could be derived from simpler uniaxial models.

4.1 Model Type A: Uniaxial Modelling

4.1.1 Objective

The premise of this model is to enable preliminary investigations into how stresses are affected by:

(a) Variable mineralogical composition throughout the sedimentary column.
(b) Stress transitions at depth as a function of diagenesis and/or overpressure.
(c) Loading/unloading processes such as uplift/erosion and glaciation, including the response of deeper sediments that have been diagenetically altered.
(d) Minor amounts of extension or compression.

This class of model can be used to determine stress distributions under boundary conditions of zero lateral strain, which is a reasonable assumption for passively subsiding sedimentary basins. By integrating characterisations of key rock types based on both published data and rock mechanics data generated in other work packages, such models offer an opportunity to develop stress profiles where data is pauce providing the mineralogy is relatively well constrained. It can therefore be considered as a means for establishing a “background” stress state. Additionally, this class of model serves as a useful means for outlining the process of developing, calibrating, and confirming material characterisations, and provides a foundation for an extension to more complex modelling.

Because of the imposed boundary conditions, this type of model has limited scope to include processes such as regional/salt tectonics. Such phenomena require 2D and 3D models, discussed in sections 4.2 and 4.3. Therefore, this type of model focuses very much on the mineralogical and diagenetic impacts on stress and pore pressure.

4.1.2 Data Sources, Construction Process and Loading

4.1.2.1 Simulation Type

The model can be run in multiple configurations:

- Effective stress analysis – in this mode it is assumed that the model responds in a drained manner and pore pressures are not evaluated.

- Coupled analysis – in this mode the mechanical and flow calculations are performed simultaneously and pore pressure changes are calculated.

Both model configurations will be explored. Due to observations linking deep minimum stress trends to overpressure and diagenesis, most effort will be accorded to the coupled modelling approach.

4.1.2.2 Geometry

The model geometry in this case is very basic and consists only of a single, rectangular initial layer with dimensions specified by the user. The geometry is automatically updated to accommodate deposition and erosion.

4.1.2.3 Material Properties

A suitable database for constitutive properties has been sourced in publications from NGI (Grande, Mondol, and Berre 2011; Grande and Mondol 2013). These datasets include various natural and synthetic samples with varied mineralogy; clay-clay and silt-clay mixtures and two different sands. The experiments were carried out in a modified triaxial cell in which as axial stress is increased the radial stress is monitored and adjusted to maintain conditions of zero lateral strain. As such data for porosity evolution with increasing effective stress is available, as in a conventional oedometer test, but also information for how the minimum stress evolves. The data for the ten tested samples is shown in Figure 4-1. Data within Grande and Mondol (2013) also provides stress-permeability data that may be used to provide inputs for coupled hydro-mechanical models. Other sources of porosity-permeability data include Yang and Aplin (2010) and Schneider et al., (1996). Characterisation of the chemical compaction processes will also be necessary, which can largely be derived from similar studies (Obradors-Prats et al. 2019) and insights derived from studies of the diagenetic impact on geomechanical properties from the Horda Platform area (M. J. Rahman et al. 2022); see Figure 4-2.

4.1.2.4 Applied Geological Loads

Simple uniaxial boundary conditions are proposed in which the model base is fixed vertically and the sides are fixed laterally.

4.1.2.4.1 Deposition

Deposition algorithms will be used to progressively add new material with rates determined based on available well information and publications. The initial thickness of the layers can be estimated based on representative initial/final porosities and the present-day thicknesses and the amount of material added can be iteratively adjusted to achieve a good match for supplied data. Ice loading can be incorporated in a similar manner and thickness estimates can be explored based on recent evaluations (SHARP Deliverable 1.1a 2022).

4.1.2.4.2 Erosion

Erosion may also be represented; it is likely that there is some uncertainty regarding the precise amount of material that has been removed. However, estimates have been sourced from relevant publications in the Horda Platform area (Baig et al. 2019). Furthermore, uplift maps have been generated already as part of the SHARP project as shown in Figure 2-2.

4.1.2.4.3 Glacial Loading

Applied glacial loading will be defined by integrating assessments and interpretations from Deliverable 1.1a (Reference). There is likely significant uncertainty associated with the timing and magnitude of imposed glacial loads and these will be explored in the modelling.

4.1.2.4.4 Temperature

Thermal loading is important for cases in which chemical compaction processes will be simulated. Several options are available:

- Thermal gradient – a representative thermal gradient is applied e.g. 30°C/km that is updated as deposition progresses.
- Coupled – the temperature field is solved based on thermal properties (conductivity, specific heat capacity) and applied flux/temperature loading.

For simplicity application of a constant thermal gradient is suggested as it might be difficult to constrain the variation of imposed thermal boundary conditions with time.

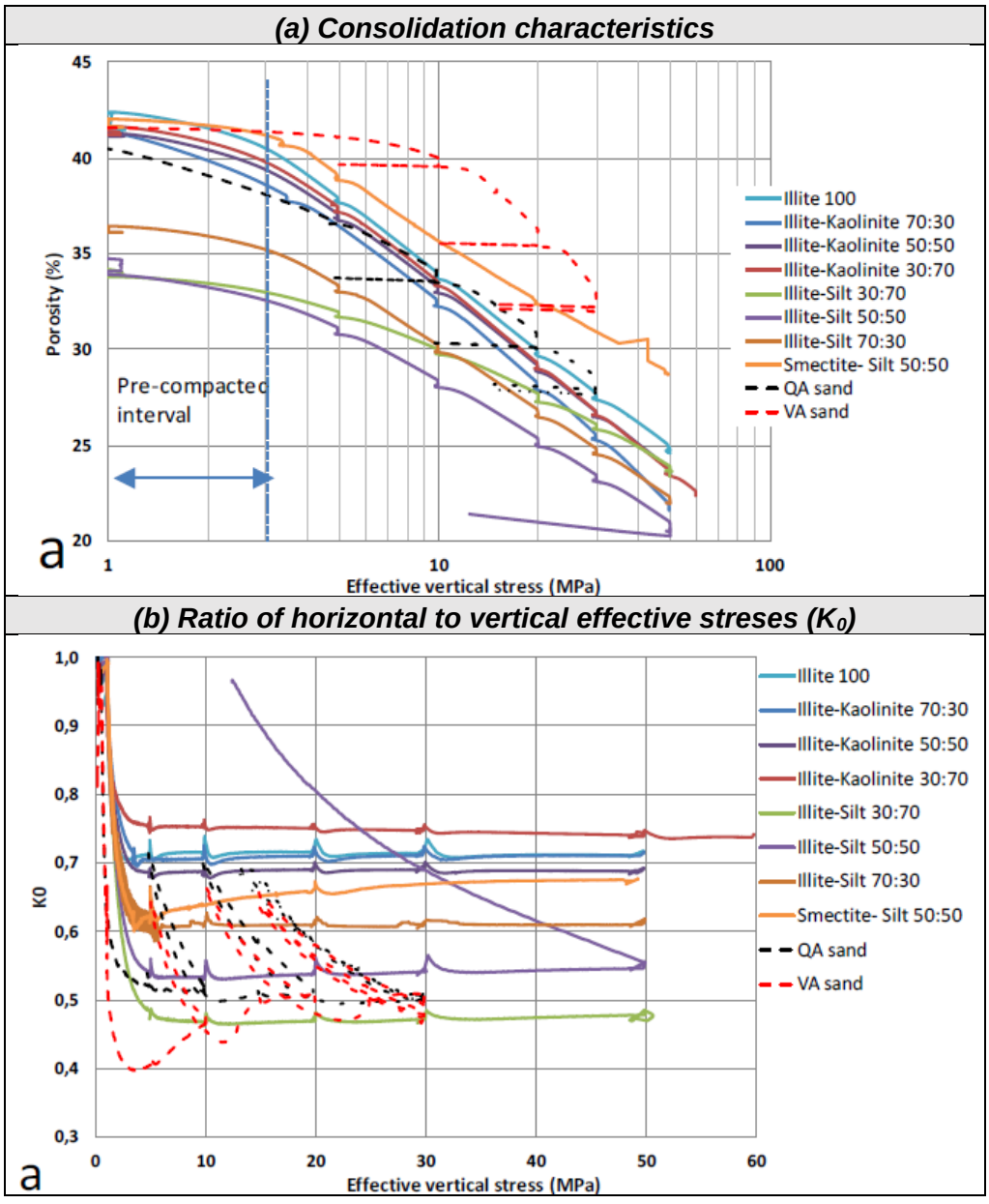

Figure 4-1 *Experimental data from Grande & Mondol (2013) showing porosity and K0 variations with mineralogical differences and under different amounts of burial and exhumation.*

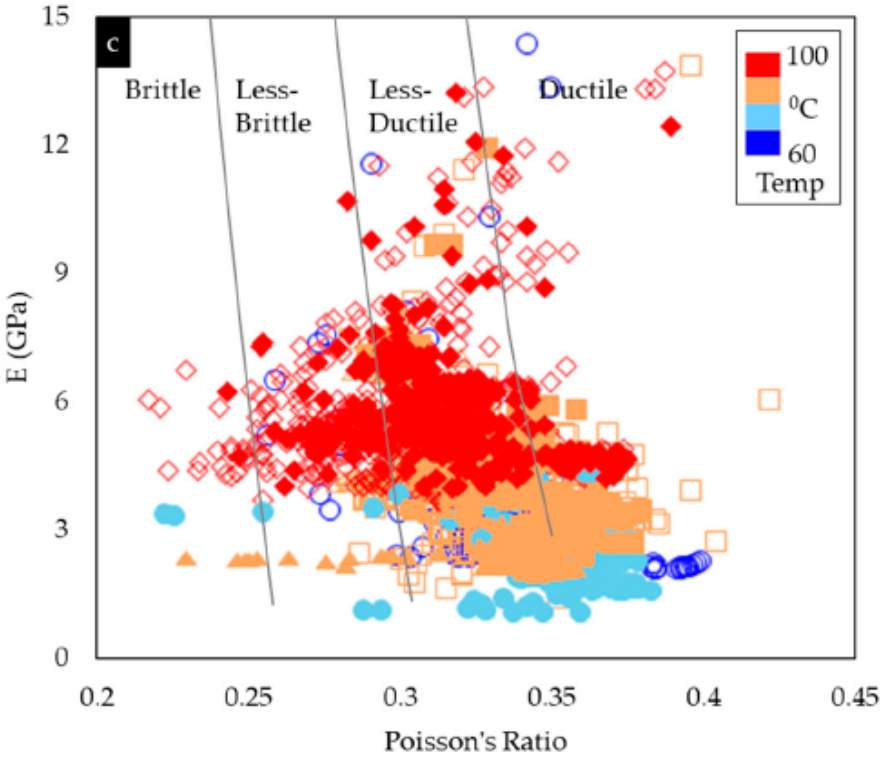

Figure 4-2 *Geomechanical properties (Young's modulus, Poisson's ratio) for the Drake Formation as a function of burial temperature* (M. J. Rahman et al. 2022)*. Note the generally ductile behaviour of the sediments that have not been chemically compacted (low temperature). More deeply buried sediments that are exposed to higher temperatures show a slight increase in compressibility and a more marked increase in stiffness.*

4.1.3 Demonstration Case

A demonstration case is developed in this section to communicate the key elements of the model and provide typical results that may be extracted from the model. Select characterisations from the database introduced above have been developed:

- Sandstone (Quartz-Arenite): Composition 94% Quartz, 6% Kaolinite.
- Siltstone: Composition 50% Silt, 50% Illite.
- Claystone: Composition 30% Illite, 70% Kaolinite.

These basic characterisations have adopted the Soft Rock 3 together with a Cam Clay poro-elastic law (models introduced in section 3.2.1.1.3). At this stage, the various options for capturing the nonlinear elastic response to unloading have not been explored fully. Once characterized, the materials can be assessed in an analysis with a single finite element to ensure the response is appropriately captured.

Comparison of experimental and numerical results indicates that the evolution of porosity with increasing effective vertical stress is well approximated for all three characterisations; Figure 4-3(a). Likewise, inspection of Figure 4-3(b) indicates that each material exhibits the correct ratio of horizontal to vertical effective stress during virgin compaction. A similar process will be repeated for the other materials in this database as part of upcoming tasks (Task 1.2: Constitutive Modelling). Once validated, the characterisations may be included in multi-element 2D/3D simulations that incorporate more complex

boundary conditions. A simple setup is shown in Figure 4-4 which features deposition of alternating clay, silt and sand over 10Ma, followed by erosion of the shallow layers over a further 5Ma. The figure shows the calculated effective vertical stress and the K_0 ratio evolving through time. The results indicate that the ratio of horizontal and vertical stresses changes significantly in the shallow section but is less affected at depth. An interrogation of model outputs is also shown in Figure 4-5.

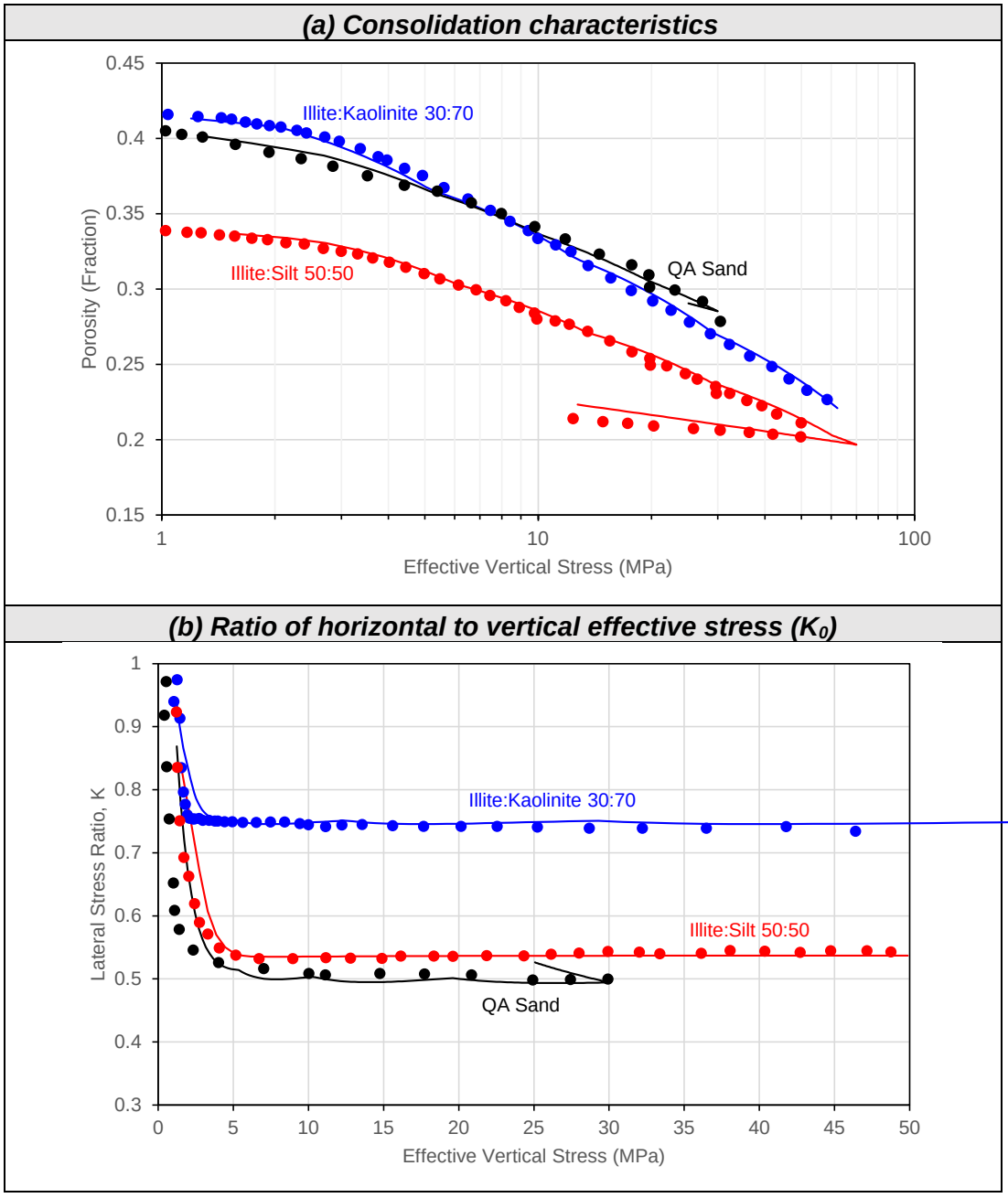

Figure 4-3 *Calibration of consolidation characteristics for differing sediment mineralogy. Solid markers represent experimental data reported in Grande & Mondol (2013), lines represent results of characterized constitutive model.*

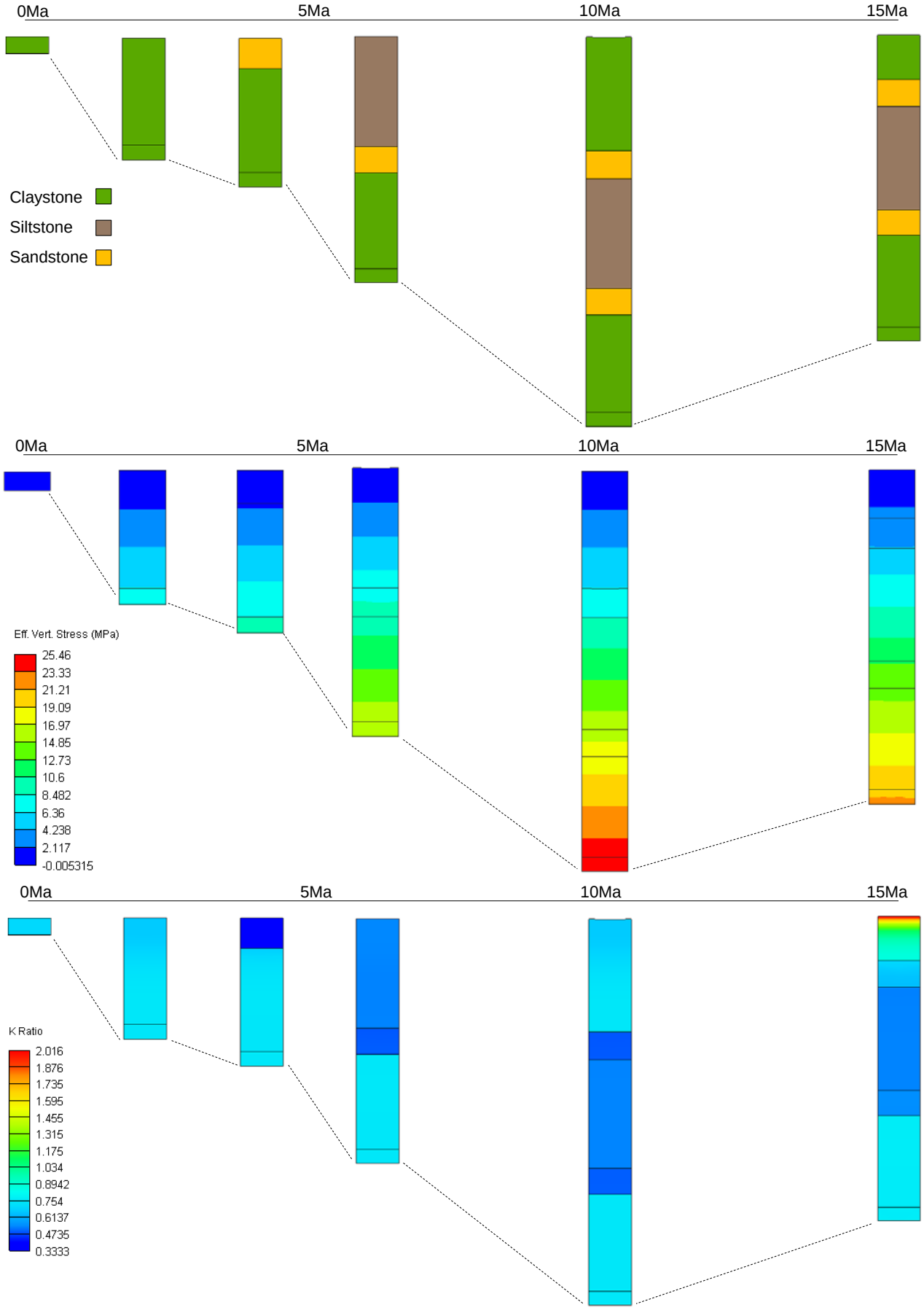

Figure 4-4 *Uniaxial model incorporating deposition of varied lithologies and subsequent erosion.*

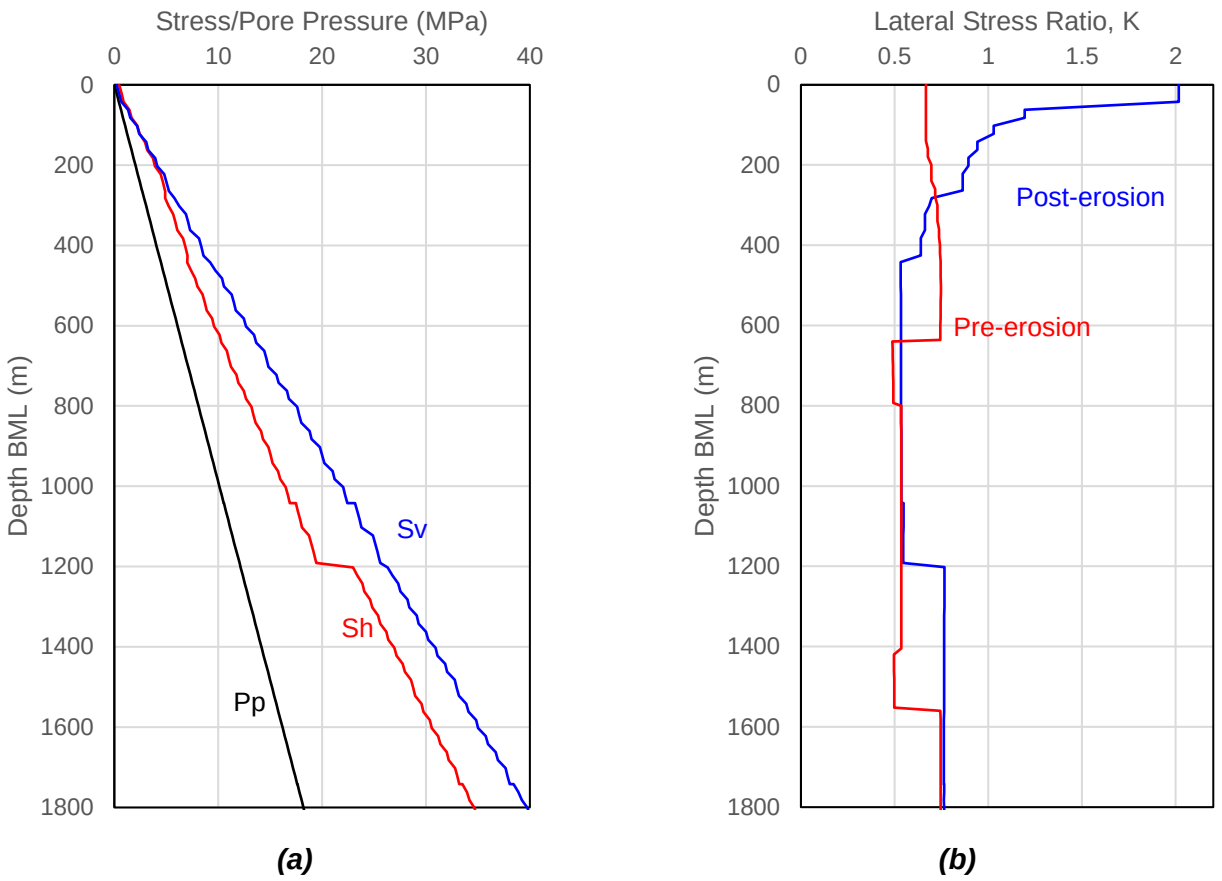

Figure 4-5 (a) *Final recovered stress distributions Pp – Pore Pressure, Sh – Effective horizontal stress, Sv – Effective vertical stress (b) Variation of lateral stress ratio with depth for pre-erosion and post-erosion configurations.*

4.1.4 Expected Modelling Outcomes

The model is expected to provide insight into the relative significance of some of the stress driver mechanisms, particularly those that are concerned with sediment mineralogy. The results predicted by the models can be checked against, or calibrated to, supplied well data and can provide a means for providing robust estimates of minimum stress in the subsurface. Uncertainty in ice thickness in the Norwegian area can be explored by exploring different mechanical and drainage properties for shallow sediments.

By extending the applied experimental data to greater depths via modelling of diagenetic processes, the causes of observed trends in stress data can be fully explored. In section 2 it has been suggested that understanding the influence of these processes is very important for seal integrity assessments.

The results from the models can be exported to give a relatively quick estimate of the *in situ* stress and pressure conditions that is compatible with the constitutive properties of the various sediments. This data would be able to complement existing workflows for 1D geomechanical modelling that form part of other work packages.

4.2 Model Type B: Regional Scale Modelling (2D/3D)

4.2.1 Objective

The aims of this model are as follows:

- Apply the characterisations developed as part of Task 1.2: Constitutive Modelling and Type A models further.
- To investigate the relative contributions from additional stress drivers along large-scale regional transects in the Northern North Sea. Some processes may be more significant than others in terms of controlling paleo and present-day stress distributions and model results should provide an indicator of this.
- To predict and analyse spatial trends in stress distribution. Early assessment of Leak-Off databases reveals both lateral e.g. East-West, and vertical trends in the minimum horizontal stress magnitude.

4.2.2 Data Sources and Construction Process

4.2.2.1 Geometry

An important initial data requirement is the geometric definition of the problem. Two potential sections have been sourced from the Northern North Sea that may be used as a basis for geometry definition (Sajjad 2013). However, it is anticipated that some specific data can be offered by entities outside of the SHARP consortium as the project progresses.

- ***NSDP82-01***

This section is aligned approximately northwest-southeast and passes from the Oygarden Fault zone in the southeast to the Magnus Basin in the northwest (Figure 4-6). Importantly, the section passes through the Horda Platform area which is of specific interest as this area is a target for storage sites.

- ***NSDP84-02***

This section is aligned approximately east-west. The section passes through the southern portions of the Horda platform in the south through the Viking Graben and into the East Shetland Platform in the east.

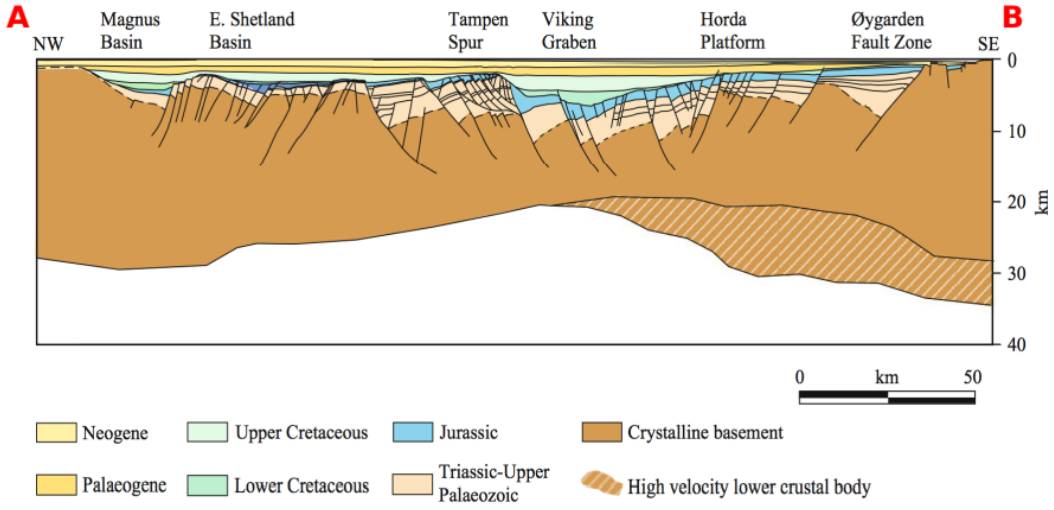

Figure 4-6 *Structure of crystalline basement and sedimentary units along regional transect NSDP82-1.*

Suitable geometry can be derived from either section. As a demonstration, the geometry of line NSDP82-01 has been digitized below and incorporated into the Elfen finite element software. Note that the faults are

represented as discrete contact surfaces which may be represented as “tied” or with frictional slip dictated by a Coulomb friction law. The corresponding finite element mesh is also shown where the level of discretization is increased in the shallow section.

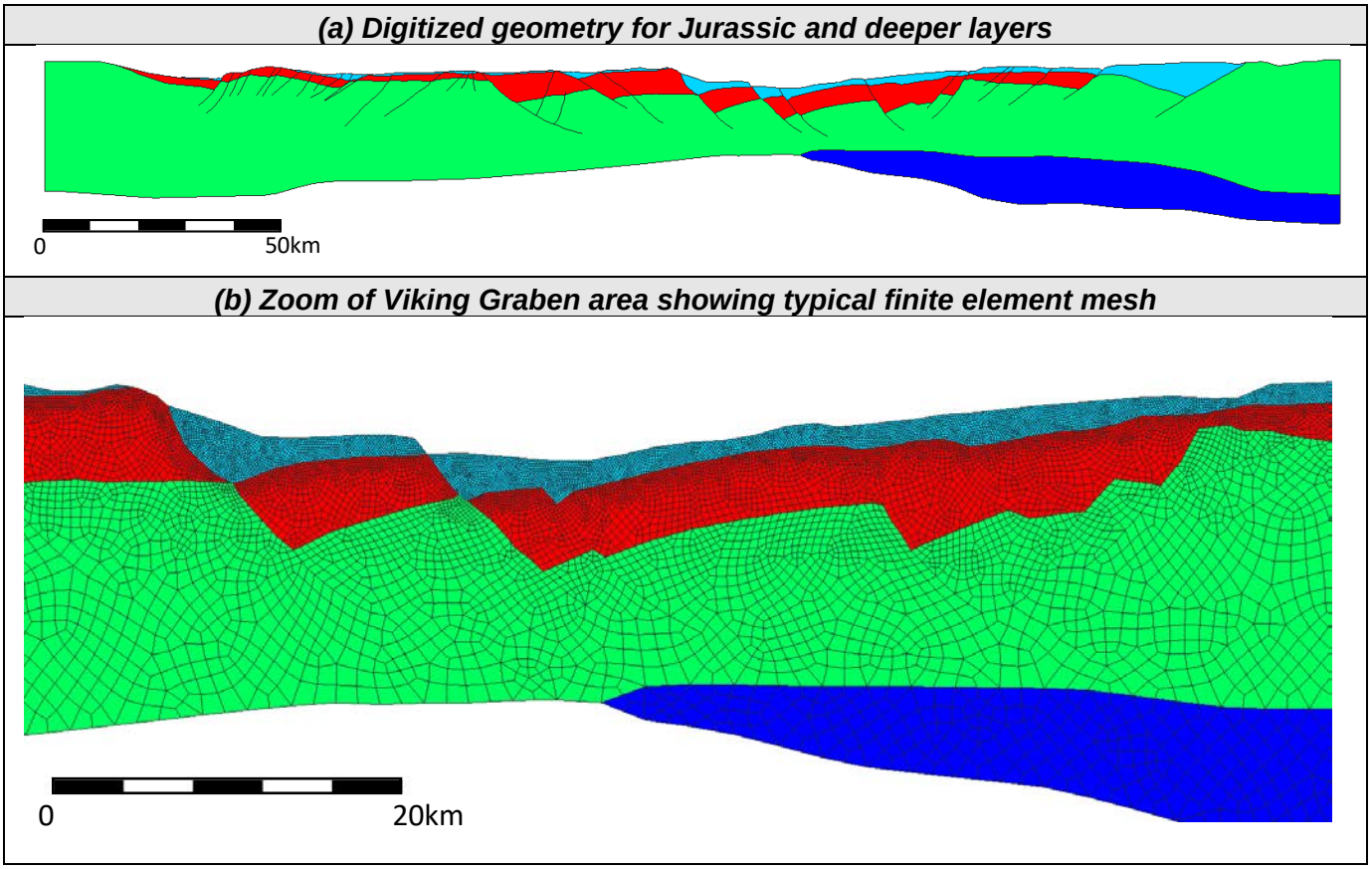

Figure 4-7 *Demonstration for constructed geometry of Triassic and older layering along NSDP82-01 (no vertical exaggeration).*

Modelling work will aim to be extended into 3D. A suitable 3D dataset to provide a basis for geometry construction that covers this area of the North Sea has not yet been sourced, though enquiries about a suitable dataset that forms part of an industry project have been made. Extending into 3D would necessitate some simplification of the model inputs and a reduction in model resolution.

4.2.2.2 Material Properties

The material properties for the shallow layers (Jurassic and younger) can be represented with the same models applied and tested as part of the Task A models. Maintaining consistency with these models will allow for the influence of laterally varying processes (erosion, uplift, ridge push) on the *in situ* stress to be better understood. Deeper layers where data will likely not be available may have to adopt assumed properties based on published studies or incorporate sensitivity analysis. Faults can be assigned as active or inactive and will use a Coulomb friction law. This would require the assignment of strength characteristics (friction angle, cohesion) which may be estimated and explored via sensitivity.

4.2.2.3 Applied Geological Loads

Some of the loading types that will be applied to the model are shown in Figure 4-8 and discussed below.

4.2.2.3.1 Basal Deformation & Lateral Shortening

For evolutionary modelling, it is often useful to have additional information to constrain boundary conditions such as imposed regional extension/compression and basal uplift. Information sourced from an MSc thesis at NTNU University (Sajjad 2013) contains a 2D Dynel® section that contains restorations at specific steps and can be used to develop optimal loading and boundary conditions for the model. The model base can also include isostatic loading to attempt to predict the rebound effect due to ice loading or erosion.

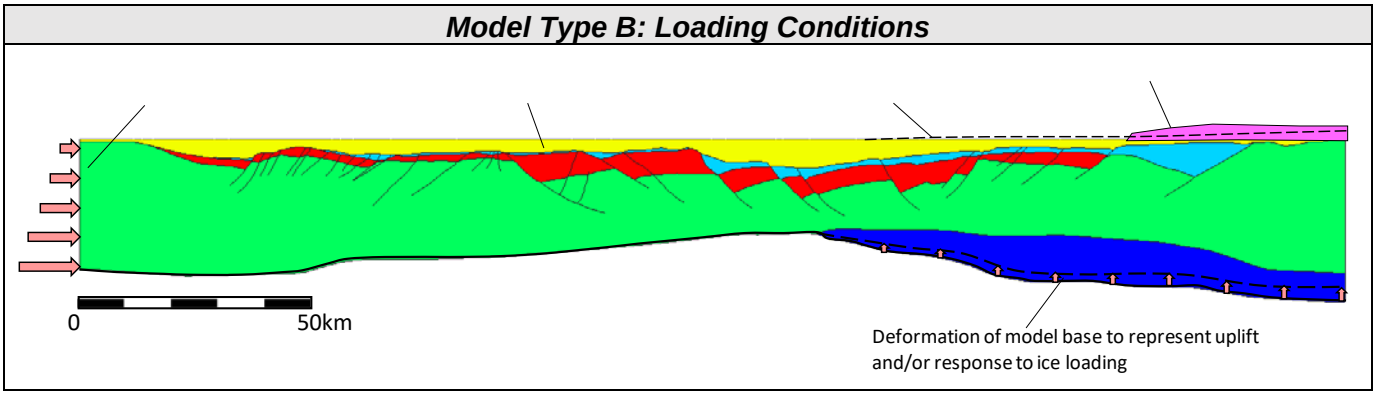

Figure 4-8 *Summary of potential imposed loads for regional scale geomechanical models in the North Sea basin.*

4.2.2.3.2 Uplift/Erosion

This is a key input into the model and may be tackled in different ways – the uplift can be prescribed directly as a load that permits imposed deformation from an initial (pre-uplift) to a final (post-uplift) configuration. When incorporating these loads the model geometry may have to be modified to a pre-uplift configuration. For erosion, a 'horizon' may be defined above which material is gradually removed, with or without uplift.

4.2.2.3.3 Glacial Processes

Constraints on ice loading such as timing, distribution, and ice thicknesses will be extracted from DV1.1a whilst also incorporating insights from the Type A models.

4.2.3 Expected Modelling Outcomes

Early models of this type are anticipated to provide estimates of stress magnitude and orientation over a wide area as dictated by the various stress drivers that are incorporated. As the model not only covers a large spatial area but extends to reasonably significant depths (to Moho), insights into stress distributions both in the deeper basement units and the sedimentary basins are expected. Consequently, the model should offer stress outputs that can be compared to focal mechanism data in the deeper units, and casing shoe measurements (FIT, LOT, xLOT) in the shallower sediments. Based on these observations some comments regarding the causes and extent of any decoupling can be made.

4.3 Model Type C: Site Specific Modelling (2D/3D)

4.3.1 Objective

The model will aim to investigate the following:

- The degree of variability in stress magnitude and orientations adjacent to salt structures such as pillows and diapirs.
- Potential decoupling of stress fields due to salt, with the existence of distinct stress regimes in pre- and post-salt intervals.
- Deformation response in the storage due to salt structures responding to recent glacial events.

4.3.2 Data Sources and Construction Process

The geometry will be conceptualized but based largely on the conditions local to the Endurance structure. Conceptualizing the definition of the problem where possible, particularly in terms of geometry, may allow for the insights gained to be applied more generally to cases where storage sites are close to salt structures.

4.3.2.1 Geometry

A representative geometry based on the Endurance structure will be constructed. The degree to which the geometry resembles the structure will depend on the nature of the data provided, however, as a minimum will represent a four-way closure above the salt. Representative layer thicknesses can be determined based on previous geomechanical models; Figure 4-9. The geometry may reflect a pre-eroded configuration such that the stress relaxation and redistribution due to the removal of post-mid Jurassic sediments can be studied. Significant halokinesis likely occurred prior to the emplacement of the upper Jurassic sequence, so starting the analysis at this time would seem appropriate.

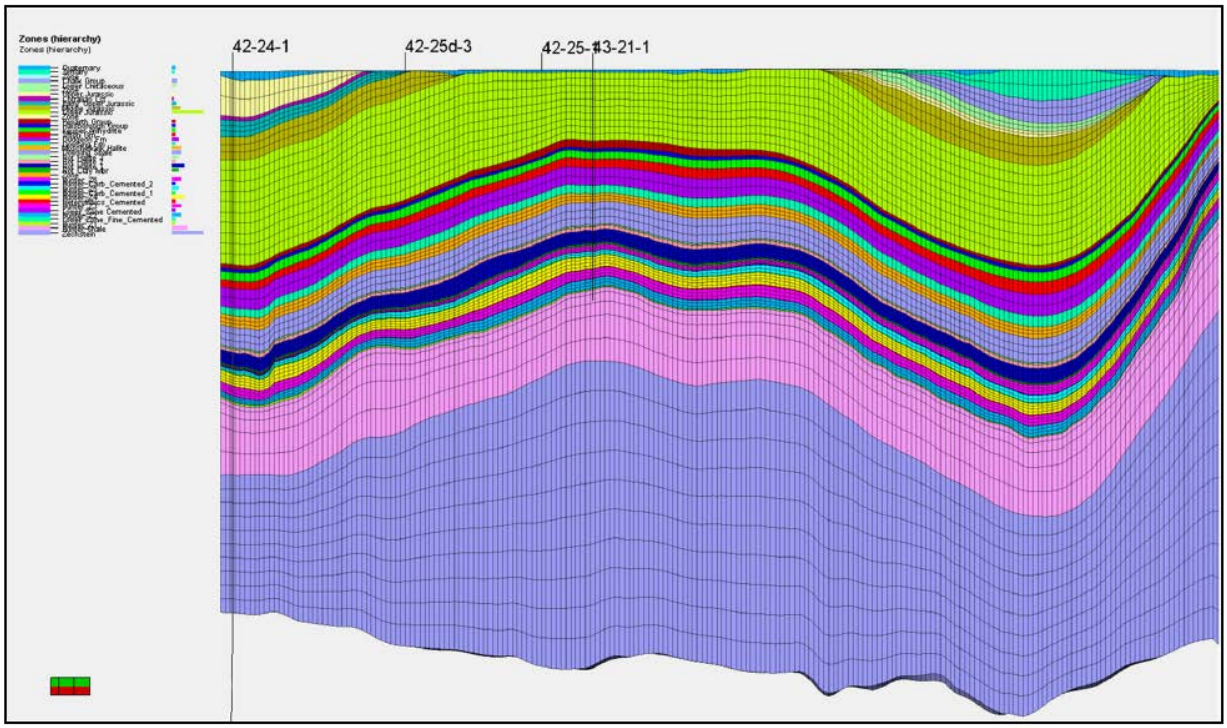

Figure 4-9 *Geometry of the Endurance storage site suitable for generating generic geometry.*

4.3.2.2 Material Properties

Representative constitutive properties for the relevant formations at Endurance have been collected within Work Package 4 Deliverable 4.1 as part of preliminary site screening. These include typical elastic properties for the key layers such as Bunter Sandstone and Bunter Shale. For the Zechstein halites, the MD constitutive model described in section 3.2.2.2 will be applied. Creep parameters based on WIPP salt can be applied (Reedlunn, Argüello, and Hansen 2022); this characterization is slightly more mobile than Zechstein Asse salt (Dusterloh et al. 2015).

4.3.2.3 Applied Geological Loads

The anticipated geological loads that will be applied are described in this section.

4.3.2.3.1 Regional Compression

The present stress state was noted to likely be strongly affected by ridge push from MidAtlantic spreading, particularly in the pre-salt interval (Williams et al. 2015). The significance of this regional compression can be explored via a far-field boundary condition. Consideration of predicted stress distributions with and without this effect can be explored.

4.3.2.3.2 Uplift/Erosion

As noted in section 4.2, the uplift can be prescribed as a direct load with an imposed deformation from an initial (pre-uplift) to a final (post-uplift) configuration. In the model, these loads may again be subject to modification to a pre-uplift configuration. Again, a ‘horizon’ may be defined above which material is gradually removed during uplift.

4.3.2.3.3 Glacial Loading

As with previous models, the inputs for loads representing glacial loading will largely be conditioned by insights reported in DV1.1a (SHARP Deliverable 1.1a 2022). Although the effects of glacioisostasy have received substantial attention, prior Thermo-Hydro-Mechanical modelling of ice loading in the North Sea is somewhat sparse, with work focusing on basin-scale loading and erosion in absence of pre-existing structures such as salt diapirs e.g Cerroni et al. (2019). Additionally, models studying the influence of ice sheets on salt diapirism tend to overestimate resultant displacements (Liszkowski 1993; Sirocko et al. 2008), or are restricted to two dimensions (Lang et al. 2014). Thus, site-specific models could also seek to investigate:

- The refinement of displacement estimates and geometry changes induced by a more realistic representation of cyclical glacial loading; incorporating a stress evolution as shown in figure 4.10
- Cyclical loading/unloading on specific geometries such as the Horda Platform and Endurance structure.
- Extending 2D models to local 3D Thermo-Hydro-Mechanical models to better constrain stress evolution and load-induced structural deformation

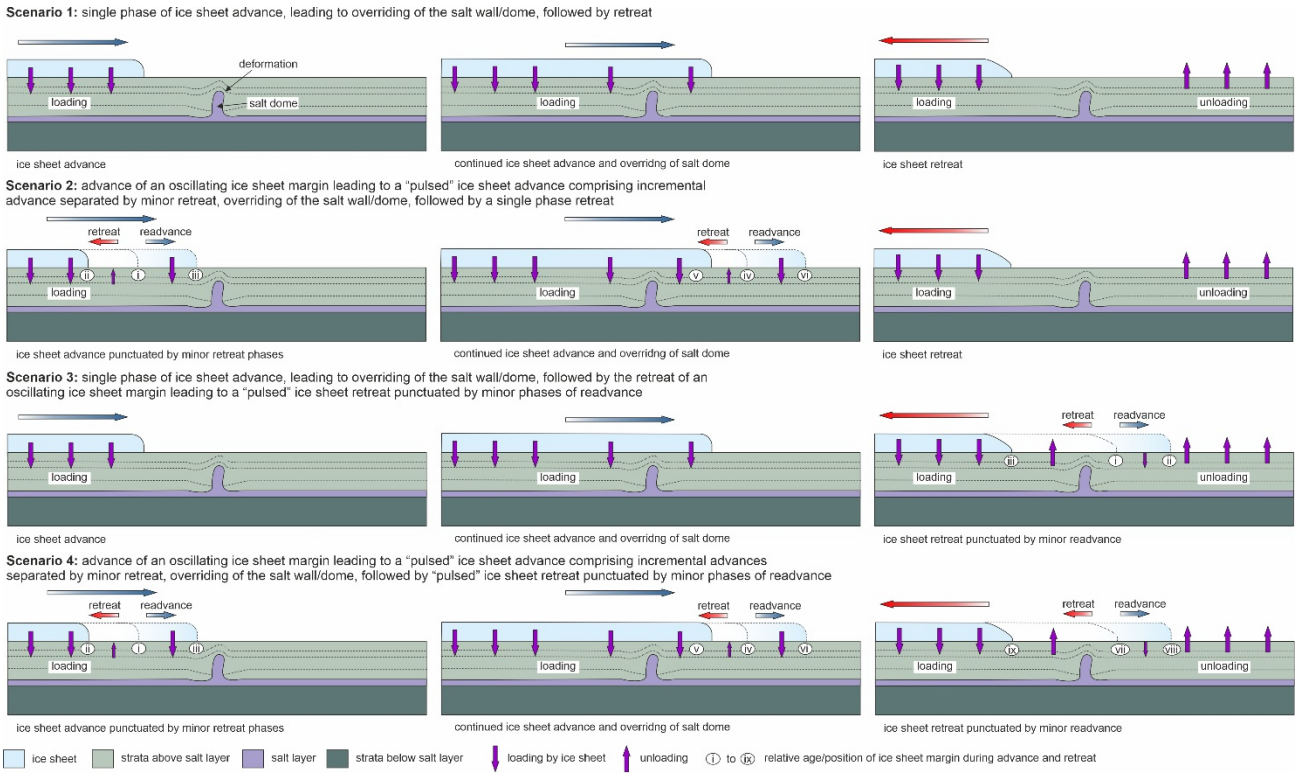

Figure 4-10 *Schematic highlighting potential loading scenarios that represent advancing and retreating ice sheets over sedimentary sequences adjacent to salt structures.*

4.3.2.3.4 Temperature

Given the thermal sensitivity of salt deformation characteristics described in Section 3.2.2,it is important to represent temperature within the model. This will likely be via a representative thermal gradient applied to the model and for simplicity, this will remain constant throughout the analysis.

4.3.3 Expected Modelling Outcomes

A primary modelling outcome of the work is expected to be exported site-specific stress distributions above the basement. Additionally, the assessment of potential decoupling from the presence of salt, causing detached stress regimes is expected, as well as the production of a realistic response of site-specific structures to quasi-cyclic glacial loading. Modelled stress outputs can again be compared/calibrated to casing shoe measurements (FIT, LOT, xLOT). An emphasized model outcome is the ability to compare the contributions of regional, relative to site-specific stress drivers.

5 Summary

A present-day understanding of *in situ* stress state is presented for the Horda Platform, Endurance Structure and Greater Bunter sandstone area, Aramis, Lisa and Nini structures (section 2). The suggested main mechanisms of stress generation include phenomena such as: ridge push, sediment and progradational loading, continental margins, glacioeustatic adjustments, and uplift/erosion. These mechanisms exist with variable magnitudes depending on the site; summarised in a stress matrix (Table 2-1). The influence of Stress-induced geometries such as faults are of variable influence across all sites. Assessing the relative significance of stress generation mechanisms is invaluable for site characterisation and formatting the mechanisms into a stress matrix allows for a more universally applicable approach to stress characterisation. A natural progression following the assessment of relevant stress drivers is the proposal of relevant geomechanical models to encapsulate significant processes present at each site. Empirical laws and relevant rheological properties implemented in models are highlighted in section 3.2. Recent modifications to relevant rheologies such as Reedlunn's (2022) characterisation of evaporite pressure-solution creep, and the effect of glacioeustatic adjustment are also considered, new for WP1. Three types of geomechanical forward models are proposed (A-C) (section 4) that explore stress in various dimensions and over differing scales, summarised below:

Model Type A – Uniaxial Modelling
This involves the generation of a 1D column to allow for preliminary investigations into how stresses are affected by mineralogical composition, potential stress transitions at depth and loading/unloading processes linked to diagenesis. Model results are fast, and can be checked against supplied well data; thus, providing estimates of minimum subsurface stress. The results would complement workflows, forming sections of the other work packages. A demonstration case is presented in section 4.1.3, showing the evolution of a cyclothemic sedimentary sequence subject to deposition and erosion over a 15Ma period.

Model Type B – Regional 2D/3D modelling
These models are generated from cross sections, with the potential for extension into three dimensions with appropriate datasets. An example geometry is presented for the Viking graben in section 4.2.2.1. Type B models provide a means for investigation into the relative contributions of *in situ* stress along large-scale transects of the Northern North Sea, as well as the analysis and prediction of spatial trends in the magnitude and orientations of stresses. Given the large depth extent, modelled stress outputs can be compared to focal mechanism data as well as shallower shoe measurements. This will give insights as to the degree of coupling between thick and thin-skinned deformation.

Model Type C – Local 2D/3D modelling
Produced from site-specific 2D/3D geometries, Type C models are able to investigate stress variability around evaporite structures, coupling of stress fields as a result of inferred decollements, and glacioeustatic responses of subsurface structures. The finer scale allows for a thorough analysis and comparison between regional and local influences on in-situ stress, with model outputs again being compared to shoe measurements such as FITs, LOTs, xLOTs etc.

Results from the models are expected to provide unique insights into the evolution, *in situ* stress state, and potential risks associated with CO2 injection into the proposed AOIs. This will undoubtedly provide information that can be offered to other work packages, as well as a general contribution to the advancement of the characterisation of safe CCS sites.

6 References

Ehers, J 1990. “Reconstructing the dynamics of the North-west European Pleistocene ice sheets” Quaternary Science reviews 9: 71-83

Wenau, S., Alves, T.M. 2020. “Salt-induced crestal faults control the formation of Quaternary tunnel valleys in the southern North Sea”. Boreas 49, 799-812

Nielsen, T., Mathiesen, A., and Bryde-Auken, M. 2008. “Base Quaternary in the Danish parts of the North Sea and Skagerrak” *Geological Survey of Denmark and Greenland Bulletin*, *15*, 37-40

Sejrup, H.P., Larsen, E., Haflidason, H., Berstad, I.M., Hjelstuen, B.O., Jonsdottir, H., King, E.L., Landvik, J.Y., Longva., O., Nygård, A., Ottesen, D., Raunholm, S., Rise, L., Stalsberg, K. 2003. Configuration, history and impact of the Norwegian Channel Ice Stream. Boreas 32, 18–36

Ask, M. V. S. 1997. “In Situ Stress from Breakouts in the Danish Sector of the North Sea.” *Marine and Petroleum Geology* 14: 231–43.

Ask, M. V. S., B. Müller, and O. Stephansson. 1996. “In Situ Stress Determination from Breakouts in the Tornquist Fan, Denmark.” *Terra Nova* 8: 575–84.

Baig, I. 2018. “Burial and Thermal Histories of Sediments in the Southwestern Barents Sea and North Sea Areas: Evidence from Integrated Compaction, Thermal Maturity and Seismic Stratigraphic Analyses.”

Baig, I., J. I. Faleide, N.H Mondol, and J. Jahren. 2019. “Burial and Exhumation History Controls on Shale Compaction and Thermal Maturity along the Norwegian North Sea Basin Margin Areas.” *Marine and Petroleum Geology* 104: 61–85.

Barnhoorn, A., W. Van Der Wal, B. L. A. Vermeersen, and M. R. Drury. 2011. “Lateral, Radial, and Temporal Variations in Upper Mantle Viscosity and Rheology under Scandinavia.” *Geochemistry, Geophysics, Geosystems* 12 (1): 1–19. https://doi.org/10.1029/2010GC003290.

BEIS. 2021. “Primary Store Geomechanical Model & Report, Key Knowledge Document, NS051-SS-REP-000-00012.”

Bjorlykke, K., and K. Hoeg. 1997. “Effects of Burial Diagenesis on Stresses, Compaction and Fluid Flow in Sedimentary Basins.” *Marine and Petroleum Geology* 14 (3): 267–76.

Bott, M. H., and N. J. Kusznir. 1984. “The Origin of Tectonic Stress in the Lithosphere.” *Tectonophysics* 105: 1–13.

Bott, M. H. P. 1991. “Ridge Push and Associated Plate Interior Stress in Normal and Hot Spot Regions.” *Tectonophysics* 200: 1–13.

Brook, M, K Shaw, C Vincent, and S Holloway. 2003. “Gestco Case Study 2a-1: Storage Potential of the Bunter Sandstone in the UK Sector of the Southern North Sea and the Adjacent Onshore Area of Eastern England.” *British Geological Survey Commissioned Report CR/03/154N*, 37.

Cameron, T. D. J., A. Crosby, P. S. Balson, D. H. Jeffery, G. K. Lott, J. Bulat, and D. J. Harrison. 1992. “United Kingdom Offshore Regional Report: The Geology of the Southern North Sea. (London: HMSO for the British Geological Survey.).”

Cartwright, J, C Kirkham, C Bertoni, N Hodgson, and K Rodriguez. 2018. “Direct Calibration of Salt Sheet Kinematics during Gravity-Driven Deformation.” *Geology* 46 (7): 623–26. https://doi.org/10.1130/G40219.1.

Cerroni, D., M. Penati, G. Porta, E. Miglio, P. Zunino, and P. Ruffo. 2019. “Multiscale Modeling of Glacial Loading by a 3D Thermo-Hydro-Mechanical Approach Including Erosion and Isostasy.” *Geosciences* 9 (465).

Chemia, Z., H. Koyi, and H. Schmeling. 2008. “Numerical Modelling of Rise and Fall of a Dense Layer in Salt Diapirs.” *Geophysical Journal International* 172 (2): 798–816.

Clausen, O. R., and J. A. Korstgård. 1993. “Small-Scale Faulting as an Indicator of Deformation Mechanism in the Tertiary Sediments of the Northern Danish Central Trough.” *Journal of Structural Geology* 15: 1343–57.

Croizé, D., S. N. Ehrenberg, K. Bjørlykke, F. Renard, and J. Jahren. 2010. “Petrophysical Properties of Bioclastic Platform Carbonates: Implications for Porosity Controls during Burial.” *Marine and Petroleum Geology* 27 (8): 1765–74.

Crook, A. J. L., S Willson, J Yu, and D Owen. 2006. “Predictive Modelling of Structure Evolution in Sandbox Experiments.” *Journal of Structural Geology* 28 (5): 729–44.

Crook, A. J.L., J. G. Yu, R. E. Flatebø, and T. G. Kristiansen. 2008. “Computational Modelling of the Rate Dependent Deformation and Liquefaction of Chalk.” *42nd U.S. Rock Mechanics - 2nd U.S.-Canada Rock Mechanics Symposium*.

Crook, A.J.L., J-G Yu, and S.M. Willson. 2002. “Development of an Orthotropic 3D Elastoplastic Material Model for Shale.” *SPE/ISRM Rock Mechanics Conference*.

Dahlen, F. A. 1981. “Isostacy and the Ambient State of Stress in the Oceanic Lithosphere.” *Journal of Geophysical Research* 86: 7801–7.

Dawson, P R, and D.E Munson. 1983. “Numerical Simulation of Creep Deformations Around a Room in a Deep Potash Mine *.” *International Journal of Rock Mechanics and Mining Sciences & Geomechanics Abstracts* 20 (1).

Day-Stirrat, R. J., A. McDonnell, and L. J. Wood. 2010. “Diagenetic and Seismic Concerns Associated with Interpretation of Deeply Buried ‘Mobile Shales.’” *AAPG Memoir*, no. 93: 5–27. https://doi.org/10.1306/13231306M93730.

Doornenbal, H., and A. Stevenson. 2010. *Petroleum Geological Atlas of the Southern Permian Basin Area, EAGE Publications*.

Dusterloh, U., K. Herchen, K. H. Lux, R. M. Günther, K. Salzer, W. Minkley, A. Hampel, J.G. Arguello, and F. Hansen. 2015. “Joint Project III on the Comparison of Constitutive Models for the Thermo-Mechanical Behavior of Rock Salt I. Overview and Results from Model Calculations of Healing of Rock Salt.” *The Mechanical Behavior of Salt VIII* 2007: 349–59. https://doi.org/10.1201/b18393-44.

Edwards, S. T. 1997. “A Study of In-Situ Stress Magnitudes in the North Sea Basin from Borehole Measurements.”

Eidvin, T., F. Riis, and E.S. Rasmussen. 2014. “Oligocene to Lower Pliocene Deposits of the Norwegian Continental Shelf, Norwegian Sea, Svalbard, Denmark and Their Relation to the Uplift of Fennoscandia: A Synthesis.” *Marine and Petroleum Geology* 56: 184–221.

Eidvin, T., and Y Rundberg. 2001. “Late Cainozoic Stratigraphy of the Tampen Area (Snorre and Visund Fields) in the Northern North Sea, with Emphasis on the Chronology of Early Neogene Sands.” *Nor. Geol. Tidsskr*. 81: 119–60.

Eijs, R. M. H. E. Van. 2015. “Neotectonic Stresses in the Permian Slochteren Formation of the Groningen Field EP201510210531.”

Faleide, J.I., R. Kyrkjebø, T. Kjennerud, R.H. Gabrielsen, H. Jordt, S. Fanavoll, and M.D. Bjerke. 2002. “Tectonic Impact on Sedimentary Processes during Cenozoic Evolution of the Northern North Sea and Surrounding Areas.” *Geological Society of London Special Publications* 196: 235–69.

Fazlikhani, H, H Fossen, R. L. Gawthorpe, J. I. Faleide, and R. E. Bell. 2017. “Basement Structure and Its Influence on the Structural Configuration of the Northern North Sea Rift.” *Tectonics* 36 (6): 1151–77. https://doi.org/10.1002/2017TC004514.

Fejerskov, M. 1996. “Determination of In-Situ Rock Stresses Related to Petroleum Activities on the Norwegian Continental Shelf. PhD Thesis at Norwegian University of Science and Technology (NTNU), Trondheim.”

Firme, P.A.L.P., D Roehl, and C Romanel. 2016. “An Assessment of the Creep Behaviour of Brazilian Salt Rocks Using the Multi-Mechanism Deformation Model.” *Acta Geotechnica* 11 (6): 1445–63. https://doi.org/10.1007/s11440-016-0451-y.

Fjeldskaar, W., and A. Amantov. 2018. “Effects of Glaciations on Sedimentary Basins.” *Journal of Geodynamics* 118: 66–81.

Fleitout, L., and C. Froidevaux. 1983. “Tectonic Stress in the Lithosphere.” *Tectonics* 2: 315–24.

Fokker, P. A. 2012. “Comparison and Translation of Cap Models in Rock Mechanics.”

Fredrich, J, A Fossum, and R Hickman. 2007. “Mineralogy of Deepwater Gulf of Mexico Salt Formations and Implications for Constitutive Behavior.” *Journal of Petroleum Science and Engineering* 57 (3–4): 354–74.

Fuchs, L., H. Schmeling, and H. Koyi. 2011. “Numerical Models of Salt Diapir Formation by Down-Building: The Role of Sedimentation Rate, Viscosity Contrast, Initial Amplitude and Wavelength.” *Geophysical Journal International*, May, no-no.

Gradmann, S, C Beaumont, and M Albertz. 2009. “Factors Controlling the Evolution of the Perdido Fold Belt, Northwestern Gulf of Mexico, Determined from Numerical Models.” *Tectonics* 28 (2): 1–28.

Grande, L., and N. H. Mondol. 2013. “Geomechanical, Hydraulic and Seismic Properties of Unconsolidated Sediments and Their Applications to Shallow Reservoirs.” In *47th US Rock Mechanics/Geomechanics Symposium, San Francisco, CA, USA*, 1–10.

Grande, L., N. H. Mondol, and T. Berre. 2011. “Horizontal Stress Development in Fine-Grained Seimdents and Mudstones during Compaction and Uplift.” In *73rd EAGE Conference & Exhibition Incorporating SPE EUROPEC, Vienna, Austria*, 1–5.

Grollimund, B, M.D Zoback, D. J. Wirput, and L. Arnesen. 2001. “Stress Orientation, Pore Pressure and Least Principal Stress in the Norwegian Sector of the North Sea,.” *Petroleum Geoscience* 7: 173–80.

Hansen, F. D., and N. L. Carter. 1983. “Semibrittle Creep of Dry and Wet Westerly Granite at 1000MPa.” In *24th*

U.S. Symposium on Rock Mechanics, Texas A&M, College Station, TX, 429–47.
Heidbach, O., M. Rajabi, X. Cui, K. Fuchs, B. Müller, J. Reinecker, K. Reiter, et al. 2018. "The World Stress Map Database Release 2016: Crustal Stress Pattern across Scales." *Tectonophysics* 744: 484–98.
Hopper, J. R., T. Funck, M. S. Stoker, U. Árting, G. Peron-Pinvidic, H. Doornenbal, and C. Gaina. 2014. *Tectonostratigraphic Atlas of the North-East Atlantic Region, Geological Survey of Denmark and Greenland, Copenhagen*.
Japsen, P., T. Bidstrup, and K. Lidmar-Bergström. 2002. "Neogene Uplift and Erosion of Southern Scandinavia Induced by the Rise of the South Swedish Dome." *Geological Society of London Special Publications* 196: 183–207.
Jørgensen, T., and R.K. Bratli. 1995. "In-Situ Stress Determination and Evaluation at the Tampen Spur Area." In *Proceedings of the Workshop on Rock Stresses in North Sea, Trondheim 13-14 February 1995*, 240–49.
Kilic, M, H. Ligtenberg, K. Hindriks, P. Schutjens, and K. Bisdom. 2022. "CO2 Storage in the Dutch Offshore K&L Blocks Using Aramis Infrastructure."
Kjeldstad, A., J. Skogseid, H. P. Langtangen, K. Bjørlykke, and K. Høeg. 2003. "Differential Loading by Prograding Sedimentary Wedges on Continental Margins: An Arch-Forming Mechanism." *Journal of Geophysical Research: Solid Earth* 108 (B1): 1–21. https://doi.org/10.1029/2001jb001145.
Lang, J, A Hampel, C Brandes, and J Winsemann. 2014. "Response of Salt Structures to Ice-Sheet Loading: Implications for Ice-Marginal and Subglacial Processes." *Quaternary Science Reviews* 101: 217–33. https://doi.org/10.1016/j.quascirev.2014.07.022.
Liszkowski, J. 1993. "The Effects of Pleistocene Ice-Sheet Loading-Deloading Cycles on the Bedrock Structure of Poland." *Folia Quaternaria* 64: 7–23.
Luo, Gang, Maria A Nikolinakou, Peter B Flemings, and Michael R Hudec. 2012. "Geomechanical Modeling of Stresses Adjacent to Salt Bodies : 1 . Uncoupled Models." *AAPG Bulletin* 96 (1): 43–64.
Maunde, A, and T. M. Alves. 2022. "Effect of Tectonic Inversion on Supra-Salt Fault Geometry and Reactivation Histories in the Southern North Sea." *Marine and Petroleum Geology* 135 (October 2021): 105401. https://doi.org/10.1016/j.marpetgeo.2021.105401.
Maystrenko, Y., D. Ottesen, and O. Olesen. 2021. "3D Thermal Effects of Cenozoic Erosion and Deposition within the Northern North Sea and Adjacent Southwestern Norway." *Norwegian Journal of Geology* 101.
Maystrenko, Y. P., M. Scheck-Wenderoth, and D. Anikiev. 2020. "3D-CEBS: Three-Dimensional Lithospheric-Scale Structural Model of the Central European Basin System and Adjacent Areas. V. 1." *GFZ Data Services*.
Mechelse, Eelco. 2017. "The In-Situ Stress Field in the Netherlands: Regional Trends, Local Deviations and an Analysis of the Stress Regimes in the Northeast of the Netherlands." *MSc Thesis*.
Muir-Wood, D. 1990. *Soil Behaviour and Critical State Soil Mechanics*. Cambridge University Press. http://www.cambridge.org/gb/knowledge/isbn/item1134715/?site_locale=en_GB.
Mukherjee, S, C. J. Talbot, and H. A. Koyi. 2010. "Viscosity Estimates of Salt in the Hormuz and Namakdan Salt Diapirs, Persian Gulf." *Geological Magazine* 147 (4): 497–507. https://doi.org/10.1017/S001675680999077X.
Müller, B., M. L. Zoback, K. Fuchs, L. Mastin, S. Gregersen, N. Pavoni, O. Stephansson, and C. Ljunggren. 1992. "Regional Patterns of Tectonic Stress in Europe." *Journal of Geophysical Research* 97.
Munson, D. E. 1997. "Constitutive Model of Creep in Rock Salt Applied to Underground Room Closure." *International Journal of Rock Mechanics and Mining Sciences & Geomechanics Abstracts* 34 (2): 233–47.
Naliboff, J., and S. J. H. Buiter. 2018. "Rift Reactivation and Migration during Multiphase Extension." *Earth and Planetary Science Letters* 421: 58–67.
Nevitt, J. M., J. M. Warren, and D. D. Pollard. 2017. "Testing Constitutive Equations for Brittle-Ductile Deformation Associated with Faulting in Granitic Rock." *Journal of Geophysical Research: Solid Earth* 122 (8): 6269–93.
Nevitt, J., D. Pollard, and J. Warren. 2012. "Constitutive Behavior of Granitic Rock at the Brittle-Ductile Transition." *Standford Rock Fracture Project* 23: 1–21.
Nielsen, L. H., R. Weibel, L. Kristensen, K. Dybkjaer, P. Japsen, M. Olivarius, T. Bidstrup, and A. Mathiesen. 2011. "Contribution to Predictions of Stratigraphy and Reservoir Properties in the Eastern Norwegian-Danish Basin." *Danmarks Og Grønlands Undersøgelse* 2011/95 (147).
Nikolinakou, M. A., P. B. Flemings, and M. R. Hudec. 2014. "Modeling Stress Evolution around a Rising Salt Diapir." *Marine and Petroleum Geology* 51 (March): 230–38.
Nikolinakou, M. A., M. Heidari, M. R. Hudec, and P. B. Flemings. 2017. "Initiation and Growth of Salt Diapirs in Tectonically Stable Settings: Upbuilding and Megaflaps." *AAPG Bulletin* 101 (6): 887–905. https://doi.org/10.1306/09021615245.
Nikolinakou, M. A., G. Luo, M. R. Hudec, and P. B. Flemings. 2012. "Geomechanical Modeling of Stresses Adjacent to Salt Bodies : 2 . Poro-Elasto-Plasticity and Coupled Overpressures." *AAPG Bulletin* 96 (1): 65–85.

Nordgård Bolås, H. M., C. Hermanrud, T. A. Schutter, and G. M. Grimsmo Teige. 2008. “Is Stress-Insensitive Chemical Compaction Responsible for High Overpressures in Deeply Buried North Sea Chalks?” *Marine and Petroleum Geology* 25 (7): 565–87. https://doi.org/10.1016/j.marpetgeo.2008.01.001.

Nygård, R., M. Gutierrez, R. Gautam, and K. Høeg. 2004. “Compaction Behavior of Argillaceous Sediments as Function of Diagenesis.” *Marine and Petroleum Geology* 21 (3): 349–62. https://doi.org/10.1016/j.marpetgeo.2004.01.002.

Obradors-Prats, J., M. Rouainia, A. C. Aplin, and A. J.L. Crook. 2019. “A Diagenesis Model for Geomechanical Simulations: Formulation and Implications for Pore Pressure and Development of Geological Structures.” *Journal of Geophysical Research: Solid Earth* 124 (5): 4452–72. https://doi.org/10.1029/2018JB016673.

Pascal, C., and R. H. Gabrielsen. 2001. “Numerical Modeling of Cenozoic Stress Patterns in the Mid-Norwegian Margin and the Northern North Sea.” *Tectonics* 20: 585–99.

Peltonen, C., Ø. Marcussen, K. Bjørlykke, and J. Jahren. 2009. “Clay Mineral Diagenesis and Quartz Cementation in Mudstones: The Effects of Smectite to Illite Reaction on Rock Properties.” *Marine and Petroleum Geology* 26: 887–98.

Peric, D., and A. J. L. Crook. 2004. “Computational Strategies for Predictive Geology with Reference to Salt Tectonics.” *Computer Methods in Applied Mechanics and Engineering* 193 (48–51): 5195–5222.

Peryt, M. T., M. Geluk, A. Mathiesen, J. Paul, and K. Smith. 2010. “Zechstein.” In *Petroleum Geological Atlas of the Southern Permian Basin Area, Eds: H. Doornenbal, and A. Stevenson, EAGE Publications*, 123–47.

Prasse, P., J. Wookey, J. M. Kendall, D. Roberts, and M. Dutko. 2020. “Seismic Anisotropy in Deforming Halite: Evidence from the Mahogany Salt Body.” *Geophysical Journal International* 223 (3): 1672–87. https://doi.org/10.1093/gji/ggaa402.

Rahman, J., M. Fawad, and N. H. Mondol. 2020. “Organic-Rich Shale Caprock Properties of Potential CO2 Storage Sites in the Northern North Sea, Offshore Norway.” *Marine and Petroleum Geology* 122.

Rahman, M. J., M. Fawad, J. Jahren, and N. H. Mondol. 2022. “Influence of Depositional and Diagenetic Processes on Caprock Properties of CO2 Storage Sites in the Northern North Sea, Offshore Norway.” *Geosciences (Switzerland)* 12 (5).

Rance, J. M., M. L. Profit, S. J. Dee, and D. T. Roberts. 2013. “Predicting the Paleo Evolution of Overpressured Geological Structures.” In *47th ARMA Rock Mechanics and Geomechanics Symposium, San Francisco, California*.

Reedlunn, B., J. G. Argüello, and F. D. Hansen. 2022. “A Reinvestigation into Munson’s Model for Room Closure in Bedded Rock Salt.” *International Journal of Rock Mechanics and Mining Sciences* 151 (January): 105007. https://doi.org/10.1016/j.ijrmms.2021.105007.

Riis, F. 1996. “Quantification of Cenozoic Vertical Movements of Scandinavia by Correlation of Morphological Surfaces with Offshore Data.” *Glob. Planet. Chang.* 12: 331–57.

Roberts, D. T., A. J.L. Crook, J. A. Cartwright, M. L. Profit, and J. M. Rance. 2014. “The Evolution of Polygonal Fault Systems: Insights from Geomechanical Forward Modeling.” *48th US Rock Mechanics / Geomechanics Symposium 2014* 1 (May 2016): 488–502.

Sajjad, N. 2013. “Structural Restoration of Mesozoic Rifting Phases in the Northern North Sea,” no. June: 66. http://hdl.handle.net/11250/240239.

Schneider, F., J.L. Potdevin, S. Wolf, and I. Faille. 1996. “Mechanical and Chemical Compaction Model for Sedimentary Basin Simulators.” *Tectonophysics* 263 (1–4): 307–17. https://doi.org/10.1016/S0040-1951(96)00027-3.

Schofield, A., and P. Wroth. 1968. *Critical State Soil Mechanics*.

Sejrup, H.P., E.L. King, I. Aarseth, H. Haflidason, and A. Elverhøi. 1996. “Quaternary Erosion and Depositional Processes: Western Norwegian Fjords, Norwegian Channel and North Sea Fan.” *Geological Society of London Special Publications*, 187–202.

SHARP Deliverable 1.1a. 2022. “Report - Glacial Contributions to In Situ Stress. Authors: E. Phillips, J. Hopper, C.F. Forsberg, L. Grande.”

SHARP Deliverable 4.1. 2022. “Report on Initial Assessments of Rock-Failure Risks for Case Studies. Authors: J.D.O Williams, P. Ringrose, M. Fyhn, K. Bisdom.”

Sirocko, F., K. Reicherter, R. Lehne, Ch. Hübscher, and W. Winsemann, J. Stackebrandt. 2008. “Glaciation, Salt and the Present Landscape.” In *Littke, R., Bayer, U.,Gajewski, D., Nelskamp, S. (Eds.), Dynamics of Complex Intracontinental Basins - the Central European Basin System. Springer, Berlin*, 233–45.

Sørensen, M. B., P. H. Voss, J. Havskov, S. Gregersen, and K. Atakan. 2011. “The Seismotectonics of Western Skagerrak.” *Journal of Seismology* 15: 599–611.

Statoil. 2016. “Sub-Surface Report Smeaheia: Mulighetsstudie Planlegging Og Prosjektering Av et CO2-Lager På

Norskkontinentalsokkel OED 15/1785 Dokument A, Undergrunnsrapport Smeaheia."
Stein, S., S. Cloethingh, N. H. Sleep, and R. Wortel. 1989. "Passive Margin Earthquakes Stresses and Rheology." In *Earthquakes at North Atlantic Passive Margins, Neoetectonics and Postglacial Rebound (Eds. Gregersen and Basham)*.
Stewart, S. A, and M. P. Coward. 1995. "Synthesis of Salt Tectonics in the Southern North Sea, UK." *Petroleum Geology* 12 (5): 457–75.
Thigpen, J. R., D. Roberts, J. K. Snow, C. D. Walker, and A. Bere. 2019. "Integrating Kinematic Restoration and Forward Finite Element Simulations to Constrain the Evolution of Salt Diapirism and Overburden Deformation in Evaporite Basins." *Journal of Structural Geology* 118 (October 2018): 68–86. https://doi.org/10.1016/j.jsg.2018.10.003.
Thompson, N., J.S. Andrews, L. Wu, and R. Meneguolo. 2022. "Characterization of the In-Situ Stress on the Horda Platform – A Study from the Northern Lights Eos Well." *International Journal of Greenhouse Gas Control* 114.
Thompson, N., J.S Andrews, H. Reitan, and N.E. Teixeira Rodrigues. 2022. "SPE-209525-MS Data Mining of In-Situ Stress Database Towards Development of Regionaland Global Stress Trends and Pore Pressure Relationships." In *SPE Norway Subsurface Conference Held in Bergen, Norway, 27 April 2022*.
Thornton, D. A., and A. J. L. Crook. 2013. "Predictive Modeling of the Evolution of Fault Structure: 3-D Modeling and Coupled Geomechanical/Flow Simulation." In *47th ARMA Rock Mechanics and Geomechanics Symposium, San Francisco, California*.
Urai, J.L., Z. Schléder, C.J. Spiers, and P.A. Kukla. 2008. "Flow and Transport Properties of Salt Rocks." In *Flow and Transport Properties of Salt Rocks, in Littke, R., Bayer, U., Gajewski, D. and Nelskamp, S.,Eds., Dynamics of Complex Intracontinental Basins: The Central European Basin System: Springer-Verlag, Berlin, Heidelberg*, 277–90.
Urai, J.L., and C.J. Spiers. 2007. "The Effect of Grain Boundary Water on Deformation Mechanisms and Rheology of Rocksalt During Long-Term Deformation." In *Wallner, M., Lux, K., Minkley, W. and Jr., H.H. Eds., Proceedings of the 6th Conference on the Mechanical Behaviour of Salt: Taylor and Francis, London*, 149–58.
Verweij, J. M., H. J. Simmelink, J. Underschultz, and N. Witmans. 2012. "Pressure and Fluid Dynamic Characterisation of the Dutch Subsurface." *Geologie En Mijnbouw/Netherlands Journal of Geosciences* 91 (4): 465–90. https://doi.org/10.1017/S0016774600000342.
Wal, W. Van Der, A. Barnhoorn, P. Stocchi, S. Gradmann, P. Wu, M. Drury, and B. Vermeersen. 2013. "Glacial Isostatic Adjustment Model with Composite 3-D Earth Rheology for Fennoscandia." *Geophysical Journal International* 194 (1): 61–77.
Wangen, M. 2000. "Generation of Overpressure by Cementation of Pore Space in Sedimentary Rocks." *Geophysical Journal International* 143: 608–20.
Weibel, R., M. Olivarius, L. Kristensen, H. Friis, M. L. Hjuler, C. Kjøller, A. Mathiesen, and L. H. Nielsen. 2017. "Predicting Permeability of Low-Enthalpy Geothermal Reservoirs: A Case Study from the Upper Triassic – Lower Jurassic Gassum Formation, Norwegian–Danish Basin." *Geothermics* 65: 135–57.
Weibel, R., M. Olivarius, H. Vosgerau, A. Mathiesen, L. Kristensen, C. M. Nielsen, and L. H. Nielsen. 2020. "Overview of Potential Geothermal Reservoirs in Denmark." *Netherlands Journal of Geosciences* 99.
White Rose. 2016. "K43 : Field Development Report."
Williams, J. D.O., M. W. Fellgett, A. Kingdon, and J. P. Williamson. 2015. "In-Situ Stress Orientations in the UK Southern North Sea: Regional Trends, Deviations and Detachment of the Post-Zechstein Stress Field." *Marine and Petroleum Geology* 67: 769–84. https://doi.org/10.1016/j.marpetgeo.2015.06.008.
Willson, S.M., A.F. Fossum, and J.T. Fredrich. 2002. "Assessment of Salt Loading on Well Casings." https://doi.org/10.2118/74562-ms.
Wu, L., E. Skurtveit, N. Thompson, E. Michie, H. Fossen, A. Braathen, Q. Fisher, A. Lidstone, and B Bostrøm. 2022. "Contaiment Risk Assessment and Management of CO2 Storage on the Horda Platform." In *16th International Conference of Greenhouse Gas Control Technologies, GHGT-16*.
Wu, L., R. Thorsen, S. Ottesen, R. Meneguolo, K. Hartvedt, P. Ringrose, and B. Nazarian. 2021. "Significance of Fault Seal in Assessing Co2 Storage Capacity and Containment Risks – an Example from the Horda Platform, Northern North Sea." *Petroleum Geoscience* 27 (3). https://doi.org/10.1144/petgeo2020-102.
Yale, D. P. 2003. "Fault and Stress Magnitude Controls on Variations in the Orientation of in Situ Stress." *Geological Society Special Publication* 209: 55–64. https://doi.org/10.1144/GSL.SP.2003.209.01.06.
Yang, Y., and A. C. Aplin. 2010. "A Permeability–Porosity Relationship for Mudstones." *Marine and Petroleum Geology* 27 (8): 1692–97.
Yassir, N. A., and A. Zerwer. 1997. "Stress Regimes in the Gulf Coast, Offshore Louisiana: Data from Well-Bore Breakout Analysis." *AAPG Bulletin* 81 (2): 293–307. https://doi.org/10.1306/522b4311-1727-11d7-

8645000102c1865d.

A. Appendix of Currently Available Data Sets and Relevant Publications

The table below contains a summary of datasets that have been identified as potential sources of data/constraint in geomechanical modelling studies. The list is not exhaustive. It is anticipated that additional data will be offered via other work packages and project partners.

Model Input	***Source/Reference***	***Dataset Type****	***Relevant Storage Site(s)***	***Comments***
Geometry	Sajjad (2013)	Thesis	Horda Platform/Northern North Sea	MSc thesis containing 2D cross sections through Northern North Sea.
	Y. P. Maystrenko, Scheck-Wenderoth, and Anikiev (2020)	Publication Open Source (CC BY 4.0)	General Southern North Sea e.g. Endurance/GBSS, Aramis, Lisa, Nini	Database covering a large area of the Central European Basins and Southern North Sea over large depth ranges.
	Equinor/Gassnova Smeaheia dataset	Dataset Open Source (CC BY 4.0)	Smeaheia/Horda Platform	Well tops data. Geometry for Smeaheia area.
	Profile 22500 Fossen SHARP project.ai	Proprietary (SHARP)	Horda Platform/Northern North Sea	Regional section provided by H. Fossen (UiO).
Constitutive Properties	Grande and Mondol (2013)	Proprietary (NGI)	All	10. no material characterisations for constraining porosity and K_0 evolution under loading/unloading. Additional hydraulic/velocity data.
	Grande, Mondol, and Berre (2011)	Proprietary (NGI)	All	10. no material characterisations for constraining porosity and K_0 evolution under loading/unloading.
	BEIS (2021)	White Paper	Endurance/GBSS	Summary of material properties for Endurance site.
	Rockfield Material Database (Sandstones)	Open Source (CC BY 4.0)	All	A selection of characterisations for well-known sandstones developed

				using data from publications under CC BY 4.0 licence.
	Equinor/Gassnova Smeaheia dataset	Open Source (CC BY 4.0)	Smeaheia/Horda Platform	Rock mechanical data for Smeaheia site e.g. elastic moduli, strength.
	Nygård et al. (2004)	Publication	All	Information to constrain the influence of diagenetic processes on sediment mechanical properties.
	Obradors-Prats et al. (2019)	Publication	All	Guidance on incorporating diagenetic processes into geomechanical simulations.
	SHARP Deliverable 3.2	TBC	Endurance, Aramis, Nini, Lisa	SHARP report containing summary of material properties available for various storage sites.
Loading	SHARP Deliverable 1.1a 2022	Report (SHARP)	All	Constraints on extent, timings and magnitudes of glacial loading/unloading.
	Sajjad (2013)	Thesis	Horda Platform/ Northern North Sea	MSc thesis containing restorations along 2 no. seismic lines.
Calibration Data	Equinor/Gassnova Smeaheia dataset	Open Source (CC BY 4.0)	Smeaheia/Horda Platform	Shoe test measurements from wells 31/6-3, 31/6-6, 32/2-1, 32/4-1 including 6 no. LOT and 1 no. FIT.
	BEIS (2021)	White Paper	Endurance/GBSS	Shoe test measurements from wells around the endurance site. 10 no. FIT tests, 2 no. LOT tests, 4 no. microfrac tests.
	Dutch Stress Map	Dataset Open Source	Aramis/Dutch Sector	Database of stress information compiled by TNO.
	World Stress Map (Heidbach et al. 2018)	Database	All sites	Global database of SHmax orientations

Appendix Table A- 1 Summary of available datasets.